POLSKA AKADEMIA UMIEJĘTNOŚCI
KOMISJA PALEOGEOGRAFII CZWARTORZĘDU

FOLIA QUATERNARIA 80

ADAMANTIOS SAMPSON,
MAŁGORZATA KACZANOWSKA, JANUSZ K. KOZŁOWSKI
with collaboration of
CONSTANTIN ATHANASSAS, YANNIS BASSIAKOS,
IOANNIS LIRITZIS, NICOLAOS LASKARIS,
IRENA TSERMEGAS

MESOLITHIC OCCUPATIONS AND ENVIRONMENTS ON THE ISLAND OF IKARIA, AEGEAN, GREECE

KRAKÓW 2012

Redaktor tomu:
Witold Zuchiewicz

Redaktor techniczny:
Jarosław Brzoskowski

Projekt
„Fundamenty neolitycznej Europy: początki zróżnicowania wczesnego neolitu
na kultury z ceramiką malowaną i kultury »impresso-carolium« na południu Bałkanów”
został sfinansowany z środków Narodowego Centrum Nauki.

ISSN 0015-573X

POLSKA AKADEMIA UMIEJĘTNOŚCI
KRAKÓW 2012

Oficyna Wydawniczo-Drukarska „Secesja”
31-016 Kraków, ul. Sławkowska 17
oficynasecesja@tlen.pl

Obj.: ark. wyd. 5,50; ark. druk. 5,75; nakład 300 egz.

CONTENTS

FOLIA QUATERNARIA 80, KRAKÓW 2012, 5-40
PL ISSN 0015-573X

MESOLITHIC OCCUPATIONS AND ENVIRONMENTS ON THE ISLAND OF IKARIA, AEGEAN, GREECE

ADAMANTIOS SAMPSON, MAŁGORZATA KACZANOWSKA, JANUSZ K. KOZŁOWSKI
with collaboration of
CONSTANTIN ATHANASSAS, YANNIS BASSIAKOS, IOANNIS LIRITZIS,
NICOLAOS LASKARIS, IRENA TSERMEGAS

A b s t r a c t. The most important Mesolithic site on the Island of Ikaria, Kerame 1, extends 80 m along the sloping edge of the cliff and is up to 40 m wide. The site is a sum of repeated sojourns of Mesolithic groups that had left behind concentrations of lithic artefacts, which were subsequently displaced by post-depositional agents, first of all by erosion. As a result, the site reveals now a large concentration of finds in Trenches E, C, and G. Moreover, post-depositional agents caused the destruction of permanent features such as the hearths associated with the various *khsemenitsas*, or – possibly – stone rings surrounding the dwelling structures. Only in trenches D, B and E the remains of a circular stone rings, probably around hearths, were registered. The lithic industry of Kerame 1 displays considerable similarity to the site of Maroulas on Kythnos; the techno-morphological differences are, probably, the effect of differing raw materials structure at Kerame 1 and at Maroulas. At Kerame 1, the distant interregional contacts and the influx of extralocal raw materials (documented by the flow of obsidian nodules from Melos and Yali) caused that production in a full cycle was carried out on-site. Thus, there was no specialization of lithic production, and unworked nodules of raw material were exploited in the particular social clusters in a full cycle, whose outcome were tools to be used by a given unit. Regretfully, because organic materials (also bones) have not been preserved we have no data to determine seasonality at Kerame 1. Nevertheless, we can say with all certainty that Mesolithic groups visiting Kerame 1 were mobile, which is evidenced by the network of interregional contacts. The most noticeable similarity between Kerame 1 and Maroulas can be accounted for by the chronological closeness of the two sites. The AMS determinations from Maroulas concentrate in the first half of the 9th millenium cal. BC (Facorellis et al. 2010). Similarly, the dates from obsidian dehydration from Kerame 1 (if their broad standard deviation is overlooked) correspond to the first half of the 9th millenium cal. BC.

K e y w o r d s: Mesolithic, OSL dating, obsidian hydration dating, early seafaring, Neolithization, Early Holocene, Aegean Basin

A u t h o r s' a d d r e s s e s: CONSTANTIN ATHANASSAS and YANNIS BASSIAKOS, Group of Ancient Metal and Palaeoenvironmental Studies, Laboratory of Archaeometry, Institute of Materials Science NCSR "Demokritos", 15310 Agios Paraskevi, Greece; MAŁGORZATA KACZANOWSKA, Archaeological Museum in Kraków, Senacka 3, 31-002 Kraków, Poland, E-mail: mak@ma.krakow.pl; JANUSZ K. KOZŁOWSKI, Institute of Archaeology, Jagiellonian University, Gołębia 11, 31-007 Kraków, Poland, E-mail: janusz.kozlowski@uj.edu.pl; NICOLAOS LASKARIS, 8 Ipirou street, Argostoli, 28100 Kefalonia, Greece; IOANNIS LIRITZIS, Laboratory of Archaeometry, University of the Aegean, Department of Mediterranean Studies, Rhodos, Greece, E-mail: liritzis@rhodes.aegean.gr; ADAMANTIOS SAMPSON, University of the Aegean, Department of Mediterraean Studies, Rhodes, Greece, E-mail: adsampson@gmail.com; IRENA TSERMEGAS, Department of Geomorphology, Faculty of Geography and Regional Studies, University of Warsaw, Krakowskie Przedmieście 30, 20-927 Warszawa, Poland, E-mail: argiro@uw.edu.pl

INTRODUCTION

Ikaria is a large island (255 km^2) which remained isolated due to its deprivation of natural ports and its rough and mountainous formation since antiquity (Fig. 1). The archaeological research has been scarce so far, and the prehistory of the island has been totally obscured. Occasional surface surveys conducted by a high-school teacher KATSAROS (2006) have led to the collection of stone axes and plenty of obsidian that show a substantial Neolithic activity. This limited prehistoric collection is found today in the Archaeological Museum of Agios Kirikos and establishes a balanced distribution of prehistoric findings in the whole island.

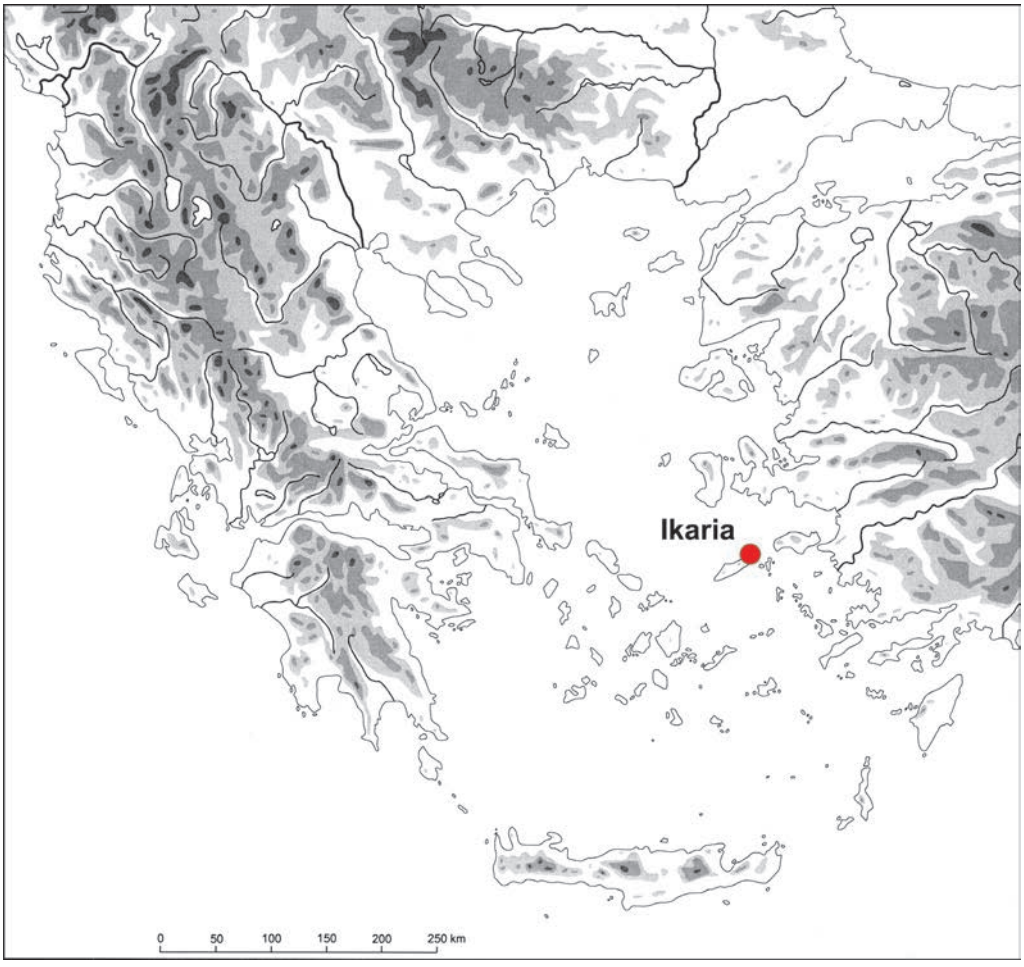

Fig. 1. Ikaria Island on the Aegean Sea

Since 2003, new prehistoric sites have been located in the western and eastern sides of the island and, more importantly, in the area between Agios Kirikos and Faros. In 2004, a systematic survey of the island was started with students of the University of the Aegean and more than 20 sites were located. In the area between Agios Kirikos and Faros, five sites have been located, which, judging from the type of stone industry, could be dated to a pre-Neolithic period (Fig. 2). This is exceptionally important because so far no findings of that age have ever been located in the eastern Aegean or in the coast of Asia Minor which lies across. It must be stressed out that no pottery has been spotted at any of these sites.

In Nyfi, very close to the Mesolithic site Nyfi 2 on the sea, a segment of a Late Neolithic settlement is preserved featuring remnants of rectangular buildings. Moreover, further smaller Neolithic sites have been located along the NE coast of the island on eroded capes.

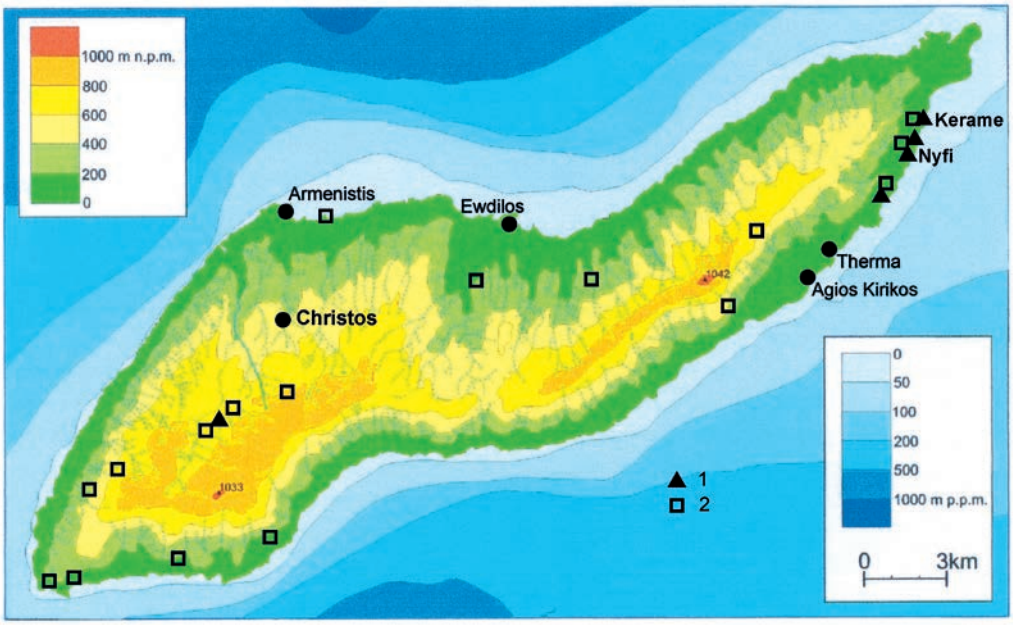

Fig. 2. Map of Ikaria with archaeological sites: A – Mesolithic, B – Neolithic

The fact that five sites featuring Mesolithic stone industry have been found, and others from the Neolithic, is indicative of a network of sites and not just of casual usage of the area. Kerame 1 is interpreted as a major site of the Mesolithic, which would be even larger if we added to it the eroded segment of the peninsula (Fig. 3).

It is important that all Neolithic and pre-Neolithic sites, except one at Glaredo near Agios Kirikos, are situated close to the coast and face a considerably secluded sea area, which is confined by Ikaria and Samos in the north, and the islands of Fourni.

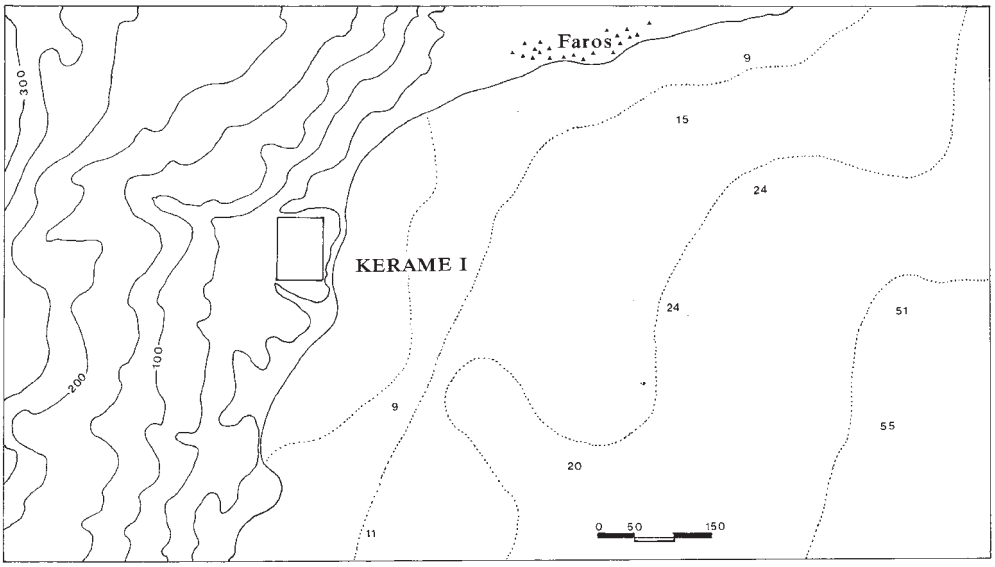

Fig. 3. Topographic map of the region of Kerame 1 site

Fig. 4. Kerame 1. View from the south

Fig. 5. Kerame 1. View on the archaeological excavations

The site of Kerame 1 is found 8 km from the town of Agios Kirikos on the main road leading to the airport of Ikaria. It is a peninsula with precipitous banks stretching into the sea (Fig. 4). In the past, it extended much farther as it is indicated by large rocks fallen to the sea owing to either earthquakes or natural erosion. It can be assumed that only the westernmost part of the site has been preserved, while its main part was ruined by erosion and the collapse of rocks to the sea.

Recent land and submarine geological researches in the area confirm that the peninsula extended many tens of metres into the sea. Prior to the excavation, artefacts of obsidian and flint were collected from the surface of the whole area which is slightly inclined to the east. A concentration of artefacts existed in the eastern side of the site. The artefacts were far fewer than expected and it is likely that, even though stone artefacts occur over an area of 8,000 m^2, they are mostly concentrated in the flat eastern part of the site, which must have constituted the westernmost part of the settlement.

Less than 70 metres from Kerame 1 to the west, another site was located with coarse ware, obsidian and ground stone tools. It is a Neolithic site (Kerame 2) that can be dated on the basis of pottery and the obsidian tools to the Late Neolithic.

The research in the area lasted 3 weeks in 2007 and 3 weeks in 2008. Archaeologists and students of archaeology from the University of the Aegean and the Athens University participated in the project. A topographic grid was made and 11 trenches were opened (Fig. 5). The profiles of the trenches were drawn and it was observed that the layers form the same sequence. Three layers were uncovered, among which the thickest (0.20-0.30 m) consists of pure brown loamy soil, followed by the second (0.20 m) one, which consists of light brown sandy-loamy-clayey sediment with small- or large-size stones, whereas the third one mainly consists of gravel.

EXCAVATIONS AT KERAME 1

Trench A

It was opened in the inner part of the site. In Spit 1, the soil was very hard and contained small stones. Down to Spit 4 (0.35 m) the soil continued to be hard but large stones appeared. Contrary to the western side, the soil in the eastern side of the trench did not contain stones and the soil was softer. The excavation was discontinued in the western part of the trench at a depth of 0.60 m. Artefacts were very rare (15 specimens including individual end-scrapers and notched-denticulated tools).

Trench B

Trench B measured 4 x 3 m. In Spits 1 and 2, the soil was rather soft and contained stones of medium size and lumps of ochre. In Squares 1-3, flint and obsidian artefacts

were found totaling to 256 specimens, including 4 backed pieces, 5 retouched flakes, 5 denticulated-notched tools and single side-scrapers. Large stones existed in sq. 1 in Spit 3 (0.25 m.). In Squares 5 and 9, the soil from Spit 3 became very hard and did not contain artefacts. Accumulated stones were also found in sq. 12 at a depth of 0.30 m. In Spits 4 and 5 soil was harder. In Squares 9, 11 and 12 excavation proceeded deeper. In Spit 6, soil became soft and contained gravels and medium-size stones. Spits 7 and 8 was excavated in Squares 8, 9, 11, and 12, where a layer of gravel and large pieces of serpentine appeared. In the south-eastern corner of the trench a quarter of a circle made from medium-size stones was exhibited, possibly a trace of a hearth (Fig. 6).

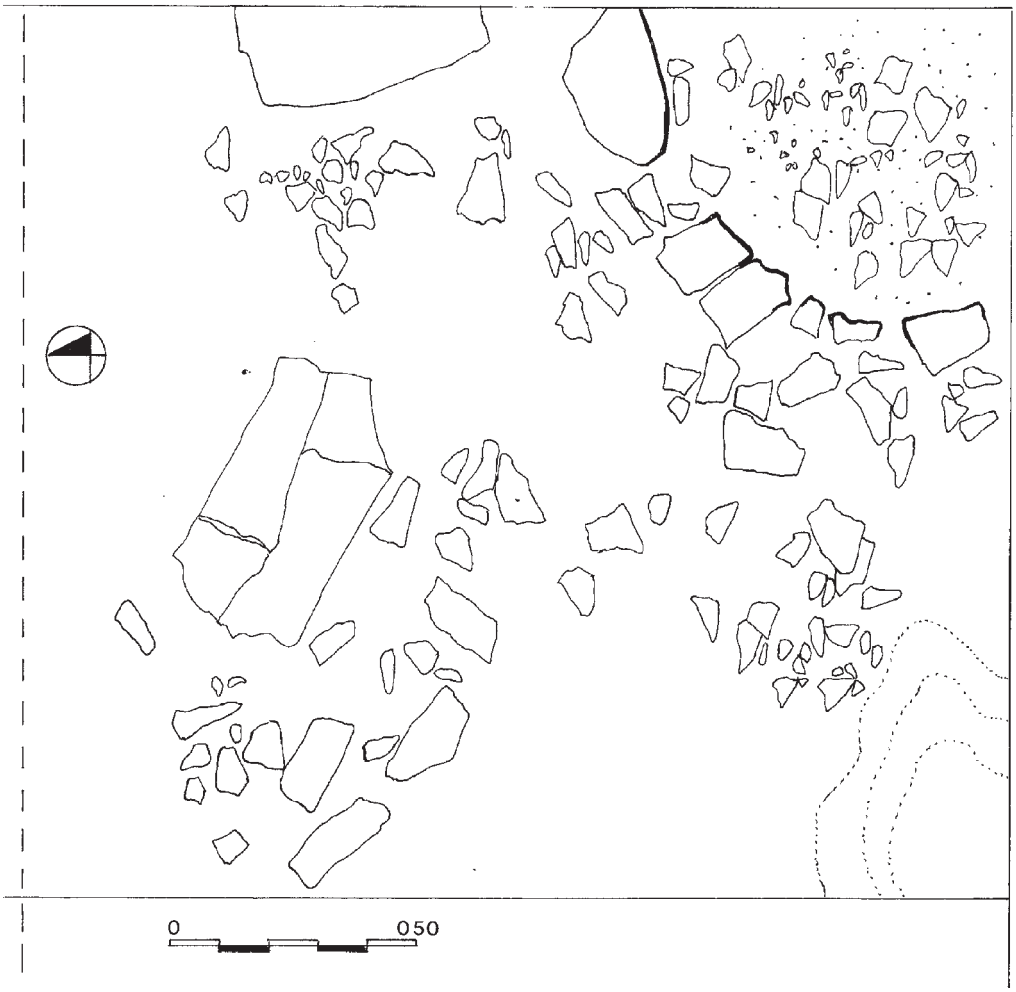

Fig. 6. Kerame 1. Stone structure in Trench B

Trench C

North of Trench E, Trench C was opened which measured 4 x 2 m. In Squares 1, 2, 7 and 8, excavation advanced in Spits 1-3 into a soil almost cleared of stones. In Square 1, a layer of gravel was present to a depth of 30 cm. In the remaining part of the trench the excavation advanced to Spits 2 and 3. The soil was clean, dark brown, with small stones. In Spits 1-3 artefacts of flint and obsidian were found. The total number of lithics is 513 including some cores and retouched tools (5 notched-denticulated tools, single truncations, retouched flakes and side-scrapers). In the upper portion of Spit 4, in Squares 7 and 8, a layer of gravel was found on one side, while on the other very soft dark soil appeared. In Squares 1 and 2 in Spit 4 there were large stones.

Trench D

A trench measuring 4 x 3 m was opened in the area between Trenches B and G. In Spits 1 and 2, 126 flint and obsidian artefacts were found, including 6 end-scrapers, 5 becs/perforators, and a single backed piece. At 0.45m depth, a large block of reddish breccia appeared and around it numerous stones of small and medium size were found. Spit 4 reached soft soil that contained stones of medium size. In the eastern side (Squares. 4, 8 and 12) in Spit 6 and 7, the soil was still soft while it contained stones of medium size. In the eastern side, the excavation reached 0.80 m. In Square 11, after large chunks were removed, the excavation continued down to Spits 7 and 8. The soil was soft with numerous small gravels. The natural bedrock appeared at a depth of 0.90 m. In Trenches G and D, the stratigraphical sequence is the same as in Trench B. Near the northern wall of the trench, some medium-size stones formed a circle (Fig. 7), probably a part of a hearth.

Fig. 7. Kerame 1. Stone structure in Trench D

Trench E

In the area between Trenches G and D, Trench E was dug measuring 4 x 2 m. Due to the difference in elevation, spit 1 reached 0.20 m on one side of the trench. The soil was brown and soft and contained 396 lithic artefacts. A concentration of cores and debitage products was found in this trench. Retouched tools are represented by 7 end-scrapers, 6 becs/perforators, 5 notched-denticulated tools and single truncations, backed implements, retouched flakes, and side-scrapers. In Spits 2 and 3, the soil was softer and contained stones of small and medium size. In the southern half of the trench, at a depth of 0.45 m, large slabs in a horizontal position appeared, while around these smaller stones existed. In the northern half of the trench the excavation reached a depth of 0.40 m. The soil was soft, but from Spit 2 numerous small and large stones appeared at the bottom of the trench. Subsequently, a westward extension of the trench was made in order to establish continuation of large stones. The result was that irregular large stones appeared close to the surface, while finds were absent. Some of stones in the central part of the trench form a circle (Fig. 8), possibly a trace of a hearth.

Trench F

In Trench F, measuring 2 x 2 m, from Spits 1 and 2 the soil was hard with large stones and few finds (79 artefacts including one end-scraper). The excavation discontinued at Spit 3. Adjacent to Trench F, an area was uncovered where compact bedrock appeared. This area constituted probably a palaeosurface used by the Mesolithic occupants of the settlement. If finds had existed, they would have been washed away into the sea.

Trench G

Trench G, measuring 4 x 2 m, is situated northeast of Trench B on the ground level. Spit 1 yielded stone artefacts. In Spits 2 and 3, soil continued to be soft and contained small stones. In Spit 3 the artefacts were fewer. In the SW corner in the 3rd layer of Trench G, a large group of stones was found that resembled a stone pavement, whereas in the SE corner no stones were unearthed and the soil was soft. In the fourth layer of the trench, at its northern side, large stones came to the surface and the artefacts were considerably fewer. The total number of artefacts is 895, including cores and tools (6 end-scrapers, single becs/perforators, truncations and a side-scraper). In Spit 4 and 5 in Squares 5 and 6, large stones lay horizontally. The soil was soft and contained gravel without artefacts (depth 0.40 m). In Spits 5 and 6, a homogeneous layer of gravel appeared that extended throughout the whole area of the trench under the large stones. In the southern part of the trench (Squares 7, 8), at a depth of 0.35-0.40 m, a stone structure could constitute a kind of wall (?) (Fig. 9). It is likely that due to the intensive cultivation at Kerame stones were displaced and some structures were destroyed. The southern side of trench yielded a large quantity of stone artefacts in Spits 1 and 2. In Spit 3, however, finds were almost non-existent. The stratigraphy of Trench G showed three basic layers. The first layer, with a thickness of 0.30 m, is a clean brown soil, while the

Fig. 8. Kerame 1. Stone structure in Trench E

second layer, of the same thickness, is light brown with small stones. The third layer consists of a concentration of gravel.

Trench H

It was dug in an area with the inclination from the west to the east. In Spit 1, the soil was hard and contained numerous stones and also stone artefacts. In Spit 2, the soil was softer and contained fewer artefacts. The total number of artefacts is 270, including 6 end-scrapers, some denticulated-notched tools and backed pieces. In Spit 3 in Square 1, a large stone and a layer of gravel appeared, which in other trenches (B, G, D and E) was found lower down.

Trench I

North of Trench H, Trench I was dug, measuring 4 x 3 m, and the first two layers yielded many obsidian and flint stone artefacts. At a depth of 0.30 m large stones were found, which, however, do not seem to belong to larger structures. Under the dense bushes, the ground was soft and contained stone artefacts. In Spit 2 stone artefacts continued to occur, but the layer of gravel was already present. In Spit 3 in Square 2,

Fig. 9. Kerame 1. Trench G: stone wall (?)

soil continued with some artefacts. The total number of artefacts is small (89); tools are represented by a denticulated-notched implement and a truncation only. It can be seen that the more we advance to the interior of the site the sediments and the artefacts were fewer. Even if the walls for cultivation created benches that retained the soil, the erosion that the site suffered during the last 10-11 millenia must have been major.

Trench J

Trench J, measuring 4 x 3 m, was opened to the north of Trench G. The ground was perfectly flat and at the surface some lithic artefacts were collected. In Spit 1, the soil was light brown and contained artefacts. Small stones were present in Spit 2 in Square 1, while in the same square in the next spit there were large stones continuing in Square 2. In Spits 2 and 3 in Squares 3 and 6, mainly obsidian artefacts were found. In Square 1 in Spits 3 and 4, under the stones, dark brown soil occurred, while in most squares a barren layer of gravel appeared. In Squares 8 and 9 humid, soft, dark brown soil continued.

Trench K

Trench K, measuring 3 x 2 m, was dug in the northernmost sloping part of the site, where the deposits were soft and stone-free. In Spit 1, the soil was light brown and contained very few finds. In Spit 2, the finds were also few while in Spit 3 numerous small stones were present in hard soil without artefacts. In this trench, some cores, numerous becs/perforators (10) and single backed pieces, side scrapers and notched-denticulated tools were found.

STRATIGRAPHY OF THE SITE AND SCATTER-PATTERN OF FINDS

Lithic artefacts were stratified only in the two uppermost lithostratigraphical units, namely (Figs. 10, 11):

1. a loamy yellow-brown unit, up to 30 cm thick, containing weakly river-rounded small fragments of limestones, sandstones, shale and quartz veins. In this layer, several shells attributed to *Helix*,probably *Helix lucorum*, were found in trenches L and H. *Helix lucorum* is living in relatively dry or medium humid environments;
2. a more sandy unit, brown-reddish in colour, up to 20 cm thick, containing sharp-eged and weakly rounded chunks of similar rocks. In this unit, few small shells were found (Trench D, wall E, depth 54 cm; and Trench G, Spit 2), belonging to genus *Helicopsis* (probably *Helicopsis smyrnocretica* Germain) (determined by S.W. Alexandrowicz). *Helicopsis smyrnocretica* is living now in relatively dry or medium humid open or partially shady environments.

At the interface of the two formations, in some sectors of the site (e.g., Trench B), there occur interbedded gravels and small stones.

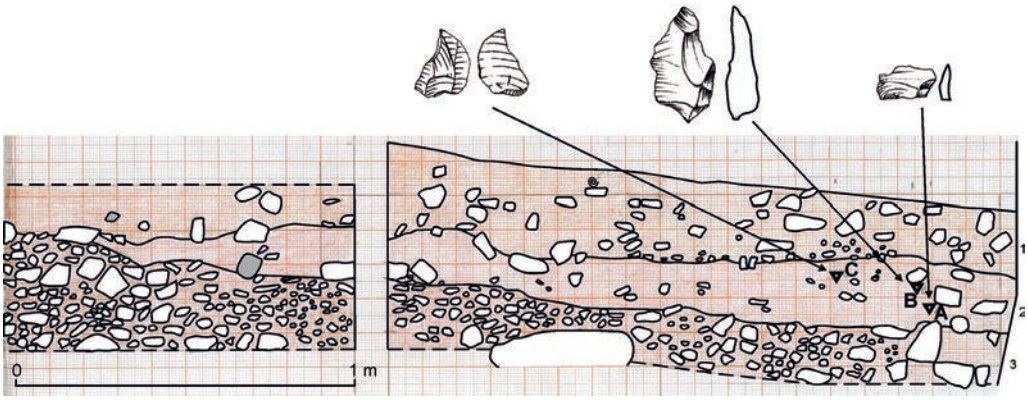

Fig. 10. Kerame 1. Trench B, profile (wall E)

The top of unit 2 is unconformable; at places this layer is eroded (Trench B) and unit 1 overlies directly sterile layer 3. Below its top, this layer consists of debris embedded within a matrix of dark-brown clay-loamy stratified material, directly on limestone blocks.

Profiles of Trenches B and D were analysed in detail (Figs. 10, 11). Unit 1 in the trenches contained, typical of the Mesolithic assemblage from Kerame 1, high end-

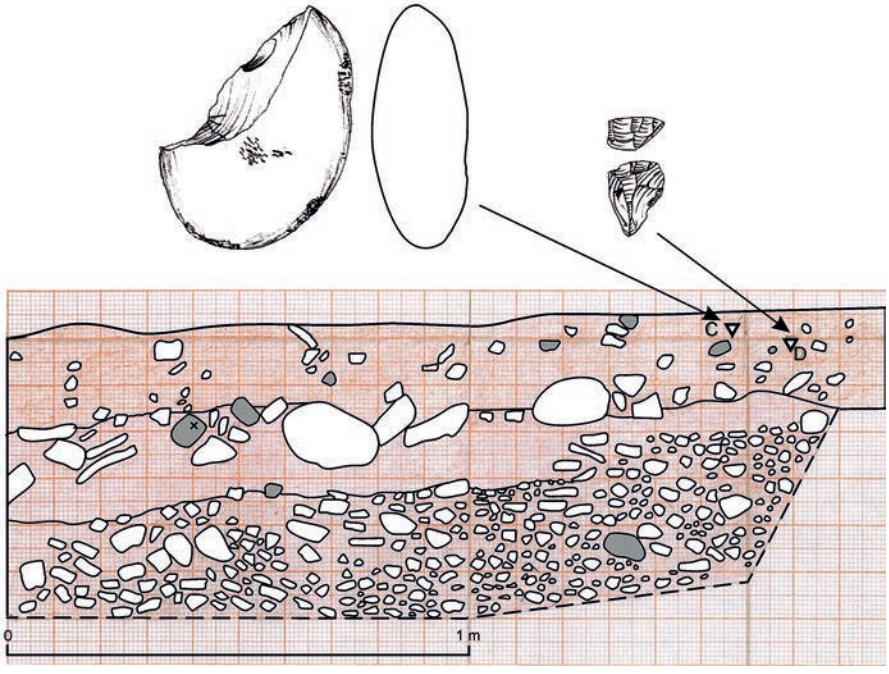

Fig. 11. Kerame 1. Trench D, profile (wall S)

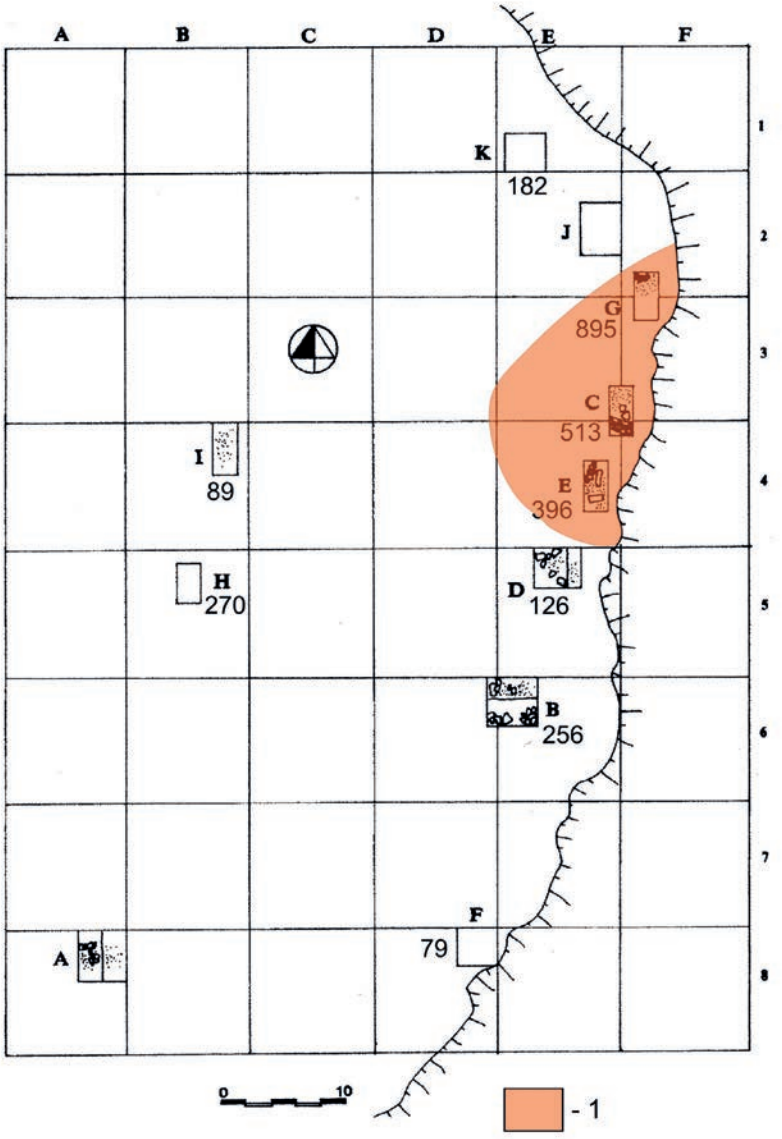

Fig. 12. Kerame 1. Distribution of trenches with numbers of artefacts: 1 – area of the highest concentration of artefacts

scrapers from white-patinated flint, denticulated-notched tools from Melian obsidian, and from white-patinated flint, also a broken quartz pebble with use-wears. Unit 2 contained flakes from beige and white-patinated flint and obsidian chips.

Lithic artefacts within unit 1 and unit 2 are not stratified at their original position, but were displaced in the course of sedimentation of these two units. The post-depositional processes re-modelled the original surface on which artefacts rested. Thus, all the finds

are stratified at secondary position within units 1 and 2. This is confirmed by dispersed OSL dates from layers 1 and 2 (Athanassas and Bassiakos in this volume).

An exception could be the situation in Trench D, next to wall N, and in trenches B and E, where a semicircular stone structure about 1 m in diameter, which could be a hearth ring, was situated (Figs. 6-8). Trench D contained relatively few artefacts in comparison with the trenches father north along the cliff. Thus, the assumption is confirmed that in trenches G, C, E concentrations of finds had been accumulated due to post-depositional agents.

The scatter-pattern of finds in the various trenches showed that there are no specific concentrations of definite categories of finds at the site. Categories of finds in the various trenches occur in the same proportions, which are the same as the ratios in the whole collection. This is particularly well observable in trenches E, C, G that are situated along the cliff and where finds are most numerous (Fig. 12). The main direction of displacement of finds was from the north (NNE), partially from the zone which is now cut off. If we consider that in Trench F a concentration of smallest finds (chips) was discovered, we can assume that in the process of slope-washing to the south, finds were sorted according to their size.

No anthropogenic structures like *kshemenitsas* have been registered, perhaps except the stone rings around the hearths. No remains that would indicate dwelling structures were found.

MESOLITHIC INDUSTRY FROM KERAME 1

Raw materials

Figure 13 shows that the most important role belonged to three raw materials: grey and dark grey, nearly black obsidian probably originating from Melos, white patinated flint or flints possibly of local origin, and black transparent obsidian with numerous opaque spherulites from the island of Yali. Other raw materials were also used, among others, local quartz, but their role was minor.

Unquestionably, obsidians were extra-local raw materials. They were supplied to Ikaria by the sea. In a straight line, the distance between Ikaria and Melos is about 170 km. Somewhat closer, at a distance of 120 km, are situated obsidian deposits on the island of Antiparos, which is a high quality obsidian (Georgiadis 2008). Obsidian from Antiparos occurs as small concretions, no more than 5 cm in diameter, but this was sufficient for the industry from Kerame 1. It should be emphasized that, so far, obsidian from Antiparos was known from the Late Neolithic only. However, only few specimens of obsidian were analysed (see Appendix) and the results indicate the provenance of these samples from Melos, other obsidian specimens have been determined by macroscopic analysis only.

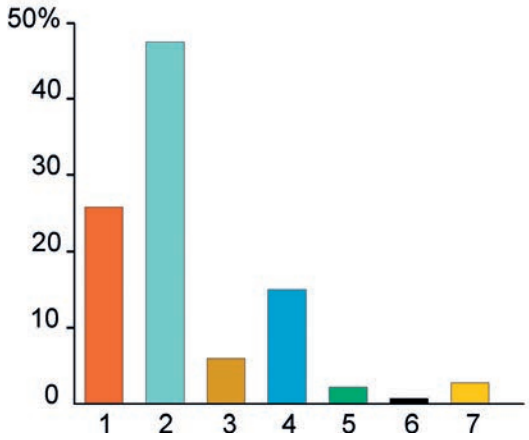

Fig. 13. Kerame 1. Raw material structure: 1 – Melian obsidian, 2 – white patinated flints, 3 – beige flint, 4 – obsidian from Yali, 5 – quartz, 6 – rhiolite, 7 – others

Obsidian from Yali is of lower quality and with poorer cleavage. Macroscopically it is easily identifiable. At Kerame 1, it accounts for 15% of the inventory. Obsidian was also supplied by the sea from the island of Yali to the southeast from Ikaria. Both in the case of this raw material and obsidian from Melos, seafaring and sea-transport were made easier by the existence of a chain of islands that joined the island with obsidian deposits with Ikaria.

The most abundant raw material are flints covered with white-patina, which makes their more precise identification impossible. These flints may have originated from Mesozoic formations in the central part of Ikaria and/or from the eastern and south--eastern areas of the coast, i.e., from a relatively small distance away from the site. Other raw materials that were exploited, such as quartz or rhyolite, are also of local origin.

Structure of major technological groups

The site of Kerame 1 yielded 3,737 stone artefacts, mostly Mesolithic ones, but also including several ones representing a younger (Neolithic) admixture. The most numerous category are flakes and splinters (1,102 – 29.4%). Chips, too, constitute a large group (less than 15 mm) which account for 21.9% of the inventory. In general, the structure of major technological categories is typical for sites where a full production cycle took place. In this respect, no essential differences exist between local and extralocal raw materials (Fig. 14).

The microlithic nature of the industry from Kerame 1, the small size of tools, of which 5% are less than 15 mm, allow us to assume that some artefacts ascribed to chips could be blanks for tool production. Chips, flakes, splinters and indeterminate fragments constitute together 57.3% of the inventory. This proportion is similar to that from the site of Maroulas on Kythnos (SAMPSON et al. 2010). Just like at Maroulas, at Kerame

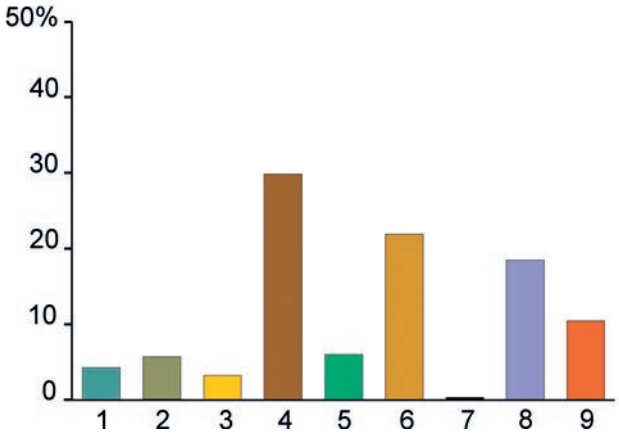

Fig. 14. Kerame 1. Major technological groups: 1 – cores, 2 – splintered pieces, 3 – blades, 4 – flakes, 5 – fragments, 6 – chips, 7 – unworked nodules, 8 – chunks, 9 – retouched tools

1 splintered technique was of importance. This technique enabled thrifty exploitation of raw materials, especially of obsidian, which was imported from considerable distances. The proportion of tools (about 10% of the total inventory) indicates that most tools were produced on-site.

Cores

Cores that document a full reduction cycle on-site are represented by 157 specimens including 70 fragments. Most of them are made from white-patinated flints (104 specimens). Other cores are made from Melian obsidian (13 specimens), obsidian from Yali (15 specimens), beige flint with a weathered surface (12 specimens), quartz, rhyolite or lava (3), hematite (1 specimen), and black lava (2 specimens). Moreover, unworked split quartz pebbles (4 specimens) and hematite fragments (4 specimens) were also encountered.

Numerous cores show an advanced stage of reduction; nevertheless, there are 30 initial cores which include: quartz plaquettes with single scars (Pl. 1:1, 2), and a core on a chunk of white-patinated flint with a prepared platform and a single scar (Pl. 1:3). These specimens are small (3.2 – 2.2 cm); hypermicrolithic specimens are numerous (< 2.0 cm – 18 specimens). One of the hypermicrolithic cores was made on an older patinated artefact (Melian obsidian).

Most cores evidence reduction from one platform, in most cases a single-blow platform, exceptionally a platform prepared by centripetal scars, or a thermal surface. Cores that were used to obtain flake or blade-flake blanks are as a rule sub-conical, from 1.5 to 3.0 cm high (Pl. 1:4–8). Hypermicrolithic cores for bladelets also occur (1.0–1.5 cm high) including sub-conical ones (Pl. 1:9; two are from obsidian – Pl. 2:1,4), with a narrow flaking surface (made on obsidian concretions from Yali – Pl. 2:5,6), sometimes

with a flat and broad flaking surface (Pl. 2:2). The reduction of hypermicrolithic cores was sometimes continued until the residual stage. In the residual stage, these cores were used for flake production (Pl. 2:3).

Reduction conducted from two opposed platforms was used, too, for the production of microlithic bladelets: these were cores with a rectangular, narrow flaking surface, partially extending onto cores sides. Cores of this type exhibit scars from side or back preparation (Pl. 2:7,8), or from lateral crest. Double-platform cores are sometimes hypermicrolithic (Pl. 2:9,10) or mediolithic (Pl. 2:11); in the latter case they were used for flake production.

Reduction from two opposite platforms was conducted on two flat sides of a core. This techniques was used when the objective were bladelet-flake blanks; it is possible that such cores are residual stages of single-platform cores (Pl. 2:12-14) leading to the hypermicrolithic stage in the case of cores from Melian obsidian (Pl. 2:15-17) and white-patinated flint (Pl. 2:18).

Change-of-orientation was predominantly employed in less advanced stages of reduction in order to obtain flake blanks. The two biggest cores from Kerame 1 (found in Trench H on the surface – Pl. 3:1, and Trench C, Spit 2 – Pl. 3:2) show perpendicular flake scars. Also occur cores with repeated change-of-orientation, in a more advanced stages of reduction, both medio- and microlithic (Pl. 3:3,4; 4:1). A different reduction model is represented by medium-size sub-discoidal flake cores, exploited on one as well as on two sides (Pl. 4:2,3).

In the reconstruction of reduction sequences, core fragments have not been taken into account as they cannot be ascribed to a definite sequence.

A doubtful specimen is a single-platform blade core on a flat concretion of white-patinated flint. The specimen shows relatively large blade scars, which may indicate that this specimen is a Neolithic admixture. This core was found in Trench G, Spit 1 (Pl. 4:4). Core distribution in various trenches is as follows: most cores were found in trenches C, G and K (16–23 specimens); trenches B and E contained 9 specimens each, trenches D, F, H and I 3–6 cores each, and only trenches A and L yielded one core each. Hence, it can be assumed that local production of blanks (mainly from white-patinated flint) concentrated in trenches C, G and K.

Splintered pieces

The site of Kerame 1 yielded 210 splintered pieces and their fragments. The most common raw material for their production was obsidian from Melos (102 specimens – 88.5%). In the case of white-patinated flint, splintered technique was used less often (64 specimens – 30.5%). Moreover, splintered pieces from obsidian from Yali also occur (27 specimens – 12%). Other raw materials are represented by single specimens.

Most splintered pieces are medium-size: from 1 to 38 mm long and from 5 to 20 mm wide. Splintered pieces made from Melian obsidian are smallest and most exhausted (11–25 mm long; Pl. 4:5).

Splintered pieces are frequently made on flakes, and sometimes bladelets. Among specimens from Melian obsidian, quadripolar splintered pieces (5) occur that are not represented by other raw materials. Splintered pieces made from obsidian from Yali have similar dimensions. Specimens from local quartz (16–39 mm long) as well as those from white-patinated flint (12–38 mm - Pl. 4:6) are slightly larger.

The most common type are bipolar splintered pieces: one- and two-sided. They were made on fine bladelets, flakes, and sometimes on cores in final stages of reduction. An attempt was made to transform microlithic splintered pieces from Melian obsidian into tools using marginal (Pl. 4:7) or notched retouch (Pl. 4:8). These operations indicate a thrifty economy of exploitation of this raw material.

It is difficult to determine whether splintered pieces without secondary retouch functioned as tools or whether they were used for blank production. Only 31 splinters have been preserved at the site, mostly (21) from Melian obsidian. Some splinters of small dimensions may have not been collected in the course of exploration although dry-sieving was used.

Flakes

Flakes are the most numerous group of artefacts (1,102); to this group we have also ascribed 7 tablets and 7 trimming flakes and splinters, which is 30.02% of the whole collection. The raw materials composition is provided in Table 1.1

Table 1

Kerame 1. Raw materials of flakes

	N	%
Melian obsidian	195	17.4
White patinated flints	671	60.1
Beige flint	82	7.3
Obsidian from Ghiali	80	7.1
Quartz	32	2.8
Rhyolite	15	1.3
Others	49	3.6
Total	1,116	100.0

Flake dimensions range from 9 to 59 mm in length and from 5 to 52 mm in width. Flake thickness is from 2 to 19 mm. Analysis of flakes from the various types of raw materials revealed that specimens from Melian obsidian are slightly smaller (length – 10–12 mm, width – 6–25 mm, thickness – 2–9 mm) than specimens made from white-patinated flint (length – 9–43 mm, width – 5–46 mm, thickness – 2–19 mm). Flakes from quartz are largest (length – 22–59 mm, width – 20–52 mm). The dimensions of specimens from obsidian from Yali are similar to those of specimens from Melian obsidian (length – 12–17 mm, width – 15–20 mm).

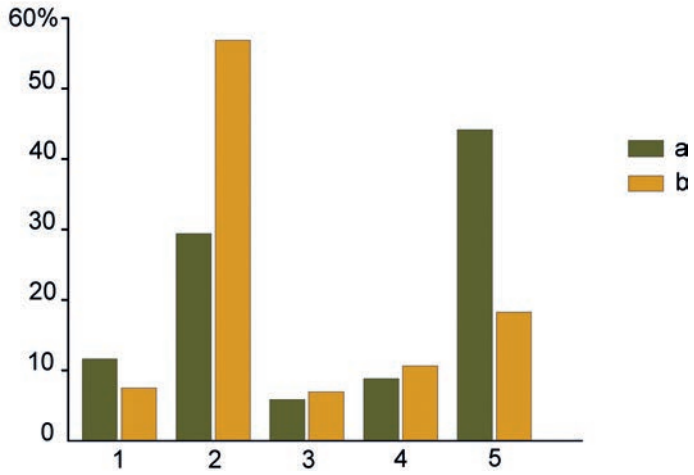

Fig. 15. Kerame 1. Platform types of flakes: A – Melian obsidian, B – white patinated flints.
1 – unprepared, 2 – formed by single blow, 3 – dihedral, 4 – facetted, 5 – linear or punctiform

The technique of platform preparation of flake cores from Melian obsidian and from white-patinated flint differ. Single-blow platforms show a higher frequency among flakes from white-patinated flint, whereas the frequency of facetted platforms is low, equally among the various raw materials (Fig. 15). The high proportion of single-blow platforms could be the result of a method of core preparation but also core retrimming by tablet detachment. Flake detachment technique from obsidian cores shaped linear or punctiform platforms (44.1%).

In the relatively numerous series of flakes from both types of obsidian there was only one cortical flake and several flakes with lateral cortex. Most flakes show parallel scars (50%), and flakes with perpendicular scars from core preparation or change-of-orientation are fairly numerous (29.4%). Moreover, there were flakes with blade scars and blade and flake scars on the dorsal side. It can be assumed, therefore, that the method of detachment of flakes and of blades from obsidian cores was similar.

Cores from white-patinated flint were, just like obsidian cores, often reduced without preparation. Retrimming was, as a rule, restricted to the correction of coring angle by tablet removal, also – when core orientation was used – to detachment of trimming flakes.

Many flakes show traces of nibbling and retouch on small sections of edges. It is difficult to decide whether they are the effect of use or damage caused by post-depositional processes.

Chips

The site of Kerame 1 yielded 820 chips accounting for 21.9% of the total inventory. At the site of Maroulas the proportion of chips is similar, i.e. 18.77% (Sampson et al. 2010). This proportion is not particularly high considering that in the Mesolithic layers of the

site of Cave 1 at Klisoura (Kaczanowska et al. 2010) this group constituted as much as 42.7%. Chips come from retouch or from core reduction and core rejuvenation. Chips from Melian obsidian (387 specimens – 47.2%) are the most numerous group. This is a higher proportion than the average for this raw material for the whole site (25.7%). Chips from white-patinated flint – the raw material that dominates at the site of Kerame 1 – are less numerous (279 – 34.1%). Chips from white-patinated flint come from tool production more often than chips from other raw materials. Chips from obsidian from Yali account for 15.6% (128) of all chips. In the investigated series there was only one chip made from quartz. Other raw materials are represented by single items.

Blades

There were 121 blades (3.2%). Several specimens with parallel lateral edges and straight interscar ridges can be assumed to be a Neolithic admixture. A small two-sided trimming blade also belongs in this group (Pl. 4:9).

Blades were made from obsidian (53 specimens of which two are probably Neolithic), and from white-patinated flint (44 specimens). Moreover, blades were produced from Yali flint (10 spec.), beige flint (8 spec.), quartz (3 spec.), rhyolite (1 spec.), and from cream-coloured, smooth, opaque flint (1 spec.).

Most blades have been preserved as fragments. Only 32 specimens are intact. The blades are from 11 to 35 mm long. Only one blade differs from the others as it is 52 mm long, made from cream-coloured, smooth, high quality flint. This blade probably represents a younger admixture.

Besides raw materials, also techniques of blade production vary. Specimens from Melian obsidian are small (length – 19–19 mm, width – 5–13 mm). The presence of a cortical blade confirms that also unworked nodules of raw material were brought to the site. Most nodules were worked without a preparation phase; preparation was only sporadically used which is evidenced by a single trimming blade. Blade core platforms were shaped by a single-blow. Among preserved butts, specimens with punctiform and linear butts were most frequent. Bulbs of obsidian blades are as a rule flat. It is likely that some blades were obtained by means of splintered technique.

Blades made from white-patinated flint are slightly larger (18–33 mm long and 7–19 mm wide). Core platforms were formed by a single-blow or were natural surfaces. Sporadically, platforms were prepared by a series of detachments, which is evidenced by the presence of facetted and *dièdre* butts. Core reduction technique shaping punctiform or linear butts was less frequent, too.

Change-of-orientation of cores is documented by the presence of blades with opposite and perpendicular dorsal pattern of scars.

Chunks

A series of chunks and waste items (682) made from a variety of raw materials is present at the site. Chunks of white-patinated flint were most numerous (300 specimens

– 43,9%). Chunks from obsidian from Yali are next in number. This obsidian has poor cleavage and in the course of working large quantity of waste remained (217 – 31.8%). Chunks from beige flint with strongly weathered surface are fairly numerous (70 – 10,2%). There were, besides, 11 chunks of local quartz. Single chunks of, probably, local raw materials such as, for instance, calcite and yellowish jasper also occurred. Moreover, 9 polihedral hematite crystals, partially polished, were found as well.

Tools

The entire collection from Kerame 1 numbered 297 retouched tools. Specimens with impact fractures (3) and with proximal notches (2 specimens – possibly half-products of microliths), and 72 fragments of indeterminate tools were counted separately. The restricted indices of major tool groups have been calculated on the basis of the total number of retouched tools (297). The most numerous groups are retouched flakes (22.2%) and denticulated-notched tools (19.5%), followed by becs-perforators (18.8%) and end-scrapers (15.5%). The frequency of techno-morphological groups is provided in Table 2, including 74 unidentified fragments and 10 artefacts attributed to the Neolithic.

Table 2

Kerame 1. Major tool categories

Tool category	N	% (with fragments and admixtures)	Group index (calculated on the base of 297 items)
End-scrapers	50	12.8	16.8
Burins	2	0.5	0.7
Becs and perforators	56	14.4	18.8
Truncations	15	3.8	5.0
Trapezes	3	0.8	1.0
Backed pieces	32	8.2	10.8
Retouched flakes	66	16.9	22.2
Raclettes	4	1.0	1.3
Denticulated-notched tools	58	14.9	19.5
Inserts with impact fracture	3	0.8	1.0
Side-scrapers	11	2.8	3.7
Bladelets with notches	2	0.5	0.7
Neolithic admixtures	10	2.6	-
Hammerstones/grinders	4	1.0	1.3
Others and fragments	74	19.0	-
Total	390		

End-scrapers

The collection included 46 end-scrapers and 4 end-scrapers combined with other tools. The most frequent raw material for their production was white-patinated flint (34); less numerous are specimens from Melian obsidian (5), from obsidian from Yali (3), from beige flint with a weathered surface (4), from opaque, smooth, beige flint (1), from quartz (1), and rhyolite or lava (3).

Among end-scrapers, blade specimens are rare: only four including a specimen on a blade-flake. These are: two short end-scrapers (Pl. 5:1,2 – the latter specimen has lateral retouch), a mediolithic end-scraper (Pl. 5:3) and a macrolithic specimen (Pl. 5:4).

Much more numerous are end-scrapers on flakes (27 specimens). The following morpho-technological types can be distinguished:

a) mediolithic flake end-scrapers, as a rule with fronts shaped by denticulated retouch (Pl. 5:5-12). Two specimens are initial (Pl. 5:13). Fronts are usually symmetrical, slightly convex; in one case the front is oblique (Pl. 5:8);
b) short, flake end-scrapers (Pl. 5:14-17), of which one is double and one has lateral retouch (Pl. 6:1);
c) flake end-scrapers with steep retouch of sides (Pl. 6:2);
d) large, flake end-scrapers with fronts and sides shaped by denticulated retouch; these are intermediate forms to denticulated-notched tools (Pl. 6:3,4),
e) atypical, nosed flake end-scrapers (Pl. 6:5,6). One of the two specimens is a fragment, possibly made on a blade, and is closer to end-scrapers *á epaulement* (Pl. 5:6);
f) a large group comprises high end-scrapers made on thick flakes. These are, first of all, end-scrapers with straight (Pl. 6:7-11) or with ogival fronts (Pl. 6:12,13). Typical high/nosed end-scrapers (Pl. 6:14,15) also belong to this group.

Besides end-scrapers on flakes, specimens on splintered pieces were also registered that morphologically do not differ from flake specimens (Pl. 7:1-3). One of them is very small, made from Melian obsidian (Pl. 7:3).

A separate group are hypermicrolithic specimens shaped on fine flakes or splinters (Pl. 7:4-7).

Four specimens are combined end-scrapers and *becs*/perforators:

a) a short flake end-scraper with a slightly convex distal front + a proximal *bec* shaped by two Clactonian notches (Pl. 7:8);
b) an end-scraper on blade-like flake, with a slightly convex distal front + an atypical, slightly asymmetrical, proximal *bec* shaped by two retouched notches (Pl. 7:9);
c) an end-scraper on a blade-like flake + a proximal perforator alterne (Pl. 7:10);
d) a short flake end-scraper with a convex distal front + a proximal *bec* shaped by two Clactonian notches (Pl. 7:11).

End-scrapers were found in all the trenches and on the site surface. Most end-scrapers were found in trenches E (7 spec.), D and H (6 spec. each), G (5 spec.), A, B, C, F, I and L (2 spec. each).

Burins

The collection contained only two burins, both from white-patinated flint: a dihedral burin on a thick flake (Pl. 7:12), and an initial burin (or a carenoidal end-scraper) (Pl. 7:13).

Becs and perforators

This group included 56 specimens, made mainly from white-patinated flint (27 specimens), Melian obsidian (19 spec.), and obsidian from Yali (7 spec.), beige flint with a weathered surface (2 spec.), and from quartz (one specimen).

The most numerous group comprises atypical perforators with a fairly short, symmetrical point (17). They are usually medium-size, made on flakes (Pl. 7:14-20), sometimes robust (Pl. 8:1,2); blade perforators are less frequent (Pl. 8:3). Only one specimen was made from Melian obsidian. Some atypical perforators were made on microlithic flakes (Pl. 8:4-9); only one was made on a bladelet (Pl. 8:10). One atypical perforator was made on a retouched flake (Pl. 8:11), and two on splintered pieces (Pl. 8:12). The points are sometimes located asymmetrically (Pl. 8:13-16). These perforators include one double specimen (Pl. 8:17) and two perforators on blade sides (Pl. 8:18).

The group of *becs* consists of several types:

a) becs shaped by Clactonian notches on medium-size flakes (Pl. 9:1-5) and microlithic specimens (Pl. 9:6-10);

b) a double *bec* (Pl. 9:11);

c) becs shaped by alternate Clactonian notches (Pl. 9:12,13);

d) becs shaped by inversely (Pl. 9:14-16), or by obversely retouched notches;

e) multiple *becs* on large flakes resembling denticulated tools (Pl. 10:1). There are only two typical blade perforators (Pl. 10:2), of which one was shaped by alternate retouch (Pl. 10:3).

Moreover, a trihedral perforator from obsidian from Yali (Pl. 10:4) and a triple microlithic perforator (Pl. 10:5) also occurred.

Becs and perforators are evenly distributed in the various parts of the site. Only in trenches E, K and D they are slightly more numerous (10 – Trench K; 6 – Trench E; 5 – Trench D), whereas in other trenches there are one or three specimens (H, I, C, G, B). Individual specimens were found in the areas in between trenches C and D, and B and D, and some come from the surface.

Retouched truncations

The assemblage yielded truncations (a total of 15) on blades and on flakes, both mediolithic and microlithic. As a rule, they were made from Melian obsidian (7 specimens) and white-patinated flint (4 specimens). There are single items from beige flint with a weathered surface, from smooth, weakly banded beige flint, and rhyolite or lava.

Mediolithic blade truncations are represented by specimens with a convex (Pl. 10:6,7), straight (Pl. 10:8) or oblique truncation (Pl. 10,9; Sampson et al. 2008, fig. 2:7). Moreover, there were two truncations on flakes: one with a slightly concave truncation on a robust flake (Pl. 10:10), the other with the truncation shaped by inverse retouch (Pl. 10:11).

Microlithic truncations were made both on bladelets and on microflakes. In terms of the shape of truncation we can distinguish specimens with: a convex truncation (Pl. 10:12-14), a straight truncation (made from Melian obsidian – Pl. 10:15), a slightly concave oblique truncation (Pl. 10:16), and a transversal, also slightly concave, truncation (Pl. 10:17).

These specimens were distributed in trenches C, E, G, I and K.

Double truncations resembling trapezes

Three inserts of this type were registered:

a) a specimen with three steeply retouched sides made on a robust flake from white-patinated flint (Pl. 11:1);
b) a kind of atypical asymmetrical trapeze on a robust flake (blade-flake?) from beige flint with a weathered surface (Pl. 11:2);
c) a double microlithic truncation made on a bladelet (?) from Melian obsidian. The truncation was shaped by alternate retouch (Pl. 11:3).

The specimens were found in trenches B, D, G.

Backed pieces

There were 32 backed pieces in the assemblage, made from white-patinated flint (12 spec.), Melian obsidian (9 spec.), obsidian from Yali (6 spec.), and also from beige flint with a weathered surface (2 spec.). Other specimens are made from unidentified raw materials. Three groups can be distinguished:

a) arched backed pieces, both made on blades and flakes. There were 10 backed blades, all fairly small, with the convex blunted back shaped by bilateral retouch (Pl. 11:4,5), or obverse only (Pl. 11:6,7; Sampson et al. 2008, fig. 2: 3-5 – one specimen; Pl. 11:7 shows distal and proximal impact fractures). A specimen on a thicker blade had a weakly convex blunted back shaped by obverse retouch (Pl. 11:8), and another specimen was shaped by inverse retouch (Pl. 11:9). A backed blade had a straight blunted back (Sampson et al. 2008, fig. 2:2).

Moreover, there were 8 backed flakes with an arched blunted back. Five specimen were on robust flakes with the blunted back shaped by two-sided (obverse/inverse) retouch (Pl. 11:10-14). Two specimens were shaped on thinner flakes by obverse retouch (Pl. 12:1,2– the latter specimen has an impact fracture in the distal part). Finally, one specimen is with a partially retouched blunted back (Pl. 12:3).

b) three backed pieces with an angulated blunted back: two are on blades (Pl. 12:4; Sampson et al. 2008, fig. 2:6) and two on flakes (Pl. 12:5,6). The blunted backs were shaped by obverse/inverse retouch.
c) backed pieces with a straight blunted back and a retouched truncation. Four, fairly irregular specimens are on flakes (Pl. 12:7-10). Only one backed-truncated piece is on a blade (Pl. 12:11).

To the group of backed pieces we have also ascribed two specimens with a partially blunted back, made on irregular blades (Pl. 12:12,13).

The backed pieces were evenly distributed in nearly all the trenches (B – 4 specimens, B/C – 1 spec., D – 3 spec., E – 3 spec., D/E – 1 spec., H – 1 spec., I – 1 spec., L – 1 spec.). Other specimens come from the site surface.

Retouched flakes

A total of 66 retouched flakes were subdivided on the basis of the location of the retouched edge in relation to the flake axis and the type of retouch. Retouched flakes are as a rule made from white-patinated flint (45 specimens). Much less frequently they were made from Melian obsidian (14 spec.), and from obsidian from Yali (2 spec.), beige flint with a weathered surface (3 spec.), from rough grey flint (1 spec.), and from smooth opaque beige flint (1 spec.).

In terms of morphology we can distinguish:
a) flakes with lateral retouch (10 specimens) including 4 flakes shaped by steep retouch on robust blanks (Pl. 12:14-16; 13:1) and 5 shaped by fine retouch (Pl. 13:2-6); only one flake is with inverse retouch (Pl. 13:7);
b) microlithic flakes with bilateral retouch (2 spec.) from obsidian from Melos (Pl. 13:8,9);
c) flakes with transversal retouch (8 spec.) including 2 flakes with oblique retouch (Pl. 13:10,11), 2 with convex retouch (Pl. 13:12,13), and 4 with irregular obverse (Pl. 13:14,15) or inverse (Pl. 14:1,2) retouch;
d) flakes with transversal and lateral retouch (6 spec.) represented by fine flakes with obverse retouch (Pl. 14:3,4), flakes shaped by alternate retouch (Pl. 13:5-7) – all in the distal part; one specimen had transversal retouch in the proximal part (Pl. 14:8);
e) flakes with convergent retouch (7 spec.) in the distal part, symmetrical (Pl. 14:9-11) and asymmetrical (Pl. 14:12,13). One flake has this type of retouch in the proximal part (Pl. 14:14);
f) flakes with fine, irregular, partial retouch (Pl. 15:1,2).

Moreover, there were 27 fragments of retouched flakes. To the group of retouched flakes also belong four splintered pieces with marginal lateral retouch (Pl. 15:3,4) and with transversal retouch (Pl. 15:5,6).

Retouched flakes are most frequent in Trench B (5 spec.) and in between Trenches B and D (4 spec.). Other trenches yielded only 2–3 specimens (A, C, D, G, K, L) or one retouched flake (E, F, H, L).

Side-scrapers

Among a total of 11 side-scrapers, most were made from white-patinated flint (9 spec.). Individual specimens were made from Melian obsidian, from obsidian from Yali and from quartz.

All the specimens were made on flakes. Morphologically, side-scrapers are classified on the basis of position of the retouched edge in relation to the flake axis:

a) straight lateral side-scrapers; made on thick flakes with retouch extending onto the surface (Pl. 15:7,8), on a cortical flake (Pl. 15:9), and on a flake from preparation with steep retouch (Pl. 15:10);
b) lateral convex side-scrapers: on a blade-flake (Pl. 15:11), on a flake from preparation (Pl. 15:12), on a cortical flake (Pl. 15:13). One side-scraper is a distal fragment (Pl. 15:14). A microlithic side-scraper was also found (Pl. 15:15);
c) a convex transversal side-scraper (Pl. 15:16) and a *dejété* side-scraper on a robust flake shaped by steep retouch (Pl. 15:17).

Single specimens were found in the various trenches (B, C, C/D, B/D, G, K). Only Trench F provided 3 specimens.

Raclettes

Four *raclettes* were made on fine flakes: from Melian obsidian (3 spec.) and from white patinated flint (1 spec.).

Three specimens were shaped by steep, inverse and obverse retouch (Pl. 16:1-3). The smallest *raclette* was shaped by only obverse retouch (Pl. 16:4).

The *raclettes* were discovered in trenches C, E and G. One specimen was collected from the site surface.

Denticulated-notched tools

The group of denticulated-notched tools was represented by 58 artefacts, mainly made from white-patinated flint (34 spec.), less often from Melian obsidian (17 spec.), from obsidian from Yali (3 spec.), quartz (1 spec.), and from beige flint with a weathered surface (2 spec.).

There were 20 tools with retouched notches:

a) notches in the distal part of flakes retouched by obverse retouch (Pl. 16:5-11). Only one specimen had a bifacially retouched notch (Pl. 16:12);
b) two specimens with bifacially retouched proximal notches (Pl. 16:13,14);
c) five with lateral notches made on small flakes (Pl. 16:15,16), or on larger (Pl. 17:1), sometimes cortical (Pl. 17:2) or on blade-like flakes (Pl. 17:3);
d) one specimen is a thick flake with three notches: two lateral, and one proximal shaped by steep retouch (Pl. 17:4).

Three tools with Clactonian notches were made on flakes: a tool with a distal notch (Pl. 17:5), a tool with a distal notch and denticulated lateral retouch (Pl. 17:6), and a tool with a proximal notch and denticulated retouch of the edge (Pl. 17:7).

There were 17 denticulated tools:

a) the most frequent tools (10 spec.) bear denticulated, obverse (Pl. 17:8-11; 18:1-4) or alterne lateral retouch (Pl.17:12,13). Some were shaped on fairly thick flakes by steep retouch;
b) two specimens represent lateral denticulates shaped by inverse retouch (Pl. 18:5,6), and one was a lateral-distal denticulate (Pl. 18:7);
c) two specimens have distal denticulated retouch (Pl. 18:8,9);
d) two specimens are fragments of small denticulated tools (Pl. 18:10,11).

A specimen made on a blade-like flake has denticulated retouch on one edge and notched retouch on the opposite edge (Sampson et al. 2008; fig. 2:8).

Moreover, there were 17 fragments of tools with denticulated notched retouch that has been preserved on small sections of edges.

The scatter-pattern of denticulated-notched tools shows a weak concentration in trenches B, E, C (5 specimens each), possibly also in Trench I (3 specimens). Trenches A, F, H, K, L contained single tools. Similarly, in between trenches B/D, C/D and D/E single specimens were found.

Bladelets with impact fractures

There were three bladelets of this type: an unretouched bladelet with a distal impact fracture (Pl. 18:12), two bladelets with a proximal impact fracture and inverse lateral retouch (Pl. 18:13,14). All were made from Melian obsidian.

Bladelets with a proximal notch

There were two specimens of this type: one was a bladelet with a retouched notch (Pl. 18:15) which was probably a half-product of a microlith, and the other with two symmetrical Clactonian notches forming a kind of tang (and another notch at the tip). The latter specimen could have been an insert (Pl. 18:16). Both specimens were made from Melian obsidian.

Fragments of unidentified chipped tools

The collection consisted of 72 fragments of unidentified retouched tools made, as a rule, from white-patinated flint.

Worked pebbles

Only three tools were made on pebbles:

a) a quartz pebble used as a hammerstone was transversally broken which gave it the shape of a chopper (Pl. 19:1);
b) a quartz pebble was used at two tips as a hammerstone (Pl. 19:2);
c) a sandstone pebble was used as a hammerstone at one tip (Pl. 19:3).

Moreover, a fragment of hematite showed traces of possible polishing.

The artefacts were found in trenches D and L.

Neolithic admixtures

Some Neolithic artefacts were found on the surface of the site, namely:

a) two fragments of Neolithic polished axes, oval in cross-section (Pl. 20:1,2);
b) a blade from white-patinated flint, with flat, irregular ventral surface retouch in the distal part;
c) a small flake from surface retouch, made from Melian obsidian (Pl. 20:3);
d) a fragment of a regular blade with lateral, semisteep retouch, from Melian obsidian (Pl. 20:4);
e) a proximal fragment of a blade from Melian obsidian, with flat, lateral retouch of one edge (Pl. 20:5);
f) a fragment of a *lame appointée* with semisteep retouch, from white-patinated flint (Pl. 20:6);
g) a proximal fragment of a blade with fine, bilateral retouch (Pl. 20:8);
h) a fragment of a regular blade with fine alternate retouch, from beige, opaque, smooth flint (Pl. 20:7);
i) a dihedral mesial burin on a blade-like flake, from white-patinated flint (Pl. 20:9).

THE INDUSTRY FROM KERAME 1 IN COMPARISON WITH THE INDUSTRIES AT THE SITE OF MAROULAS ON THE ISLAND OF KYTHNOS

The industry from Kerame 1 shows most analogies with the early Mesolithic site of Maroulas on the island of Kythnos (Sampson et al. 2010). Similarities can be seen in core reduction processes, while some differences are caused by the different raw materials used (at Maroulas a higher, up to 56%, use of quartz and a higher frequency of exclusively Melian obsidian, up to 31%). The raw materials used at Maroulas, first of all extensive use of quartz, resulted in a specific strategy of reduction of tabular quartz fragments.

Reduction sequences and blank types

The comparison of reduction sequences from Kerame and from Maroulas can be carried out for cores from flint and obsidian, i.e., the raw materials that occur in greater quantities at both sites. The reduction sequence for single-platform cores is similar at the two sites: its objective was to obtain flake or blade-flake blanks. The only difference is that at Maroulas cores for blades or bladelet production are more frequent, although at both sites the index of bladelets is low (1.9 at Maroulas, and 1.5 at Kerame 1). At both sites, reduction was continued from one platform until the residual phase. Its result were hypermicrolithic cores (also for bladelets). Reduction from two platforms at the two sites was conducted on cores with a narrow flaking surface. However, cores with a broad flaking surface and cores with opposite flaking surfaces also occur. Change-

of-orientation, evidenced on the largest preserved cores, played an important role at Kerame 1 whereas at Maroulas change-of-orientation was carried out in the final phase of reduction.

Tools

The structure of retouched tools is, generally, similar at both sites. At Kerame 1, the frequency of backed pieces (10.8%), more numerous than truncations (6.0%), is higher than at Maroulas. At the latter site, on the other hand, both typological groups are equally represented while their frequency is together only 8.3%. At Maroulas, the indices of denticulated-notched tools (Maroulas – 25.9, Kerame 1 – 19.5) and side-scrapers are much higher (Maroulas – 7.4, Kerame 1 – 3.7). The indices of other tool groups are similar at the two sites.

End-scrapers (at Kerame 1 – 15.5%, at Maroulas – 17.9%) show a higher proportion of flake end-scrapers at Kerame 1, which is a half of all the end-scrapers, whereas at Maroulas they are a fourth of all the end-scrapers. Morphology of end-scrapers at the two sites shows close similarity: there occur specimens with lateral retouch (at Kerame denticulated retouch is more common), high end-scrapers on robust flakes as well as hypermicrolithic specimens are numerous. At both sites combination of end-scrapers+*becs* is registered, but such specimens are more numerous at Kerame 1.

At both sites burins are few (Kerame 1 – 0.7%, Maroulas – 1.2%).

Becs/perforators have similar frequencies at the two sites and morphologically are very close. These are: atypical perforators on mediolithic flakes or blade-flakes and *becs*. At Maroulas these specimens are more often with retouched rather than Clactonian notches. In both assemblages the presence of hypermicrolithic specimens is characteristic.

Despite different frequencies the truncations and backed pieces at the two sites are, generally, similar, such as: short truncations on blade-like flakes, microlithic specimens of double trapezoidal truncations. On the other hand, the groups of backed pieces differ slightly: at Maroulas these are first of all microlithic backed pieces with straight or angulated blunted back, less often arched, whereas at Kerame 1 – although small specimens, too, predominate – specimens with an arched blunted back, often on robust flakes with a strongly rounded blunted back are more numerous than at Maroulas. This difference could be the effect of different Epipalaeolithic traditions, in which two assemblages were rooted: Maroulas evolved on the tradition of the Epigravettian of Continental Greece where arched backed pieces were less frequent, and Kerame 1 evolved on the tradition of the North Aegean Epipalaeolithic (e.g., on Limnos) where regular arched backed pieces or even segments predominated.

In the two assemblages the most numerous categories are retouched flakes and denticulated-notched tools (retouched flakes: 22.2% – Kerame 1 and 16.9% – Maroulas, denticulated-notched tools: 19.5% and 25.9%, respectively). In respect of the type of retouch and its position in relation to the blank axis, these tool categories are similar

in both assemblages. It should be added that at Maroulas a major part of denticulated – notched tools was made on plaquettes.

Side-scrapers are similar, too, but at Kerame 1 they are less numerous than at Maroulas (3.7% and 7.4%, respectively). An important difference is that macrotools are absent at Kerame 1.

Between the assemblages of the "Aegean Mesolithic" the most noticeable similarity can be seen between Kerame 1 and Maroulas, which can be accounted for by the chronological closeness of the two sites. The AMS determinations from Maroulas concentrate in the first half of the 9th millenium cal. BC (Facorellis et al. 2010). Similarly, the dates from obsidian dehydration from Kerame 1 (if their broad standard deviation is overlooked) correspond to the first half of the 9th millenium cal. BC (see Laritzis and Laskaris in this volume).

THE INDUSTRY FROM KERAME 1 IN COMPARISON WITH THE INDUSTRY FROM THE MESOLITHIC LAYERS IN THE CYCLOPS CAVE ON THE ISLAND OF YOURA

Because the inventories from the Cyclops Cave (Sampson et al. 2003; Sampson 2008, 2011; Kozłowski and Kaczanowska 2009) are very small, the comparison of Kerame 1 industry and the Mesolithic industry in the Cyclops Cave can be made for only some types of artefacts. Moreover, only flint artefacts can be compared because it is uncertain whether obsidian artefacts from the Cyclops Cave can be ascribed to the Mesolithic layers. Thus, the similarity of the two industries rests in: the importance of splintered technique, the presence of high end-scrapers, truncations, retouched flakes and denticulated-notched tools, and arched backed blades. It should be added that tools at Maroulas are much larger than tools at Kerame 1.

THE INDUSTRY FROM KERAME 1 AND OTHER MESOLITHIC INDUSTRIES FROM AEGEAN ISLANDS

In recent years, in the course of field surveys conducted by A. Sampson, two other Mesolithic sites were discovered on the islands of Naxos and Chalki. Naxos provided an inventory of several tens of artefacts and Chalki of as many as several hundred. On the island of Naxos, artefacts are predomiantly made from Melian obsidian and some from flint, whereas on the island of Chalki from Melian obsidian, obsidian from Yali and brown flint (Sampson 2010).

The two inventories show that splintered technique was used, accompanied, however, by microlithic bladelet technique based on a fairly regular single-platform core. The presence of regular bladelets is a distinctive feature of the two assemblages that makes them different from other sites of the "Aegean Mesolithic". This feature, together with the presence of typical trapezes, suggests a younger age of the sites on Naxos and on Chalki, although we do not have radiometric determinations for these sites.

Other tool categories, such as perforators/*becs*, hypermicrolithic end-scrapers, short blade end-scrapers, denticulated-notched tools and retouched flakes resemble specimens from Kerame 1 and Maroulas. The morphology of truncations and, possibly – backed pieces – is also similar although at Naxos and Chalki backed pieces were made on more regular blanks.

OTHER MESOLITHIC SITES ON IKARIA

The sites extend from 1 to 3 km eastwards of Kerame 1 (Fig. 16) and reveal artefacts from white flint and obsidian from Melos and Yali. The typological analysis showed that they belong to the same period as Kerame. The closer site (Panagia), within sight at Kerame, lies on a small plateau by the main road, near a small monastery of Panagia. Flint and Yali obsidian have been found in open areas among thick shrubs. The other site (Nyfi 2) is situated at Nyfi at a distance of 40 m from the Neolithic settlement. It is a small plateau where thick sediments have been preserved. Artefacts from flint and Melos obsidian were collected on the surface. The site of Nyfi 3 is 500 m northeast of Nyfi 2. It is a low plateau, much lower than Nyfi 1 where a very thin soil has been preserved. Artefacts from flint and obsidian were collected. Another site (Sykies) which yielded Mesolithic flint artefacts is by the road 1 km west of Nyfi 1.

Nyfi 2

The site of Nyfi 2 is situated at a distance of about 2 km from the Neolithic settlement of Nyfi 1, on a small plateau where thick rubble/gravel/clayish sediments have been preserved. From the site surface, about ten artefacts made from white-patinated flint and Melian obsidian were collected. These included:

a) a flat, double-platform blade-flake core: on one side reduction was conducted from two unprepared platforms, and on the opposite side from one platform; white-patinated flint (Pl. 21:1);
b) a hypermicrolithic core on a flake, with the flaking surface on the narrow facet; Melian obsidian (Pl. 21:2);
c) three obsidian splintered pieces: a two-sided, bipolar specimen (Pl. 21:3), two hypermicrolithic specimens; one on a bladelet (Pl. 21:4), the other on a flake (Pl. 21:5);

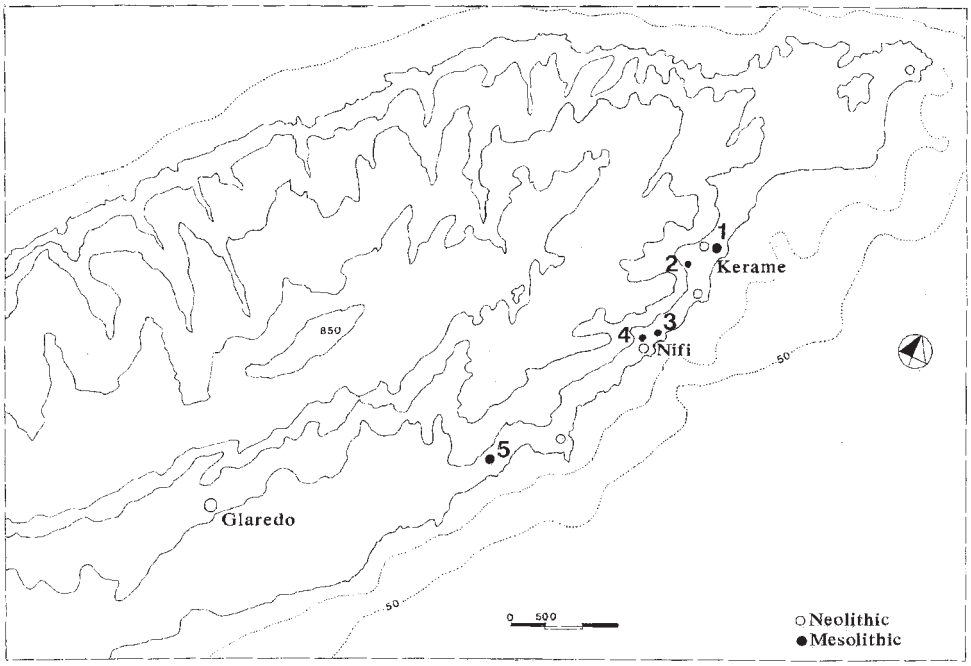

Fig. 16. Map of the Mesolithic sites near Kerame 1

d) an arched backed piece on an obsidian blade (Pl. 21:6);
e) a denticulated-notched tool on a flake with lateral-distal obverse retouch and proximal inverse retouch (Pl. 21:7).

The collection contained, besides, a transversal truncation on a macroblade from chalcedony (Pl. 21:8), and three mesial fragments of mediolithic blades from Melian obsidian; these specimens could be Neolithic (Pl. 21. 9-11).

Nyfi 3

The site of Nyfi 3 is situated 500 m to northeast of Nyfi 2, on a low elevation, lower than Nyfi 1. A thin layer of soil has been preserved. Over a small area flint and obsidian artefacts were collected:

a) a single-platform initial blade-flake core from white-patinated flint (Pl. 21:12);
b) two burin-like cores on flakes from white-patinated flint. Flaking surfaces show bladelet scars on flake sides (Pl. 21:13,14);
c) a quadripolar splintered piece from white-patinated flint (Pl. 21:15);
d) a fragment of an end-scraper in the distal part of a blade from white-patinated flint (Pl. 21:16);
e) a perforator on a quartz plaquette;
f) two flakes from white-patinated flint: one with bilateral inverse, steep retouch (Pl. 21:17), the other with partial distal retouch (Pl. 21:18);

g) a flake with a lateral notch and a denticulated-notched tool, made from Melian obsidian (Pl. 21:19);
h) 17 flake fragments: 5 made from quartz, 11 from white-patinated flint, one from Melian obsidian;
i) three chips: two from Melian obsidian and one from obsidian from Yali;
j) a fragment of a blade from white-patinated flint.

Moreover, site Nyfi 3 provided a fragment of a blade with slightly denticulated lateral retouch, made from quartz, which could be a Neolithic admixture.

CONCLUSIONS

The most important site of Kerame 1 extends 80 m along the sloping edge of the cliff and is up to 40 m wide. The site is a sum of repeated sojourns of Mesolithic groups that had left behind concentrations of lithic artefacts, which were subsequently displaced by post-depositional agents, first of all by erosion. As a result, the site reveals now a large concentration of finds in trenches E, C, and G. In respect of quantity and quality, the distribution of finds is even, without forming conspicuous groups. Moreover, post-depositional agents caused the destruction of permanent features, such as the hearths associated with various *khsemenitsas*, or – possibly – stone rings surrounding the dwelling structures. The remains of a circular stone rings around hearths were registered in Trench D, B and E. In trenches C and G large stone slabs occur, which, however, do not form intentional structures and were, in all likelihood, displaced from the higher parts of the slope by torrential slope-washing. This phenomenon is caused by torrential rains which occur on Ikaria in winter (Tsermegas 2007, see also Appendix).

Because organic materials that would correspond to the Mesolithic occupation at the site have not been preserved, a possibility that light timber structures without stone walls also existed cannot be ruled out. A major part of the site, situated beyond the present-day cliff, had been destroyed when the cliff edge retreated, as erosion of the cliff advanced.

The lithic industry displays considerable similarity to the site of Maroulas on Kythnos (Sampson et al. 2010); the techno-morphological differences are, probably, the effect of differing raw materials structure at Kerame 1 and at Maroulas. At Kerame 1, the distant interregional contacts and the influx of extra-local raw materials (documented by the flow of obsidian nodules from Melos and Yali) caused that production in a full cycle was carried out on-site. Thus, there was no specialization in lithic production, and unworked nodules of raw material were exploited in the particular social clusters in a full cycle, whose outcome were tools to be used by a given unit. Regretfully, because organic materials (also bones) have not been preserved we have no data with which to determine seasonality at Kerame 1. Nevertheless, we can say with all certainty that Mesolithic groups visiting Kerame 1 were mobile, which is evidenced by the network of interregional contacts.

The absence of organic remains (bones, palaeobotanical evidence) does nor allow to reconstruct the subsistence economy of the users of Kerame 1. The only interesting piece of evidence could be few land snail shells. Hence, we can assume that, contrary to Maroulas where large concentrations of land snails shells occur, gastropods did not play a major role in the nutrition of the users of Kerame 1. No marine shells have been discovered at the site. Moreover, contrary to Maroulas, grinding stones are absent which suggests minor importance of plant food. We can, thus, hypothesize that the subsistence economy at Kerame 1 was based primarily on fishing and hunting.

The site of Kerame 1, just as other Mesolithic sites on Ikaria, was probably situated farther away from the Early Holocene seashore as the sea level was probably lower by 30-35 m in relation to the present level (see Fig. 16). The inhabitants of the island lived in fairly dry environment, with the presence of sparse vegetation. Such environment is documented by land snails that occur in two layers with artefacts. Moreover, the presence of thermal springs could attract Mesolithic groups to settle in their vicinity.

The radiometric determinations for obsidian artefacts from Kerame 1, if we disregard the large standard deviation, suggest that Kerame 1 and Maroulas, possibly also the lower layers of the Cyclops Cave on Youra, may be contemporaneous. On the other hand, the techno-morphological arguments point to an earlier age of Kerame 1 than of the Mesolithic sites at Naxos and Chalki.

APPENDIX

GEOLOGICAL STRUCTURE AND PALAEOGEOGRAPHY OF THE SITE OF KERAME (SE IKARIA, GREECE)

IRENA TSERMEGAS

The site of Kerame I is situated on a marine terrace (GEORGALAS 1953) that encloses the Kerame bay from the south. The substratum of the area is built up of consolidated Pleistocene fanglomerates (red breccias and, locally, conglomerates of torrential fans) composed of fragments of Palaeozoic and Mesozoic crystalline rocks: crystalline schists, gneisses, phyllite, crystalline limestones, and amphibolites building the hills to the WNW of the narrow sedimentation zone stretching along the shoreline (Fig. 17). The thickness of fan deposits unconformably overlying the Lower Pliocene yellowish, at places milky, marine sandstones and conglomerates, is a dozen or so metres (KTENAS 1927, 1969; PAPANIKOLAOU 1978; GEOLOGICAL MAP… 2005).

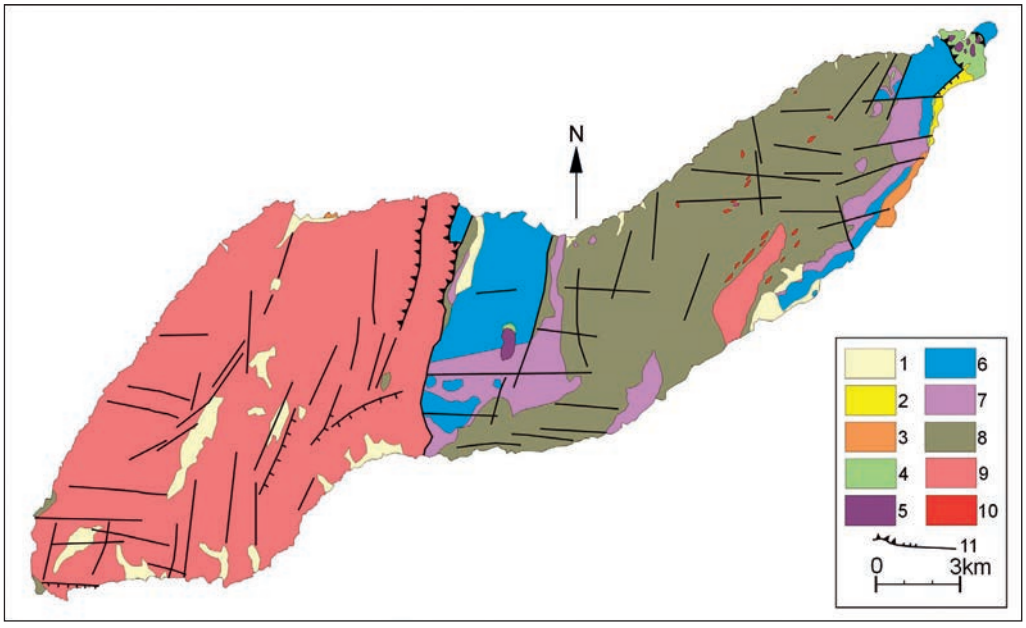

Fig. 17. Geological map of Ikaria: 1 – Holocene sediments (alluvial, littoral and slope), 2 – Pleistocene marine terraces, 3 – Pliocene marine sediments (breccia, sandstone, margles), 4 – Oligocene – Lower Miocene ophiolithic molasse, 5 – Upper Triassic crystalline limestones and dolomites, 6 – interbedded Mesozoic marbles and shales, 7 – Triassic marbles, 8 – Palaeozoic (?) gneisses, 9 – Lower Miocene granitoids, 10 – Lower Miocene pegmatites, 11 – tectonic structures

The dip of the layers building the Kerame fan and the fact that the cutting it cliff is up to 10 m high (like in the case of other fans that occur in the vicinity of Kerame, Glifadi and Nifi bays) indicate that this fan is the upper part of a major landform with a front situated several hundred metres to the east of the present shoreline, and which had been destroyed due to postglacial marine transgression (Fig. 18).

The traces of this relief are also evidenced by the 50 m depth contour. The beginning of the formation of the Kerame fan was most probably related to the maximum of the last marine regression. At about 20,000 years BP the sea level in the region of Ikaria was lower than that of the present day by at least 130 m, while the eastern edge of Ikaria was connected with the island of Fourni, Samos and with Anatolia by a narrow strip of land. However, at the end of the Pleistocene this land bridge no longer existed (Lambeck 1996).

The accumulation of sediments was favoured by the presence of a fault zone. Along this zone, the eastern part of Ikaria was uplifted in relation to the littoral foreland. This is evidenced by both the absence of Neogene sediments within the uplifted fault side as well as by the fact that the area is deeply dissected by streamcutting erosion. Together with the marine transgression the fans, like the littoral belt to SW and NE of them, became – for a short time interval – covered by the sea. Subsequently, the fans and the littoral belt were uplifted in stages. This caused that the fans were dissected and

Fig. 18. Section of the Kerame cliff

the modern proluvial deposits were accumulated several metres lower down within the beach. Although the surface of terrace is in places flat, there are no marine sediments that could suggest the age of the fans, which can only be indirectly estimated.

The information on the youngest neotectonic processes on Ikaria is unfortunately very scanty. The active fault zone forming the SE coast of the island is evidenced by the presence of numerous thermal springs in this area. The analysis of seismic reflection profiles (Lykousis et al. 1995) and a survey from the neighbouring island of Samos (Stiros et al. 2000) provide some premises; however, it is difficult on such a basis to assess the precise age of uplift.

At the beginning of the Holocene, i.e. the period to which the cultural material at the Kerame I site is ascribed, the level of the Aegean Sea in the region of eastern Ikaria was lower than the present one by no more than 30-35 m (Lambeck 1996): thus the Kerame fan had already been shaped. Since then, the shoreline must have retreated by a dozen or so metres, which means that originally the site was situated farther away from the seashore. The present elevation of the site is also most probably higher by several metres than initially. Because the materials that build the fans are easily destroyed by erosion, traces of earlier wave notches have not been preserved at the cliff foot, such as limestone cliffs in the vicinity of Demonopetra. Notches can also be seen on the NW coast of the island of Samos where the younger stages of coastal uplift have been dated at 500-3,900 years BP (Stiros et al. 2000).

At the time when the Kerame terrace was occupied by Mesolithic groups, the surface of the fan must have been no longer active. For this reason, the sediments which contain artefacts (layers 1 and 2 in the archaeological excavations) are composed of finer fractions than those lower down in the section and were, in all likelihood, deposited by slopewash processes caused by torrential rainfalls.

OBSIDIAN HYDRATION DATING FROM HYDROGEN PROFILE USING SIMS: APPLICATION TO IKARIAN SPECIMENS

Ioannis Liritzis, Nikolaos Laskaris

INTRODUCTION

The early seafaring prior to the Neolithic (ca. 7th millennium BC) constitutes a controversial issue in Aegean archaeology and generally in the Mediterranean (Sampson et al. 2010; Laskaris et al. 2011 and references therein). However, current evidence from systematic research in different parts of the Aegean started gradually changing this picture and opened up new dynamics for understanding the character of exploitation and the importance of early coastal and island environments; see the example of Crete (Kopaka and Matzanas 2009; Strasser et al. 2010), the new site of Ouriakos on the island of Lemnos (dated according to preliminary evidence to the end of the Pleistocene and possibly to the beginning of the Holocene ca. 12,000 BP; N. Eustratiou, pers. comm. 2010), and the new Middle Palaeolithic site in Agios Eustratios Island (A. Sampson, pers. comm.). Our contribution sheds new light on the Late Pleistocene/Early Holocene (ca. 12th millennium BP) exploitation of obsidian sources on the island of Melos in the Cyclades.

The main source of information for these early visits on the island of Melos comes from Franchthi cave in the Argolid. Provenance studies of the material from this site indicated its Melian origin but obsidian hydration dating was not applied to the artefacts recovered. Regarding the presence of obsidian at Youra, Kythnos, Franchthi, Ikaria, and Attica several routes could be considered as possible: a direct ones and via a *chaines operatoire* model that include distances of ca. 120 km and crossings of ca. 15-20 km between islands (Sampson 2008; Broodbank 2006, p. 209). The presence of obsidian in mainland and island sites indicates that these exploitations included successful return journeys (Broodbank 2006, p. 209).

The new obsidian hydration dates presented below (Table 3) are part of the combined work published elsewhere in Laskaris et al. (2011), and employ the novel SIMS technique and SIMS-SS method (Fig. 19), that offers a new reliable source of absolute dating. Since the archaeological evidence of the presence of obsidian in levels that antedate the food production stage could have been the result of trade or the intrusion of younger age obsidian artefacts from the overlying Neolithic layers (see the discussion

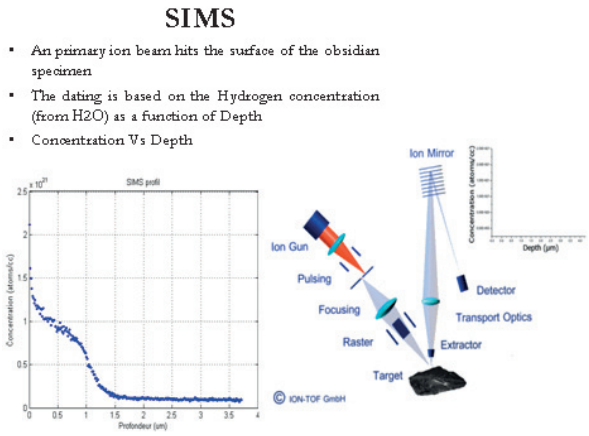

Fig. 19. SIMS apparatus showing ion gun entering surface to a few microns (essentially non destructive technique) and the obtained H+ profile (Schematic diagram of the CAMECA IonTOF ToF-SIMS instrument)

regarding Cyclops Cave on the island of Youra; Kaczanowska and Kozłowski 2008, p. 172) that exist in all sites discussed here, the novel SIMS-SS method was employed to confirm excavation data.

Table 3

SIMS-SS dates for two samples from Ikaria (Kerame site) (from Laskaris et al. 2011)

No.	Lab. No./ site	Sampling details	X_s (cm)	C_s (grmol/cc)	C_i (grmol/cc)	e^k	$D_{s,eff}$ (cm^2/year)	Age SIMS-SS (years BP)
1	RHO-891 Kerame, Ikaria	T,C, Spit 4 Sq. 5+6	3.1486e-5 ± 1.87e-6	0.00129197 ± 1.79e-5	0.000106014 ± 6.24e-6	360	1.1365e-12	11085 ± 3282
2	RHO-892 Kerame, Ikaria	Trench D Spit 4	4.90433e-5 ± 2.24e-5	0.0007287 ± 2.24e-5	9.8763e-5 ± 4.44018e-6	80	3.42e-13	10152 ± 1643

OHD – A BRIEF REVIEW

In many regions of the ancient world, obsidian, a volcanic glass, was the preferred material for stone-tool production. Fracturing obsidian exposes fresh surfaces or surface intact internal fissures, on which hydration rinds may form. The thickness of a rind increases with the age of the artefact. Rind thicknesses, measured using powerful digital optical microscopes but more accurately employing infrared spectroscopy and nuclear

analysis, can be used to date the production of artefacts. The latest advance, the novel secondary ion mass spectrometry – surface saturation (SIMS-SS) involves modeling the hydrogen concentration profile of the surface versus depth, whereas the age determination is reached via equations describing the diffusion process (Figs. 19, 20).

The reactions involved in the production of a rind and the exact diffusion mechanism by either mechanical transport or molecular interconversion is still complex and subject to research.

SIMS Hydrogen Profile & Hydration Rim

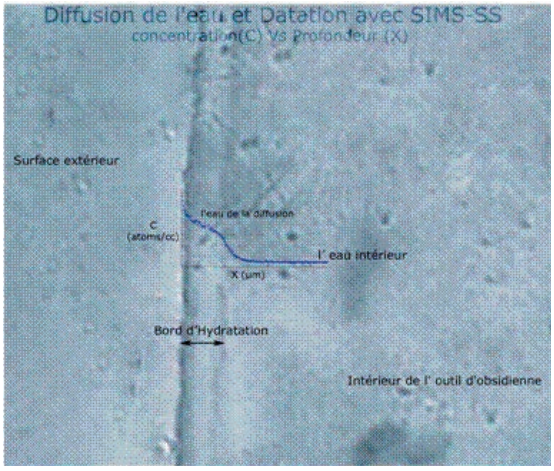

Fig. 20. SIMS hydrogen sigmoid profile overlapping the hydrated layer (rim)

Factors related to diffusion reactions affect the rate at which rinds form and progress on obsidian artefacts. These include the chemical composition of the glass, effective hydration temperature (EHT), diffusion rate, flaking, relative humidity, intrinsic water, and exposure time.

Hydration measurements can be used for relative or absolute dating and its accuracy is dependent on control of these variables. Theoretically, hydration dating has no absolute temporal limitations, but rinds tend to crumble at a thickness of 50 microns, making it difficult to date artefacts of great antiquity. With SIMS-SS, H+ profiles formed during last decades are measurable (see below). Although radiocarbon, thermoluminescence, and archaeomagnetic dating can be used to date Holocene sites, hydration dating used to be an inexpensive alternative; with the advent of the SIMS-SS method it too has become costly (Liritzis 2006)

Hydration measurements are used in three fundamentally different ways to calculate the age of artefacts. The first and earlier empirical method calibrates rind measurements with other temporal data, such as radiocarbon dates or even ceramic phases. The variation in local environmental conditions is not taken into account resulting in increased error. The second intrinsic approach is the induction method that relies on laboratory ageing experiments. Hydration is induced by exposing fresh obsidian to water vapour or

liquid water of high temperatures and pressures. Under these artificial conditions, rind formation can be modelled as a diffusion process, allowing the calculation of EHT-dependent hydration rates with an Arrhenious plot.

However, the extrapolation to ambient temperatures induces uncertainties. Estimated temperatures using thermal cells or weather station data and mathematical expressions extrapolated to the past are used for a first approximation. Among serious flaws is the fact that natural rind formation is far more complex than laboratory-induced diffusion. In SIMS-SS the shape of hydration profile is considered as the end product of diffusion that includes all environmental factors (Liritzis 2006; Liritzis and Laskaris 2010). Sample suitability is a least weathered flat surface and other tests.

The earliest attempts to use hydration measurements to date artefacts were made by Friedman and Smith (1960). Since then, hydration dating has been used widely, with some success in California and the Great Basin of the United States, Australia, and the Pacific. In these areas, numerous regional chronologies have been constructed using the calibration method. In Mesoamerica, obsidian hydration dating has usually been used to supplement more traditional chronological data.

Case studies that have critisized the method include cross-dated OHD results with ^{14}C dating, archaeomagnetism, and ceramic phasing of Mexican, Guatemalan, and Sardinian obsidians. Hydration dates of New Zealand obsidians dated to last millennium by Christopher Stevenson and his colleagues have been satisfactorily but not exactly compared with radiocarbon dates from the same context; while OHD errors spanned some two to three hundreds of years. More recently, Stevenson et al. (2004) have offered a chronology for the Hopewell Culture earthworks (ca. 200 BC–AD 500) in central Ohio with dates developed from high precision hydration layer depth profiling using SIMS, and that data suggested that long-distance exchange in obsidian occurred throughout the Hopewell period.

Ambrose (1998) gave a provisional age-depth model for hydration thicknesses for Manus Island, Papua New Guinea, for the last two thousand years based on internal crack surfaces and compared with ^{14}C age control. Among other problems, weathering and dissolution were readily observed, while the comparison with ^{14}C produced some confusion.

Although current environmental conditions can be measured, an unmeasurable error is introduced when these conditions are extrapolated to the past. A shift in EHT of just 1 K, for example, can lead to dates that err by centuries. For this reason, the two earlier hydration dating approaches relying on a $t^{1/2}$ dependent hydration rind empirical relationship, in spite of some successes, must still be considered relatively inaccurate independent chronometric techniques.

The novel SIMS-SS technique (see below) has produced ages from the Aegean Islands (third to thirteenth millennium BC), the Easter Islands (Chile), Japan (fifth to thirtieth millennium BC), Mexico, Greece, Hungary, Asia Minor, and other parts of the World. For many of these cases, the comparison with archaeological and ^{14}C data is excellent, and suggests a promising alternative (Liritzis and Stevenson 2011).

THE SIMS-SS OBSIDIAN HYDRATION DATING METHOD IN BRIEF

From the 1960s, when Friedman and Smith (1960) first report on the Obsidian Hydration Dating, the use of obsidian tools as a chronometer in archaeology has been subjected to several critiques detailed studies (see Liritzis and Laskaris 2011 and references therein)

In fact, the classical approach to obsidian hydration dating (OHD) uses optical microscopy to read hydration rims, make approximate corrections for temperature history by calculation, and computes age from experimentally derived diffusion coefficient and the square-root-of-time dependence of rim thickness on age. Though it several cases seems successful it is not widely used by archaeologists (Liritzis and Laskaris 2011).

Amongst several drawbacks is the exponent of time, the diffusion coefficient, and the extreme simplicity of the empirical age equation (Liritzis 2006).

At any rate the square-root-of-time relationship is introduced also in the SIMS-SS procedure, since in the derivation of equation (1) the Boltzmann transformation introduces a variable, η, which is inversely proportional to $t^{1/2}$ (Liritzis et al. 2004, p. 53, eq. 6).

In 2002, an alternative novel approach towards obsidian hydration dating, using SIMS, named SIMS-SS, has been initiated (Liritzis et al. 2004; Liritzis 2006), based on modelling the hydrogen profile acquired by secondary ion mass spectrometry (SIMS), following Fick's diffusion law, together with the assumption of surface saturation (SS) layer with water molecules. SIMS is based on the bombardment of the sample with a beam of primary ions and the measurement of the backscattered secondary ions emerged from the formed crater; the latter application referred as non destructive due to the fact that the area of the crater is only of a few square microns (see Fig. 19). The measured profile differs from its ideal theoretical (step function) shape and has a sigmoid (S-like) shape.

The rationale of the SIMS-SS dating method is based on the modelling of the diffused water profile, especially along the first 1– 10 μm. The formation of a saturation layer near the exterior of the obsidian tool surface is a crucial and basic parameter in the diffusion age modelling. In fact, since the cutting of an artefact by prehistoric man, water from ambient humidity enters rapidly and presumably perpendicularly to the obsidian's surface. In the first 1–5 μm the diffusion is faster and saturation occurs, while, subsequently a slower diffusion rate continues from this layer towards the interior of the blade (Liritzis et al. 2004; Liritzis 2006).

The age calculation procedure is separated into two major steps. The first step concerns the calculation of a 3rd order fitting polynomial of the SIMS profile. The second stage regards the determination of the saturation layer, i.e. its depth and concentration. The whole computing processing is embedded in stand-alone software created in Matlab (version 7.0.1) software package with a graphical user interface and executable under Windows XP (Laskaris 2010). The software uses the age equation proposed earlier (eq. 1) (Liritzis et al. 2004) in order to calculate the age in years.

$$T = \frac{(C_i - C_s)^2 \left(\frac{1.128}{1 - \frac{0.177 k C_i}{C_s}} \right)^2}{4 D_{s,eff} \left(\left. \frac{dC}{dx} \right|_{x=0} \right)^2} \quad \text{(eq. 1)}$$

In the above mentioned equation, C_i is the concentration of the intrinsic water, C_s the saturation concentration, k is a factor derived from a correlation of the non-dimensional profile with a family of curves by Crank (1975) and $D_{s,eff}$ is the effective diffusion coefficient calculated using the depth of saturation layer (X_s), with errors attached the 1 sigma standard deviation of respective data processing. In fact, $D_{s,eff}$ is empirically derived from a set of well known ages and equation 2 as the effective value of the diffusion coefficient D_s for $C=C_s$, and k is derived from the family of Crank's curves. Based on a calibration curve of well dated samples it is:

$$D_{s,eff} = a*D_s + b/ (10^{22}*D_s) = 8.051e^{-6}*Ds+0.999/(1022 * D_s), \quad \text{(eq. 2)}$$

where $D_s = (1/(dC/dx))*10^{-11}$ assuming a constant flux and taken as unity. The eq. (2) and assumption of unity is a matter of further investigation.

In fact, the combined factors of the faster diffusion rate of water in the obsidian surface, together with the kinetics of the diffusion mechanism for the water molecules and the specific stereochemical structure of obsidian, as well as the external conditions for the diffusion (temperature, relative humidity and pressure), all result in the formation of an approximately constant boundary concentration value in the external surface layers. This is the surface saturated layer (the SS layer) (Liritzis 2006). Assuming that the second diffusion – from the saturation layer to the interior of the obsidian – follows Fick's 2nd law of diffusion, the attributes of the layer (concentration and depth) are very important as initial / boundary conditions. Liritzis and Laskaris (2009, 2010) developed an accurate and safe way to determine the saturation layer. This procedure is based on the combination of the first derivative of a 3rd order polynomial that models the SIMS profile along with repeated linear regressions between the data points of the profile.

The SIMS-SS method includes a wide range of suitability criteria and procedures that reduce the propagation of errors and maximize the efficiency of the method (Liritzis and Laskaris 2009, 2010, 2011; Laskaris 2010). These criteria along with the Taylor's error propagation statistics provide overall accuracy. The most important criteria and procedures are the following: 1) the location of the surface saturation layer, SS, 2) choice of appropriate 3rd order polynomial fit of H+ profile, 3) checking appropriate surface area of interest for the profiling.

The SS layer (and resulted saturation depth X_s and concentration at this depth C_s) is located either by successive linear regressions or via first derivative and this is sensitive

to the 3rd order polynomial fitting of the profile as explained below. The latter is based upon the fitting of H+ profile by a cubic spline polynomial fit of Savitzky-Golay. From this the 1st derivative is calculated, as well as, the inflection point. Then, a simpler 3rd order polynomial is made from the starting point to the inflection point and its 1st derivative is found. It follows repeated fittings from the start to the depth of derivative and so on until a derivative with no peak is found. From all derivative peaks we keep the first and last peaks. The SS layer lies between these two peaks. Then the successive linear regressions for this part of the curve provides variable slope values near zero and the SS is recognized as the segment with the least variation (slopes around zero).

The selection of best fit 3rd order polynomial: some initial non-realistic experimental points are removed as due to the sputtering and initial surface charge, and all points of the tail as well, and apply a 3rd order fit. The R-squared is calculated storing the number of point cut at the tail. This follows repeated fits by increasing the tail points by 1-3 points and noting the R-sqr until all points of the tail are included in the fittings. Then a plot is made between the Rsqr as a function of respective tail points and two shapes are obtained one like a positive parabola and the other as a reversed parabola. For both curves there is an inflection point (peak), this is the highest/lowest Rsqr, respectively for these two shapes and corresponds to the best 3rd order polynomial fit to the data of the diffused region and the tail that represents the non diffused region.

The saturation attributes X_s and C_s are very important parameters in the dating process. Often the obsidian surface in the micro- and nano-scale is not smooth, a fact that influences the diffusion of water and subsequently the SIMS H^+ profile. Despite the data provided by the PLM (Polarized Light Microscopy) and SEM (Scanning Electron Microscopy) on the structure of the obsidian surface, such as the presence of crystallites in the micrometer scale, the AFM (Atomic Force Microscopy) provided more representative images of roughness and structure. The features of these images consist of cracks and voids, which were sometimes within the first 10 μm of the tool surface, that is within the expected hydration depth of last about 10,000 years. Based on these assumptions Liritzis et al. (2008a,b) proposed the use of SEM and AFM for the examination of the surface prior to SIMS H^+ analysis for the selection of a proper spot on it (smooth and free of inclusions) for the SIMS measurement. Occasionally, a SIMS profile may derive from an irregular surface raster (cracks, crystallite, anomalous topography). AFM as well as cation plots (Mg, F, K, Al, Si) may characterize a non disturbed from a disturbed H+ profile and thus permit a further processing of the SIMS profile and age calculation. In fact, a disturbance in F, Mg, Al results to a disturbance in H+, in other cases the F and Al are a line and Mg a standard exponential curve. In all cases a comparison of SIMS-SS ages with independent methods for a wide variety of obsidian samples from all over the World shows a satisfactory linear trend (Liritzis et al. 2008a,b; Liritzis and Laskaris 2009, 2010; Laskaris 2010). The commensurability between the archaeological expected ages and the SIMS-SS ages is quite high and reinforces the validity and wide applicability of the novel dating approach.

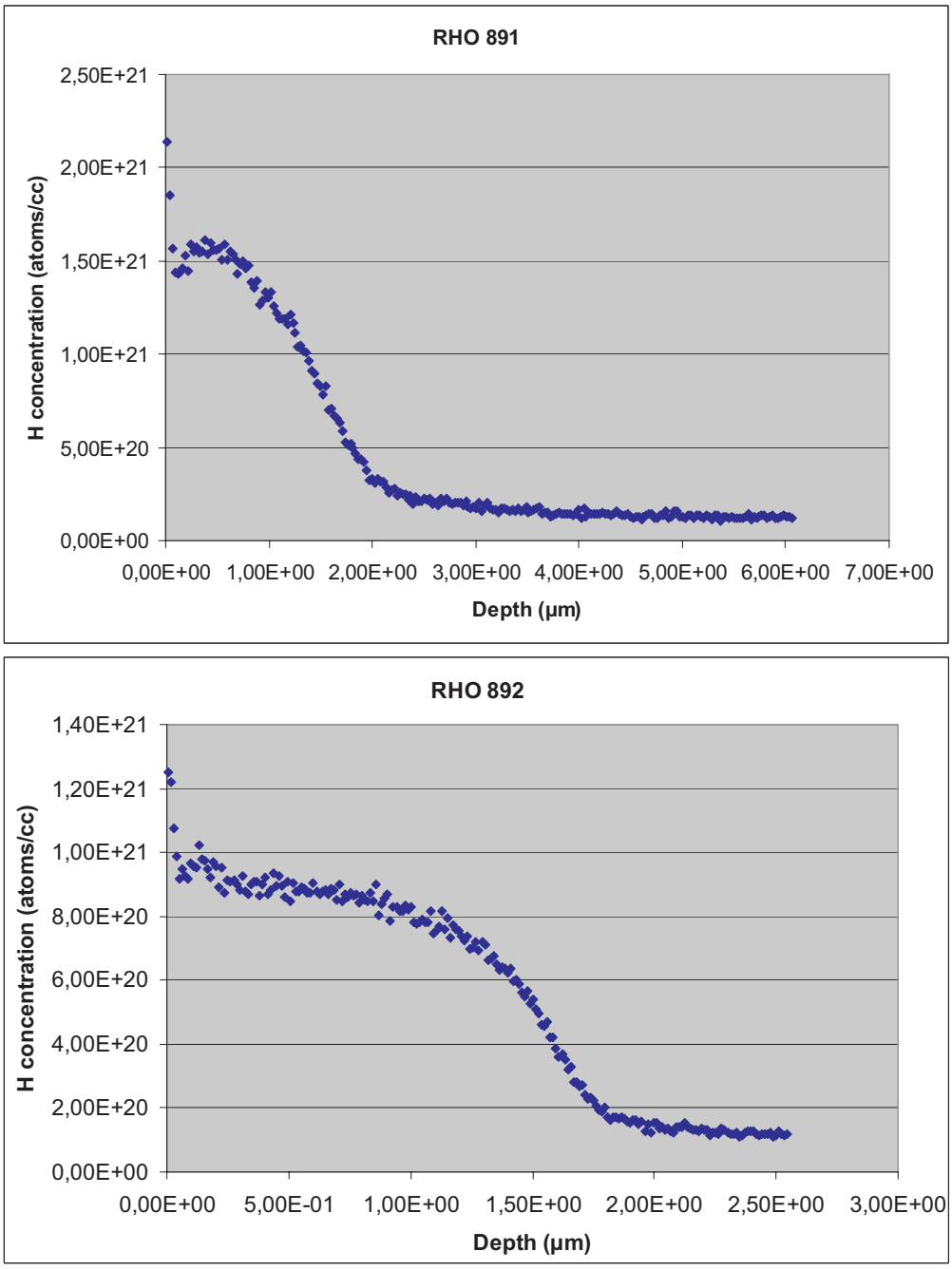

Fig. 21. Hydration profile (H^+) of two obsidian tools, for RHO-891 (a) and RHO-892 (b), of Xs (depth) and Cs (concentration). Ci is the concentration of intrinsic water (Laskaris 2010; Laskaris et al. 2011)

RESULTS

Figure 21 shows the hydration profiles of the two samples from Ikaria Island. For RHO-892, due to an initial disturbance in the exponential drop in the first μm of Mg profile, the H+ profile was not processed. A re-measured SIMS profile on another surface point gave satisfactory results (LASKARIS 2010, p. 139). The profiles of hydrogen and other cations for both analysed Ikarian samples are given in Figure 22.

The hydration profile of the H^+ (as well as other useful cations) data are experimentally measured with SIMS (quadrupole or dynamic). All procedures and criteria have been tested have been applied for both samples.

Overall, the steps for the age calculation were: 1) obtaining H+ profile by SIMS in atoms/cc and conversion to grmol/cc, 2) determination of best 3rd order polynomial for this profile, 3) testing the parabola check, 4) testing the diffusion trends of cations, 5) defining the SS layer and obtain Xs and Cs, 6) determination of k-coefficient and therefore e^k, from non-dimensional plots and compared with Crank's similar plots, 7) calculation of D_s and $D_{s,eff,}$ 8) calculation of dC/dx for x=0, and 9) calculation of age, e.g., from web page of SIMS-SS dating method at the laboratory of Archaeometry, Rhodes http://www.rhodes.aegean.gr/tms/sims-ss/ (constructed by N. Laskaris as part of his Ph.D thesis). The two ages average to10,600± 1,830 years BP pointing to the last glacial and the onset of Holocene, belonging within the Mesolithic period. Chemical analysis points to Melos sources.

DISCUSSION AND CONCLUSIONS

The dates of Table 3 provide the dating of the two obsidian artefacts (ca. 11,000 BP). It has been suggested that the exploitation of the obsidian sources on the island of Melos could have been an even earlier phenomenon in relation to what was known so far from Franchthi cave. The rest of the dates are in accordance with the evidence from Franchthi cave, where obsidian is present from the 11th millennium BP levels, while its presence continues during the Lower Mesolithic (2nd half of the 10th millennium BP), reaching its peak in the Upper Mesolithic. The SIMS-SS dates (Table 3) from the site of Kerame in Ikaria (see details in this volume) and other sites in the Aegean so far, manifest that during the Mesolithic a rather well established system of obsidian exploitation and circulation existed, a phenomenon that has its routes even earlier, as the SIMS-SS dates from sites such as the Schisto cave in Attica indicate. It is evident that the novel SIMS-SS method has important applications in the relevant work and can aid researchers to address specific questions to their excavation data.

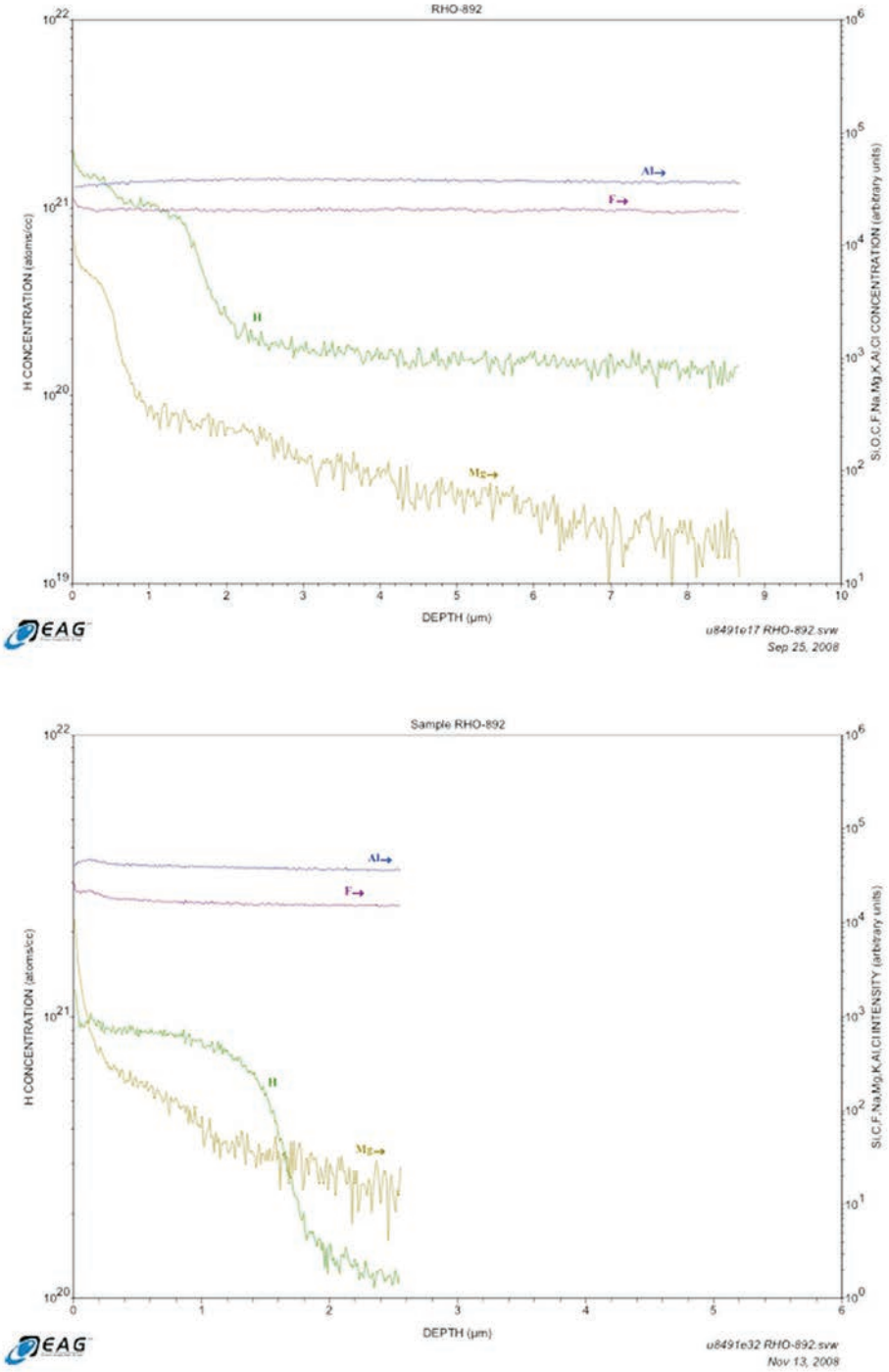

Fig. 22. a (upper) – Rho-892 due to Mg disturbance at depth < 1 μm the hydrogen profile is not utilised; b (below) – re-measured RHO-892 on another surface area. Hydrogen profile is utilised because other cations vary smoothly

ACKNOWLEDGEMENTS

I would like to thank Prof. A. Sampson for providing the samples and useful discussions. SIMS measurements were made at Virginia Tech USA Dynamic-SIMS and Evans Analytical Group USA.

OPTICALLY STIMULATED LUMINESCENCE DATING OF ARTEFACT-BEARING ARCHAEOLOGICAL LAYERS AT "KERAME", IKARIA, EASTERN AEGEAN: FIELD OBSERVATIONS, LABORATORY PROCEDURES, AND LIMITATIONS

Constantin Athanassas, Yannis Bassiakos

GEOLOGICAL AND TOPOGRAPHIC SETTING

The excavation site is located ~ 5 km southeast of Agios Kirikos and 200 m south of the road to the airport. The mean elevation of the study site is 14 m. The excavation is situated on a terrace that is relatively smooth and degrades by 2-5% seawards, terminating at a steep cliff some 3-15 m in the backshore. The terrace is composed of Quaternary breccia-conglomerates which are cemented with argillaceous-siliceous sediments. The deposits are slightly tilted towards the sea due to recent tectonic activity. The Holocene soil formation, which accommodates the archaeological artefacts, comprises a thin veneer (30-70 cm-thick) and is made up of moderately-cohesive porous argillaceous-siliceous materials. The area is covered with low vegetation (bushes) of the xerophytic type and extends beyond the excavated site in broader area of the terrace. However, vegetation was denser in recent past and specifically a few decades ago. Local vegetation was downgraded by massive and repetitive fires in the area in 1949 and 1994 (Them. Katsaros, pers. comm.)

Other terrestrial deposits that extend in the north of the local motorway, and within the vicinity of the excavated site, exhibit somewhat higher inclinations (5-10% higher than previous). These are consisted of mainly moderately-cohesive lateral debris cones, loose pebbles, conglomerate/breccia deposits and other slope deposits, originating from the weathering/erosion of carbonate and argilo-siliceous hard rocks outcropping in nearby hills and highlands.

Small waterways that traverse the slope deposits favour the transport of loose material (cobles, pebbles, etc.) contributing to the development of the Holocene soil veneer, in which the excavation trenches have been dug, but primarily they terminate through deep gaps (due to the aforesaid rock detachment) at the coastal zone and finally into the sea.

The lithic assemblage from the archaeological excavation is mostly composed of flints/cherts (of whitish-creamy-brown or light-grey colour) and obsidians. These types of rocks do not exist in the Holocene layers on the site and were mostly extralocal.

For the needs of the excavation, six trenches with orthogonal cross-sections have been dug, reaching at depths ranging between 50-70 cm each, arrayed along the terrace and at a small distance from the edge of the cliff. The sequence of the trenches is characterized by the following nomenclature and they arrayed in a WSW-ENE as follows: B, D, E, C, G and J. In situ measurements of natural environmental radioactivity for the purposes of estimation of the local dose rate (D_R) were conducted in the trenches as well as in the broader area, using a calibrated portable scintillometer "Saphymo-Steel" type "SPP-2" with a detector crystal of NaJ(Tl), having a volume of 50 cm^3 and a radioactive source consisted of Cs-137. Measurements were made considering a 2π-geometry, and the values yielded by the sedimentary terrestrial layers were on the order of 39-51 counts/sec, as it is expected for argillaceous-siliceous/calcite holocenic soil mantles. A total of five samples were collected from trenches Δ, K and Z, all coming from the vertical sides of the trenches and from depths indicated in Table 4. From trenches D and K pairs of samples were collected so as to associate the stratigraphic order with the resulting OSL dates later on.

Table 4

Depths of sampling at Kerame site

Trench	Nomenclature	Depth from surface (cm)
D	D1	23
D	D2	33
J	J1	35
J	J2	26
G	G1	24

In order to collect samples in light-tight conditions, solid steel tubes with sharp edges were employed, 7 cm in diameter. Tubes were hammered vertically against the scarps and parallel to the layers where the lithic artefacts were retrieved from. Steel tubes were penetrated horizontally to a depth of 15-18 cm by hammering the rear end of the tube so as to collect rounded core of sediment, 13-16 cm in length, without exposing the sediment to daylight. Soon after the extraction of the sediment core, sediment-containing tubes were wrapped in situ with opaque film in order to carry on their process in the laboratory und under subdued orange light conditions.

A brief description of OSL dating

Radioactivity is omnipresent in the environment even at very small amounts. Radioactivity in the environment originates from radioactive elements that are found in surrounding rocks, and mainly are uranium (U), thorium (Th) and potassium (K). An additional component of ionizing radiation falls on Earth's surface from the sky and it is called cosmic rays. Natural minerals such as quartz and feldspar are able of 'memorizing' the accumulate exposure to nuclear radiation. More specifically, minerals of this type are able to accumulate within their crystal an amount of the energy released by the surrounding radiation through time. If the crystal is stimulated by light the stored energy can be released in the form of light and this light is termed Optically Stimulated Luminescence (OSL). When light is removed from the sample, luminescence will start building up anew. The susceptibility of stored energy to sunlight in natural minerals is therefore the property exploited in OSL dating. At some later time, if the sample is stimulated by artificial light in the laboratory the intensity of luminescence signal will be dependant on the amount of absorbed nuclear radiation. If this amount of absorbed dose is divided with the rate at which the dose was absorbed it will lead to the time that has elapsed since the sample was last illuminated. This is called the OSL age.

Therefore, the estimation of an OSL age is a matter of calculation of two parameters (equation 1): the amount of absorbed dose which is called the Palaeodose and it is measured in Grays in the S.I.

$$OSL\ age\ (ka) = \frac{Paleodose\ (Gy)}{Dose\ rate\ (Gy/ka)} \qquad \text{(eq. 1)}$$

and the rate at which the dose was absorbed and it is called the dose rate and its S.I. unit is Grays/thousands of years. In OSL dating, several methods for palaeodose estimation have been introduced. However, among them, the Single Aliquot Regenerated (SAR) dose protocol is the most appropriate methodology introduced by Murray and Wintle (2000). The basic advantage of SAR over other protocols is that it deals with changes in 'sensitivity' of quartz. Changes in sensitivity are unwanted alterations in luminescence capacity due to laboratory treatments in the course of an SAR procedure. Instead of minimizing changes in sensitivity, SAR corrects for such changes. This can be achieved by using the OSL response to a constant test dose, applied after each regeneration dose, to monitor any sensitivity changes. This constant dose is called the test dose. Particularly, the SAR procedure involves splitting the sample into smaller 'sub-samples' known as 'aliquots' and replicate luminescence measurements are made on each aliquot, typically obtaining between 10 and 20 independent estimates of the palaeodose for the sample.

After the measurement of the natural OSL signal the luminescence response is regenerated by applying progressively higher artificial doses. The growth of the test dose-corrected OSL response is called the growth curve. Projection of the natural's

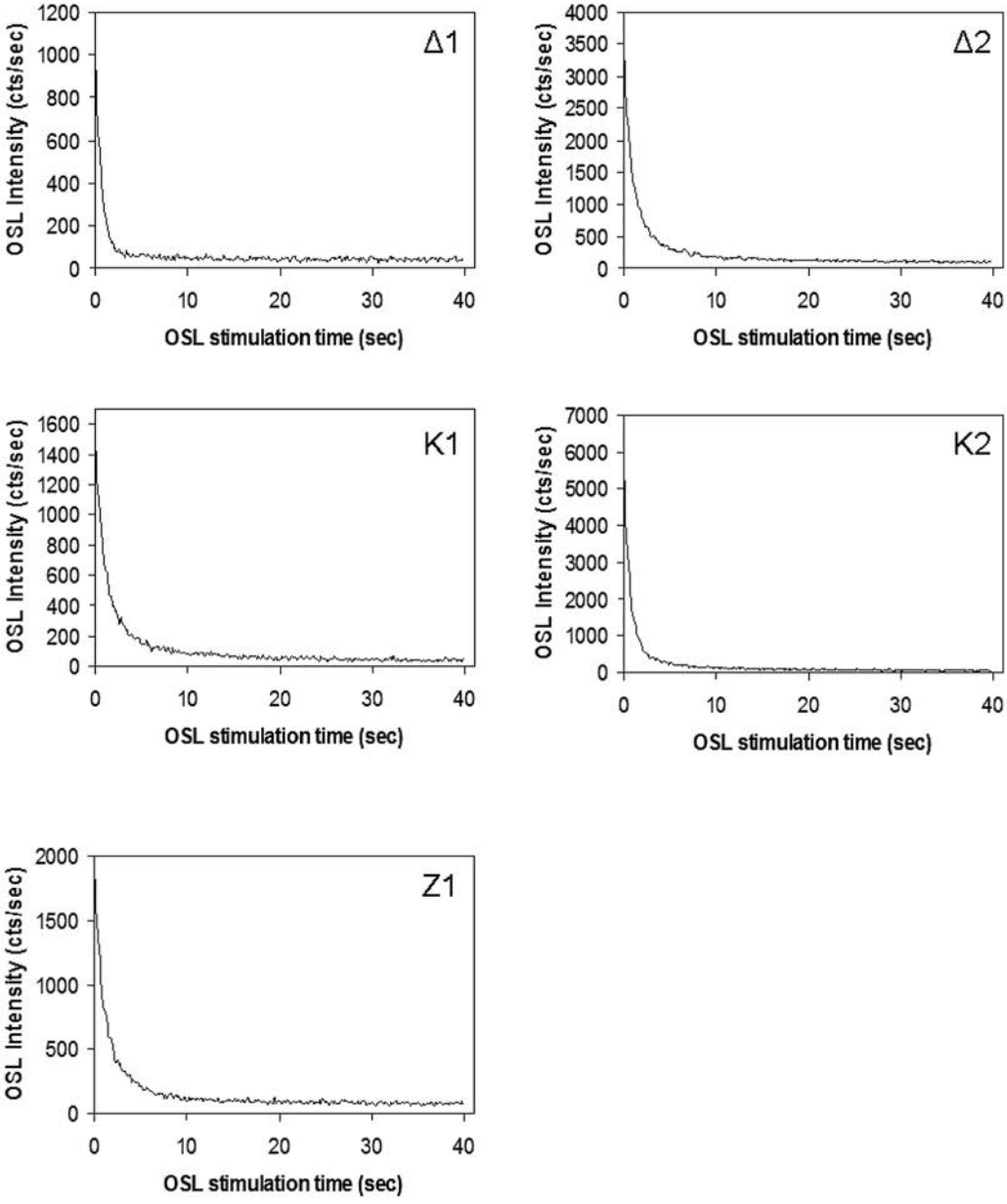

Fig. 23. Typical OSL signals (decay curves) recorded in this study

signal intensity onto the growth curve results in the inquired palaeodose. Replicate measurements of SAR on aliquots of the same sample will result in a number of individual palaeodose estimates.

Performed laboratory measurements

Samples D1, D2, J1, J2, and G1, all coming from the reddish soil horizons of the Kerame excavation, were submitted for standard chemical treatment. Quartz was the target mineral to be dated. Chemical treatments involved use of HCl (10% concentration), H_2O_2 (20% concentration), HF (40% concentration). These treatments aimed to remove/dissolve any calcite content, organic material, and eliminate the feldspar content as well as to etch quartz grains. Intermediate mechanical treatments involved dry sieving in order to isolate quartz grains in the grain-size fraction of 90-125 μm. The entire preparation was carried out under subdued orange light conditions emitted from low-pressure sodium lamps (Spooner et al. 2000). The quantity of the purified quartz was divided in sub-samples (aliquots) and mounted on stainless disks (1 cm in diameter). OSL procedures involved the measurement of 10 disks per sample. Luminescence measurements were carried out using a RISØ-TL/OSL reader.

Measurements included calculation of the palaeodose (D_e) and estimation the dose rate (D_R). The equivalent dose was estimated by running the Single-Aliquot Regenerated Dose protocol (Murray and Wintle 2000; Wintle and Murray 2006) on multiple aliquots from each sample, generating in this way a number of individual paleodoses per sample. Specifically, measurement of natural OSL signal was succeeded by the measurement of the OSL response of each sample to a series of laboratory irradiations (5, 10, 15, 0 Gy), all normalized by the OSL response to a constant laboratory dose which is known as the "test dose" (Murray and Wintle 2000). The size of the test dose was 2 Gy. Growth curves were constructed by plotting the normalised luminescence signals against the regenerated doses. Typical natural OSL signals of the samples from Ikaria acquired during the OSL measurements and the generated growth curves are given in Figures 23 and 24, respectively.

Moreover, the SAR methodology necessitated the repetition of one of the regenerated doses at the end of the SAR sequence (recycling point). This served to control the amount of "sensitivity change" by the completion of the measurement procedure. Only aliquots yielding over 90% similar OSL signals at the recycling point (recycling ratio) were further considered for chronological implications.

The mean palaeodose for each sample was estimated by averaging the apparent palaeodoses. Table 5 provides mean palaeodoses and their standard errors for each sample.

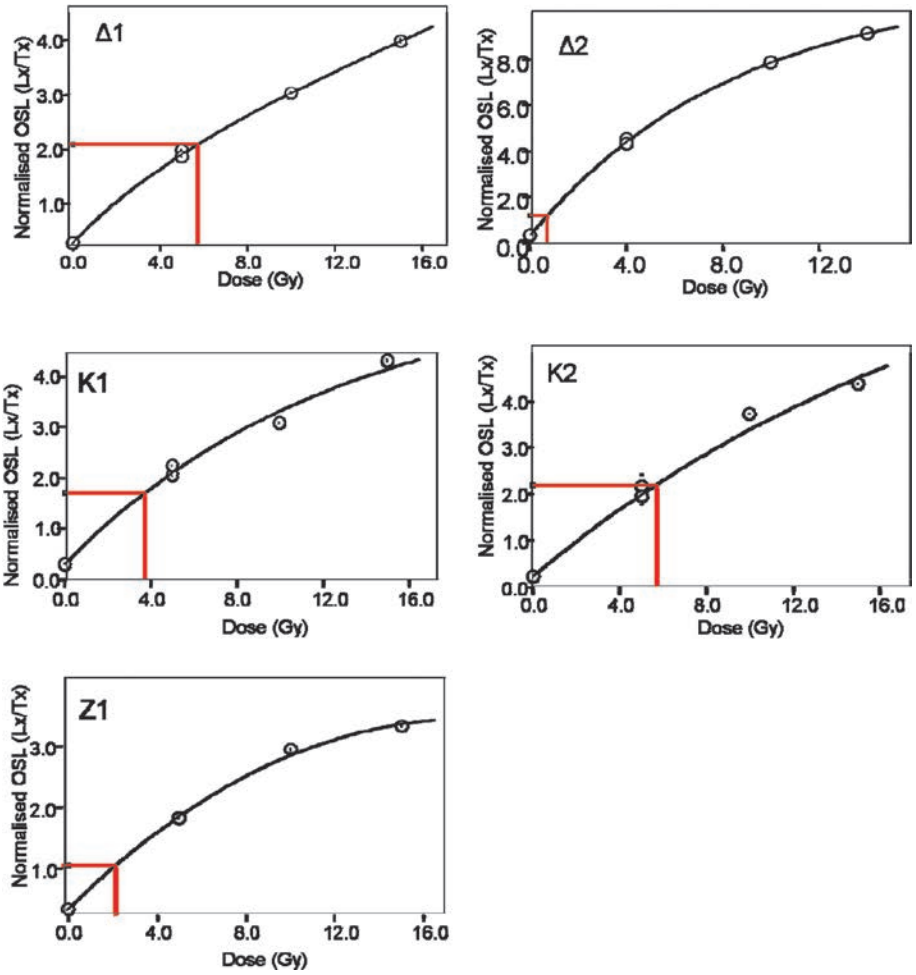

Fig. 24. Typical OSL growth curves generated in this study

Table 5

Mean palaeodoses and their standard errors

Sample	Mean palaeodose	Standard error
D1	6.7	0.6
D2	7.7	0.7
J1	3.7	0.1
J2	6.0	0.6
G1	2.1	0.2

On the subject of dose rate estimation, that involved measurement of the sample's radioelement content in U, Th and K. Concentrations of U and Th (in ppm) were estimated by means of alpha-particle spectroscopy (Michael and Zacharias 2000), while the K content (in % weight) was measured by means of scanning electron microscopy (SEM) microanalysis (EDX).

Radioelement concentrations were converted to dose rates (α-, β- and γ- dose rates) per sample by taking into account conversion factors provided by Adamiec and Aitken (1998). The total dose rate for each sample was estimated at 1.9±0.2 Gy/ka. This value has been corrected for moisture content, grain-size attenuation and cosmic ray contribution. OSL-ages were calculated based on the simplified formula shown in Equation 1. Final OSL ages for Kerame are given in Table 6.

DISCUSSION ON THE OSL DATING RESULTS AND CONCLUSIONS

Standard laboratory procedures and measurements offer the ability to check the reproducibility of the measurements as a criterion for selecting or discarding a paleodose, according to the SAR methodology proposed by Murray and Wintle (2000). These procedures ensure the avoidance of laboratory mistakes in the OSL dating of sedimentary deposits. However, the chronological data are not consistent with the archaeologically expected chronology.

Table 6

OSL ages obtained for Kerame site

P = palaeodose, DR = dose rate, ka = thousand years

Sample	P (Gy)	DR (Gy/ka)	Age (ka)
D1	6.7±0.6	1.9±0.2	3.53±0.30
D2	7.7±0.7	1.9±0.2	4.05±0.36
J1	3.7±0.1	1.9±0.2	1.94±0.02
J2	6.0±0.6	1.9±0.2	3.16±0.32
G1	2.1±0.2	1.9±0.2	1.01±0.11

Specifically striking is the inconsistency between OSL results and stratigraphic order for the pair of samples J1 and J2 (both coming from trench 'K') as it is seen from the data shown in Tables 4 and 6. Sample J1 comes from a depth of 35 cm and it underlies sample J2, which lays at 26 cm. Under normal conditions the overlaying sample J2 should yield a younger age than J1. The estimated age for the underlying sample J1 is centered on 1.94 ka (1,940 years ago) whereas the overlaying sample J2 has an age of 3.16 ka (3,940 years ago). These values are not in agreement with the stratigraphic order of the measured samples. Field observations do not suggest any type

of stratigraphic reversal. Moreover, excavational data suggest a Mesolithic age for the lithic artefacts (A. Sampson, pers. comm.). On the contrary, all ages produced here seem severely underestimated in respect to the expected chronology of the site. The observed chronological and stratigraphic discrepancies doubt the accuracy of the current OSL chronology and hence ages of Table 6 should be dealt with extreme cautiousness.

Not only OSL dating but also C-14 dating attempts resulted in similarly underestimated ages for the excavated site (A. Sampson, pers. comm.). Consequently, the failure of both, otherwise well-established, dating techniques to provide safe age estimates could be attributed to intense environmental/geochemical instabilities. Indeed, the small depths of the sampled layers render them prone to bioturbation (either natural or human-induced). It is thus not impossible that the lithic-bearing strata might have experienced several exposures a long time after their formation or sediment mixing (Lomax et al. 2007) due to vegetation changes, herding, cultivation or fires. Regarding the latter, the extensive fires that swept the soil surface in recent times could also have an impact on the geochemical composition of the subsurface. The debris from fires that were developed on soil surfaces is rich ash and charcoal. Among other components, ash contains a high percentage of potassium-rich salts. These can be readily leached in the underlying soil layers, altering the geochemical concentration and consequently the dose rate towards underestimated OSL ages. Moreover, recent enrichment in charred material could also influence the C-14 content leading again to underestimated radiocarbon dates. The impact of these unwanted phenomena would be important in the uppermost layers of the soil, where, by coincidence, studied samples come from. Based on the above it can be concluded that due to the relatively small depth of the lithic-bearing strata and the recent local environmental changes (both anthropogenic and natural), neither OSL nor C-14 dating methodologies can lead to safe age estimates for the Mesolithic sites of Kerame.

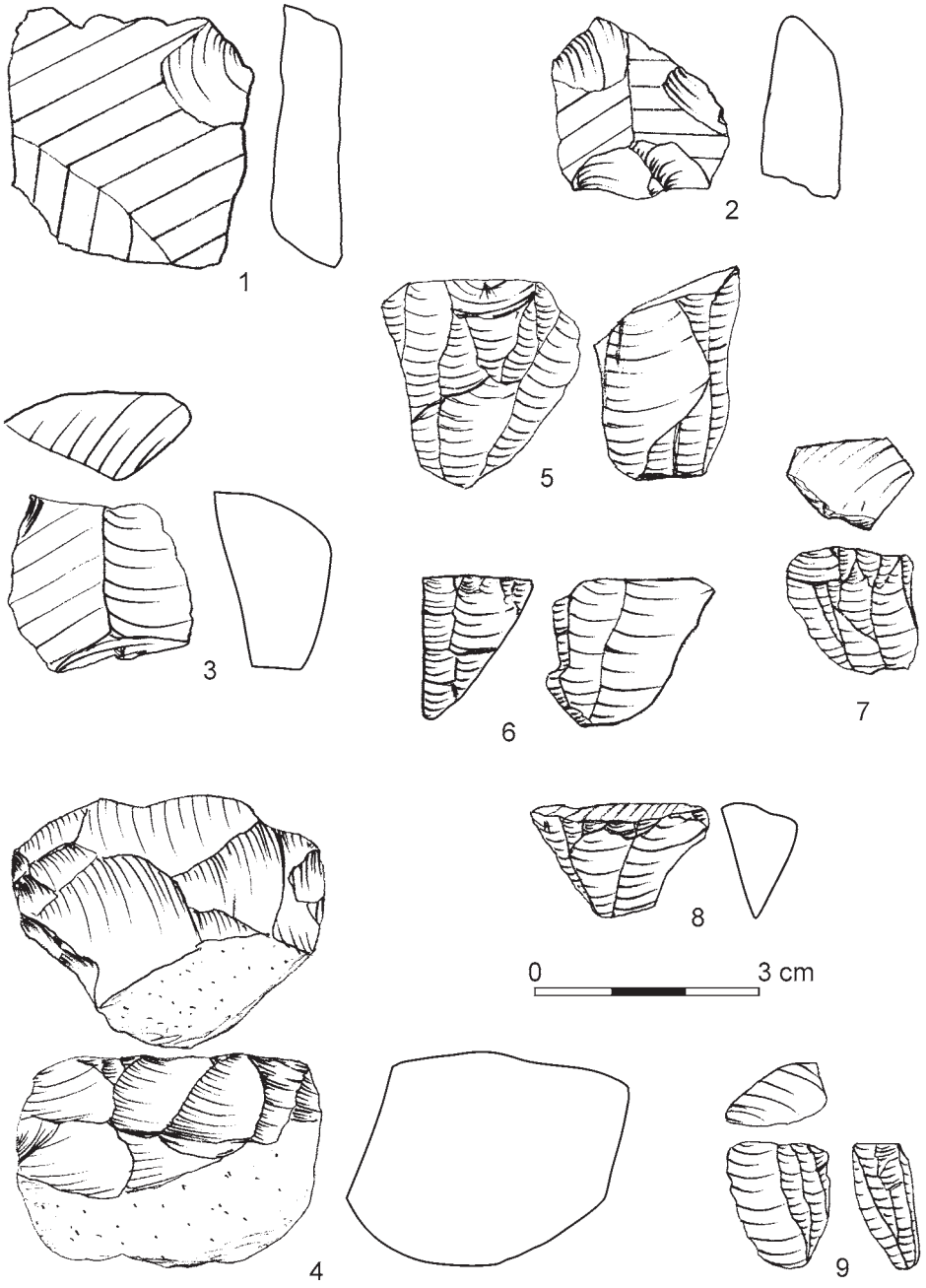

Pl. 1. Kerame 1: 1-9 – cores

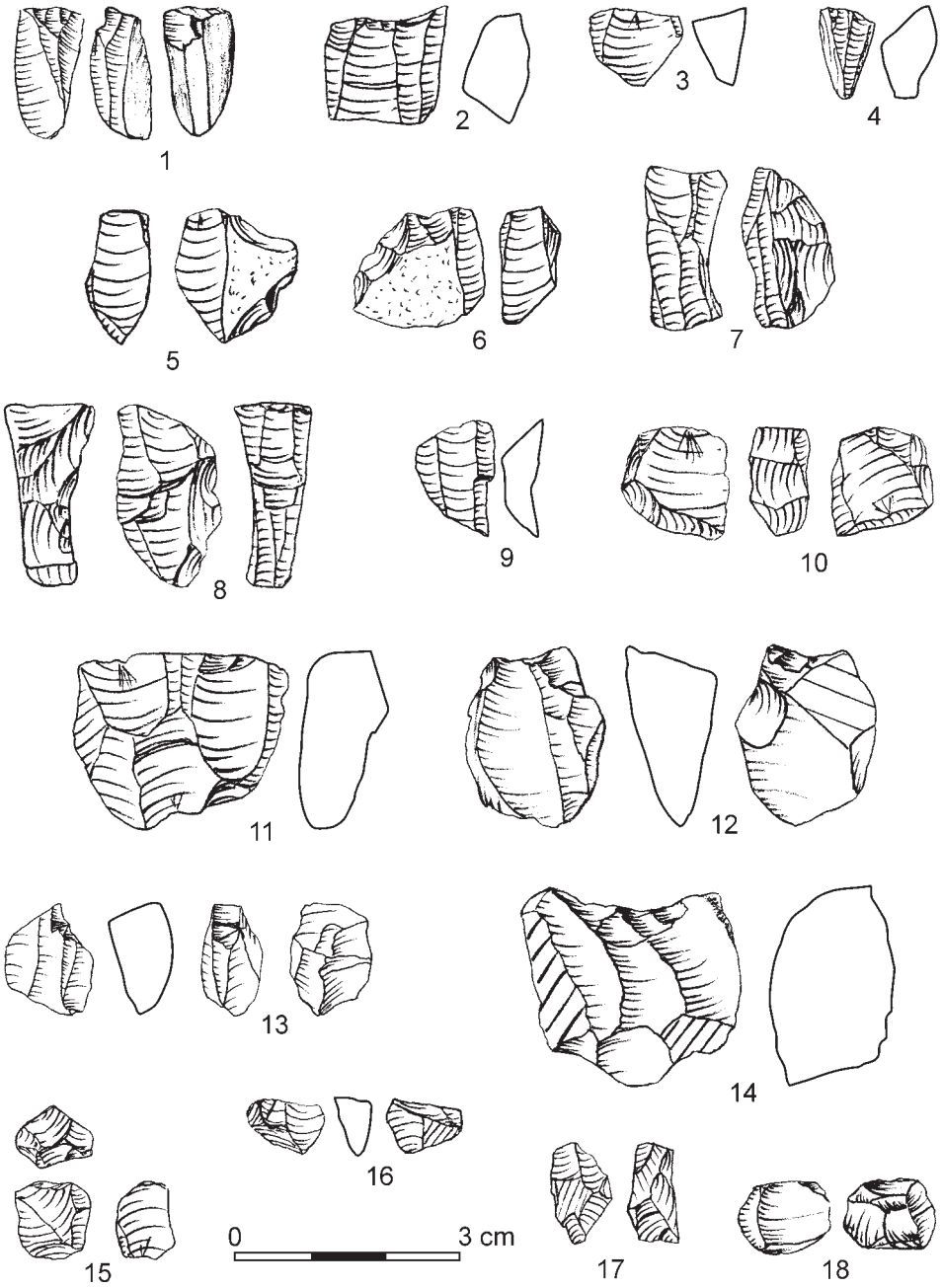

Pl. 2. Kerame 1: 1-18 – cores

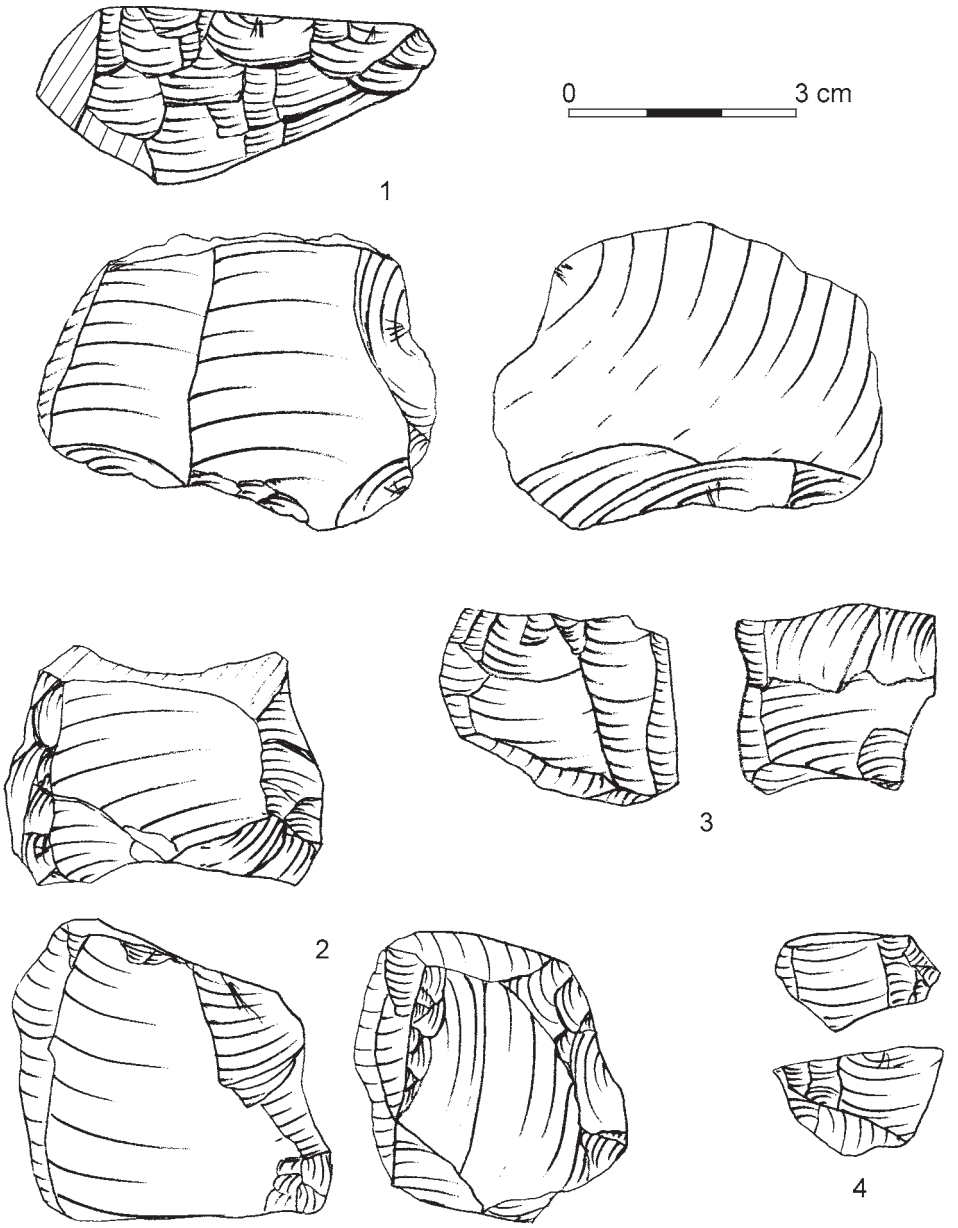

Pl. 3. Kerame 1: 1-4 – cores

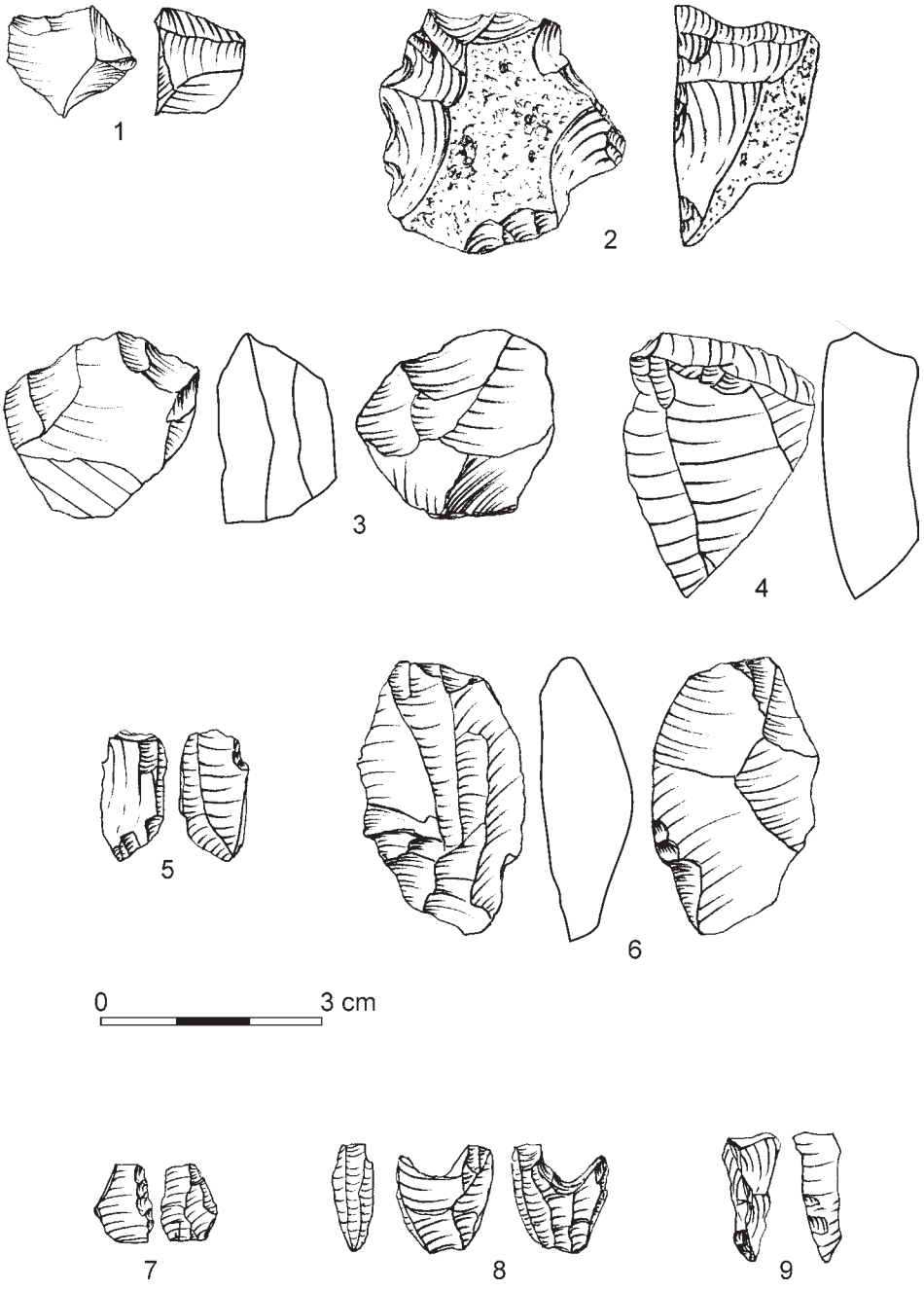

Pl. 4. Kerame 1: 1-4 – cores ; 5-8 – splintered pieces ; 9 – crested blade

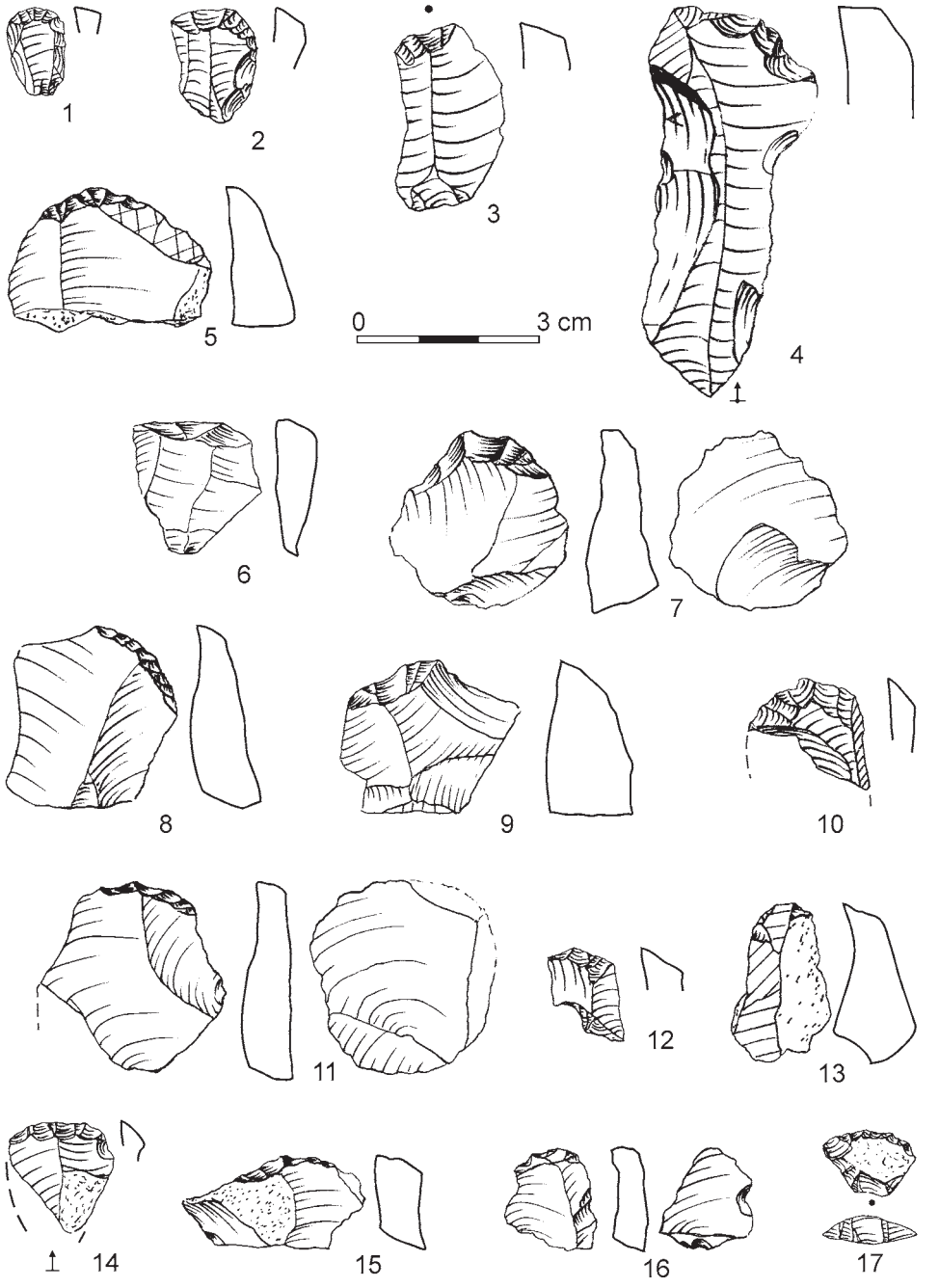

Pl. 5. Kerame 1: 1-17 – end-scrapers

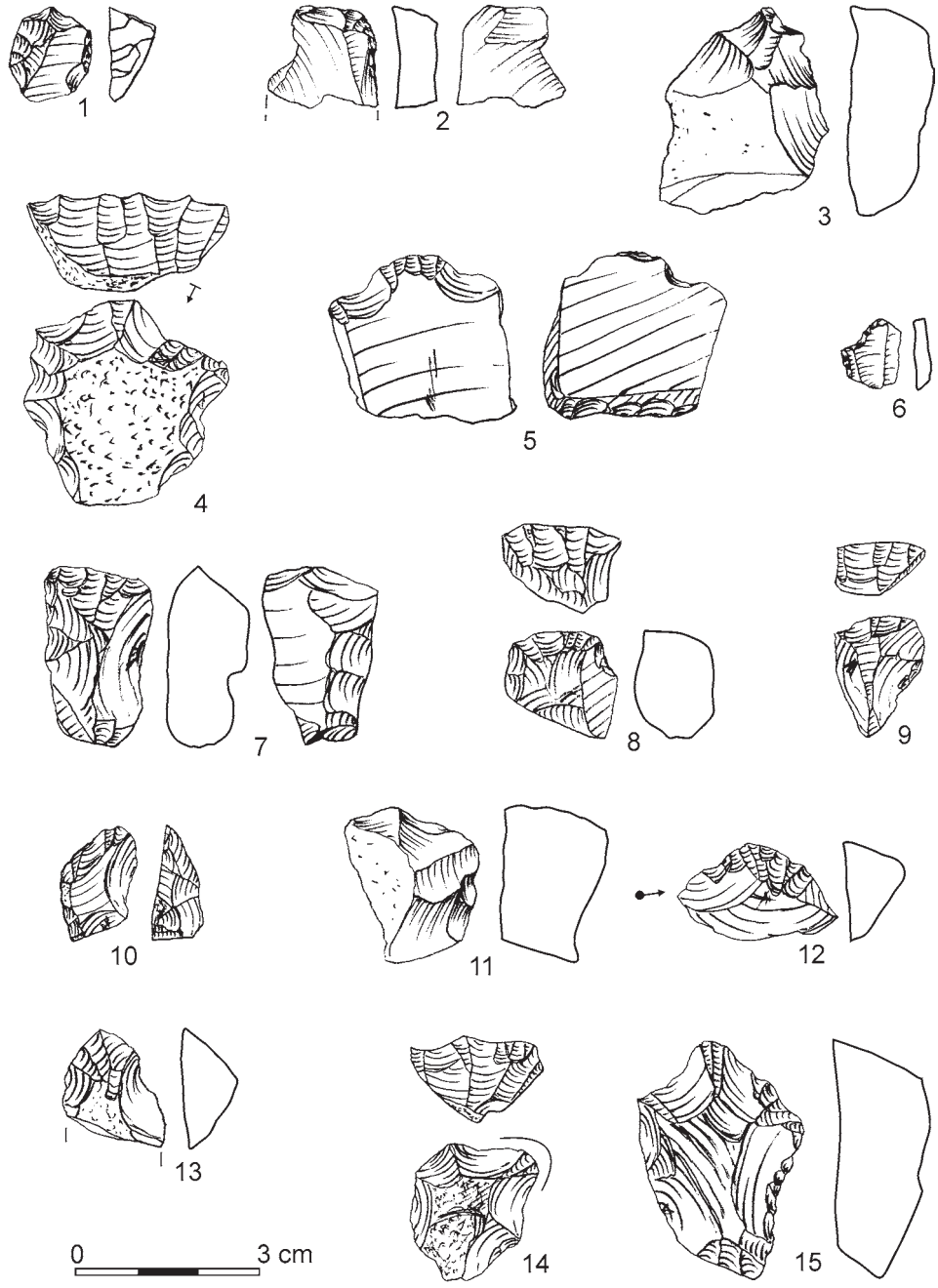

Pl. 6. Kerame 1: 1-15 – end-scrapers

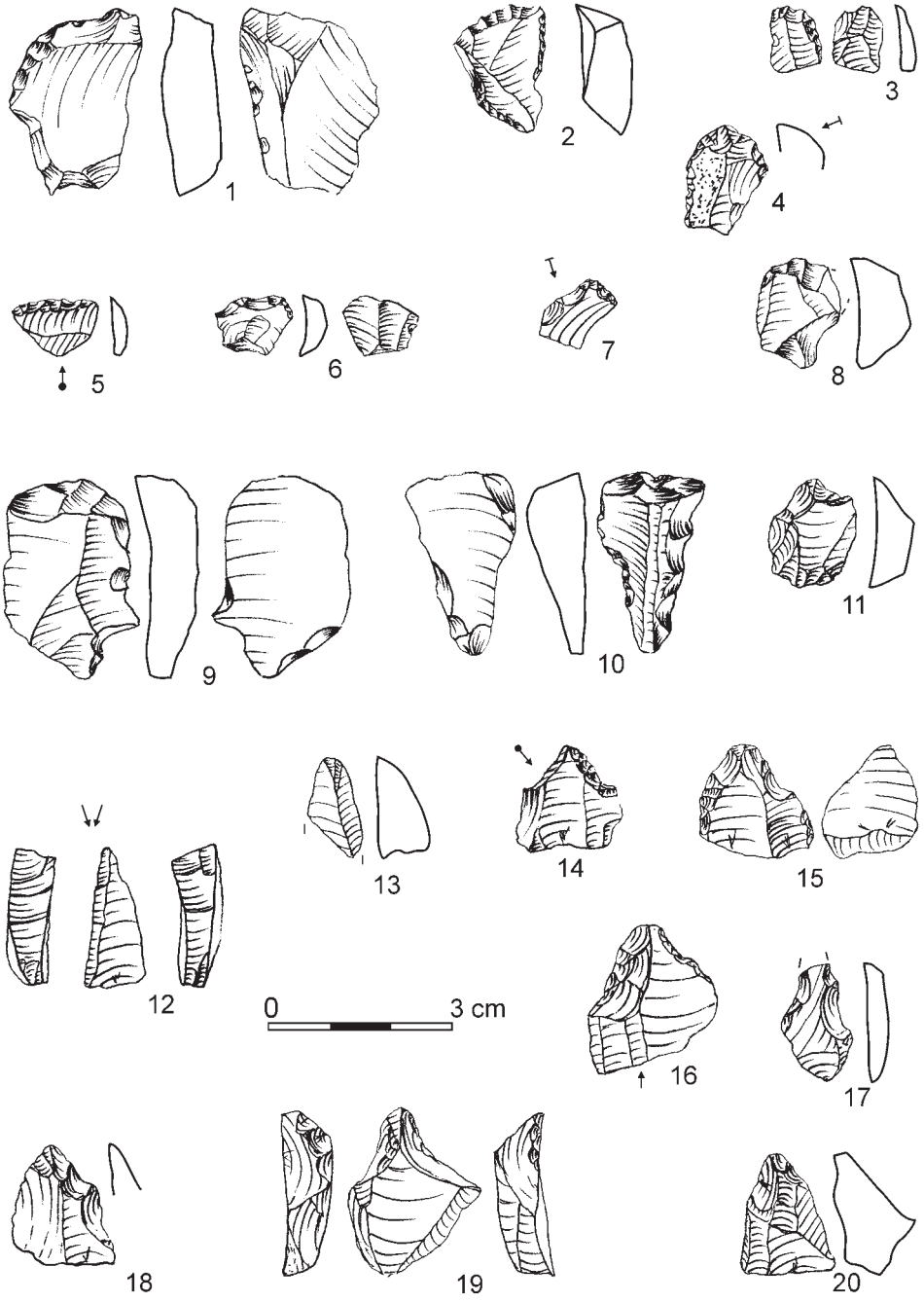

Pl. 7. Kerame 1: 1-11 – end-scrapers, 12,13 – burins, 14-20 – becs/perforators

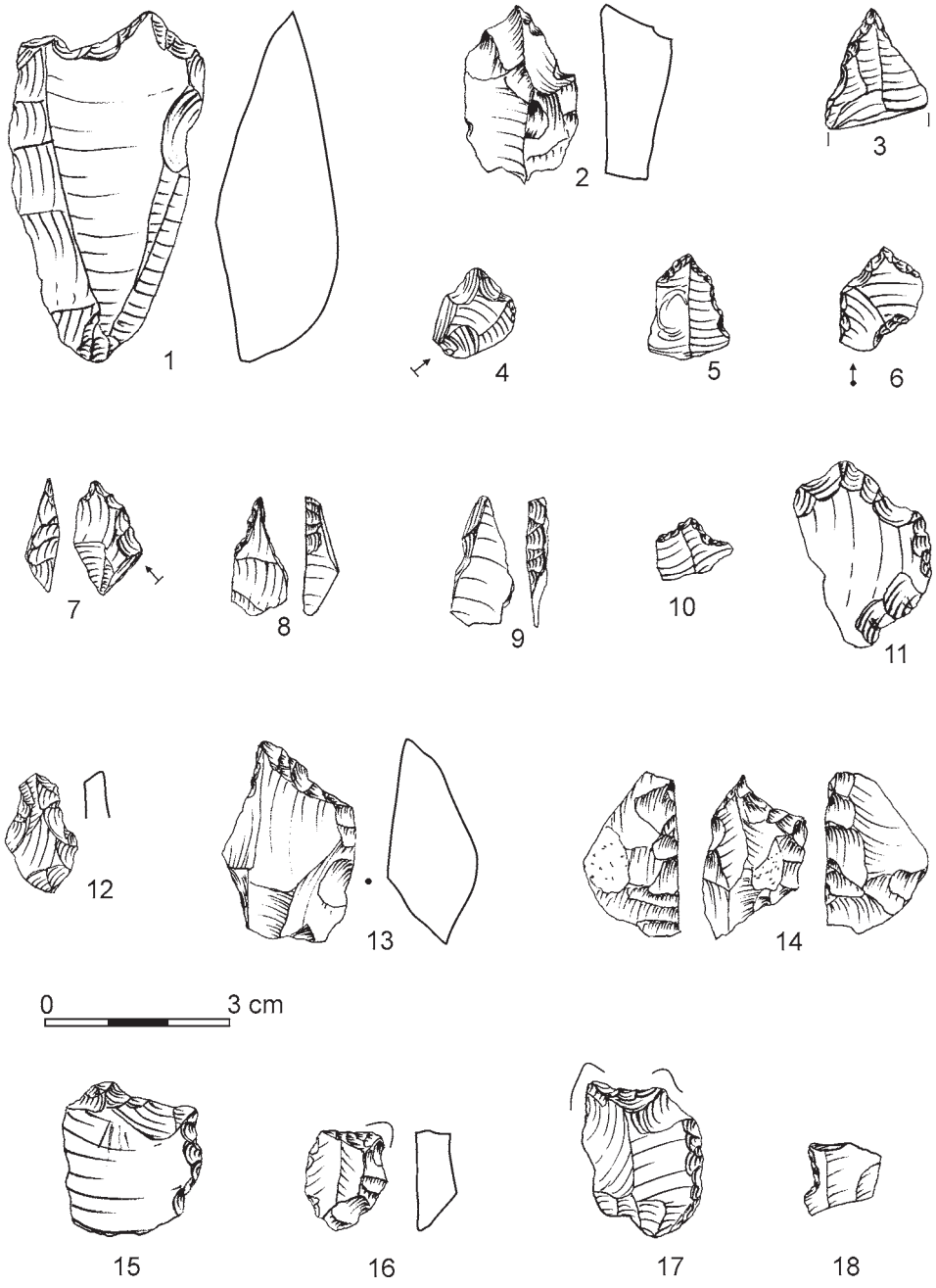

Pl. 8. Kerame 1: 1-18 – perforators/becs

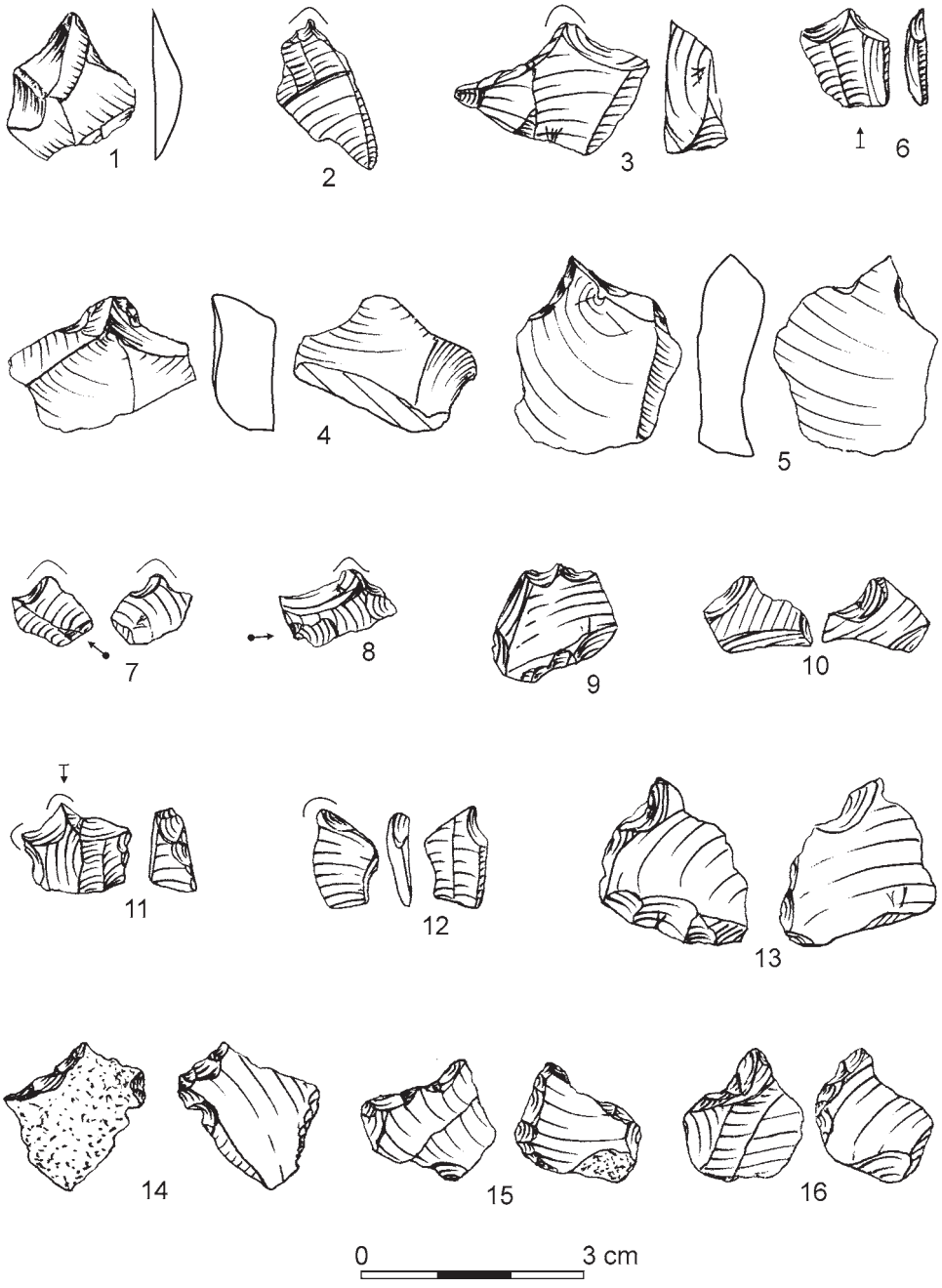

Pl. 9. Kerame 1: 1-16 – perforators/becs

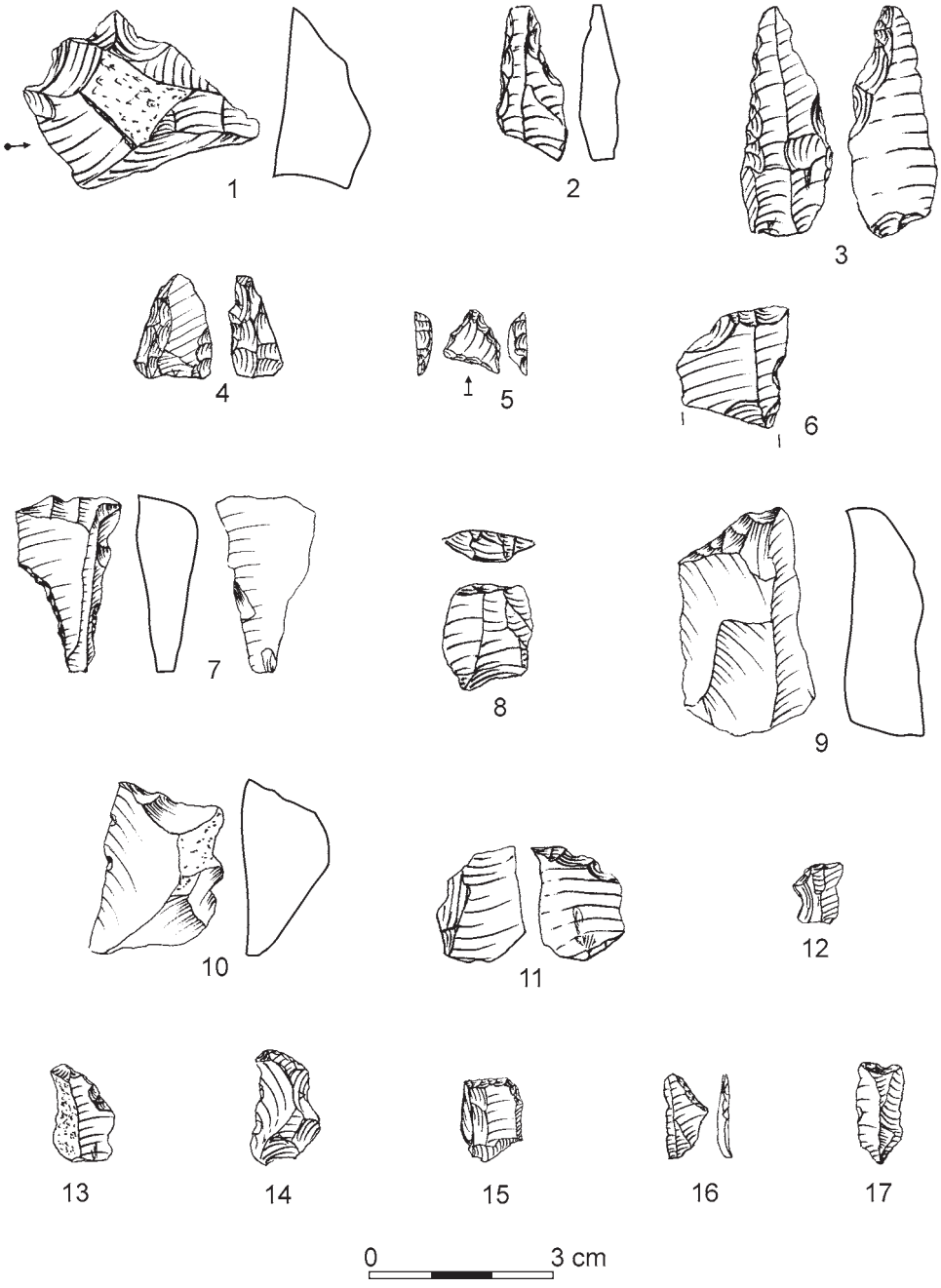

Pl. 10. Kerame 1: 1-5 – perforators/becs, 6-17 – retouched truncations

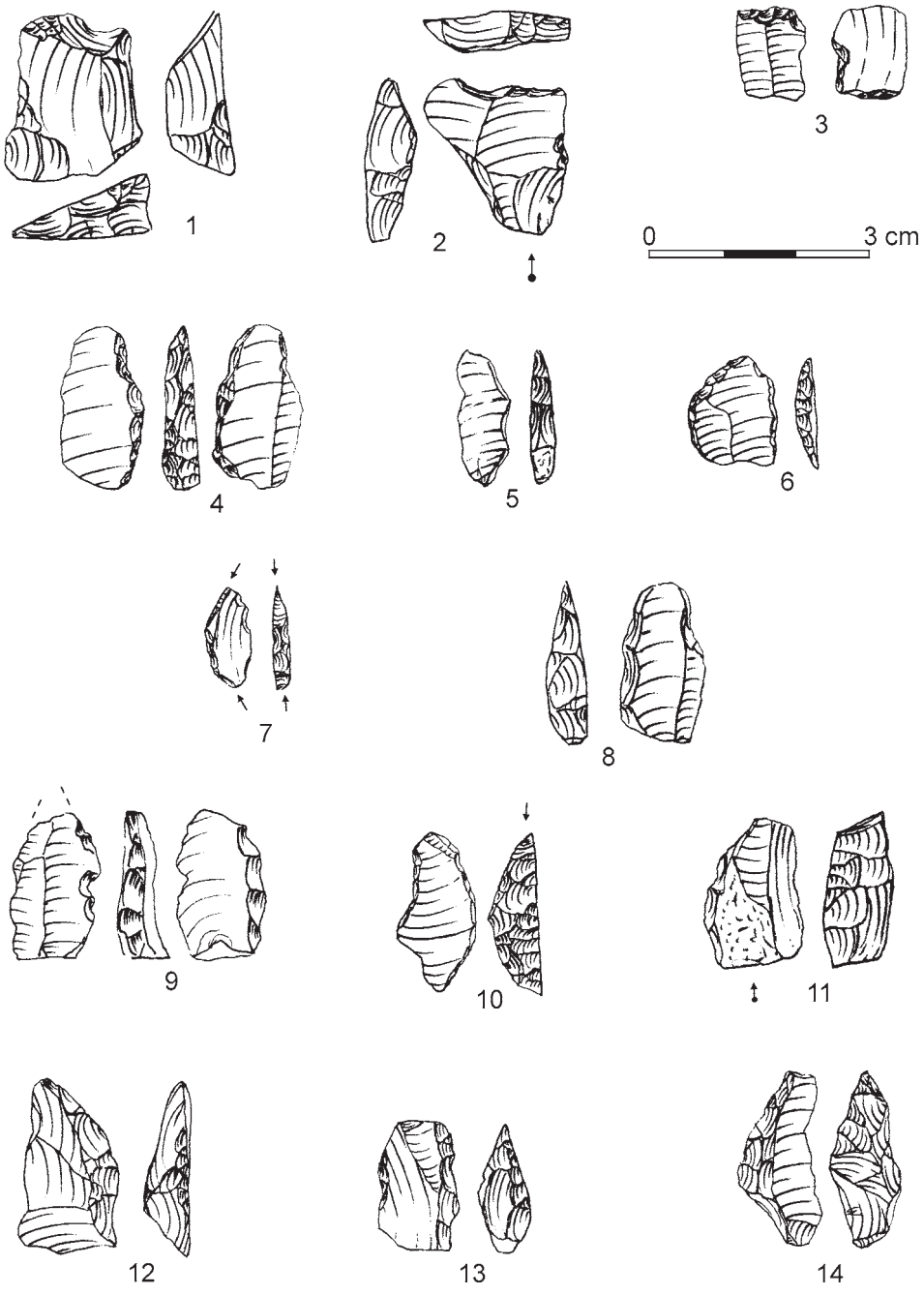

Pl. 11. Kerame 1: 1-3 – double truncations (atypical trapezes), 4-14 – backed pieces.

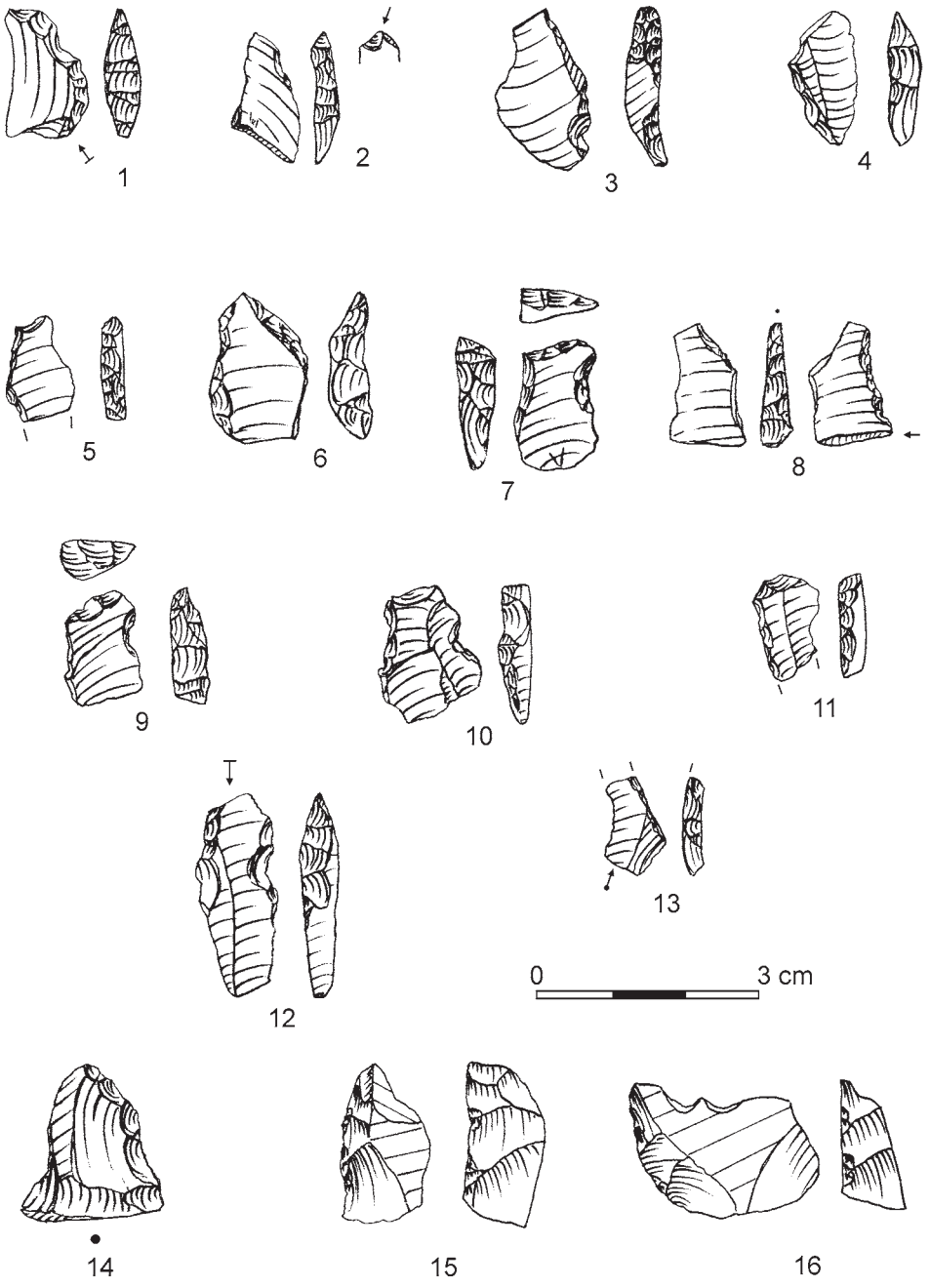

Pl. 12. Kerame 1: 1-13 – backed pieces, 14-16 – retouched flakes

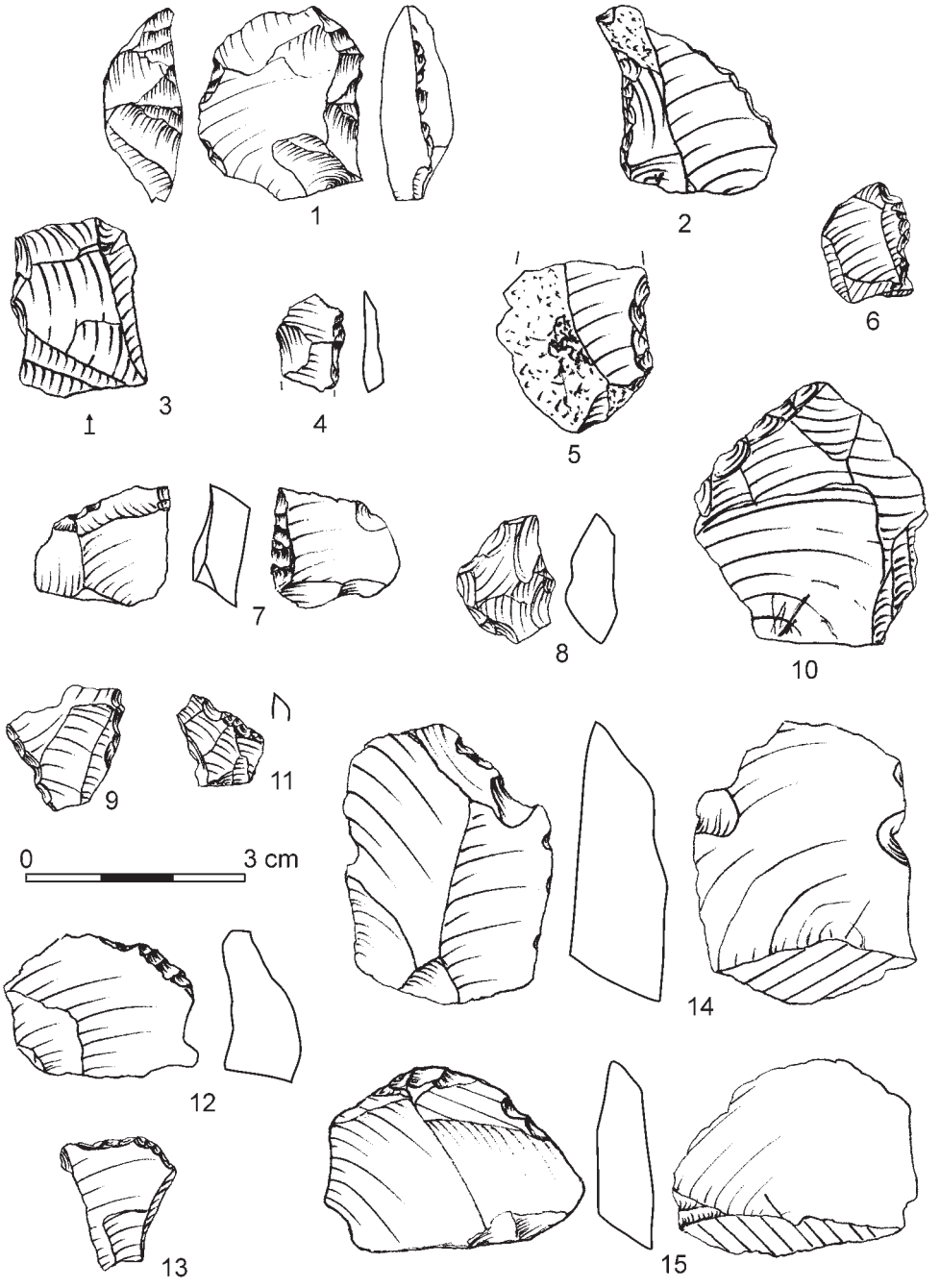

Pl. 13. Kerame 1: 1-15 – retouched flakes

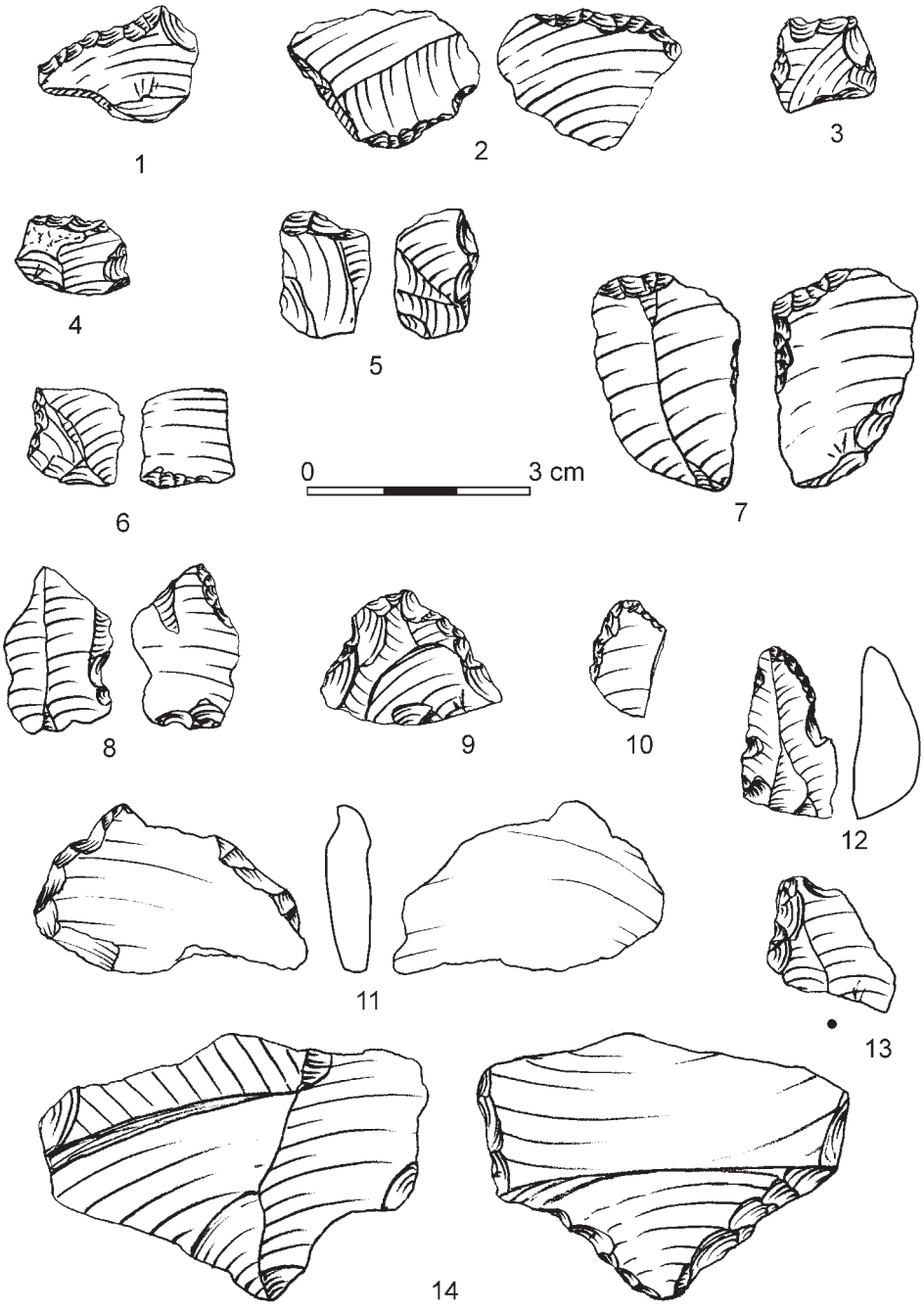

Pl. 14. Kerame 1: 1-14 – retouched flakes

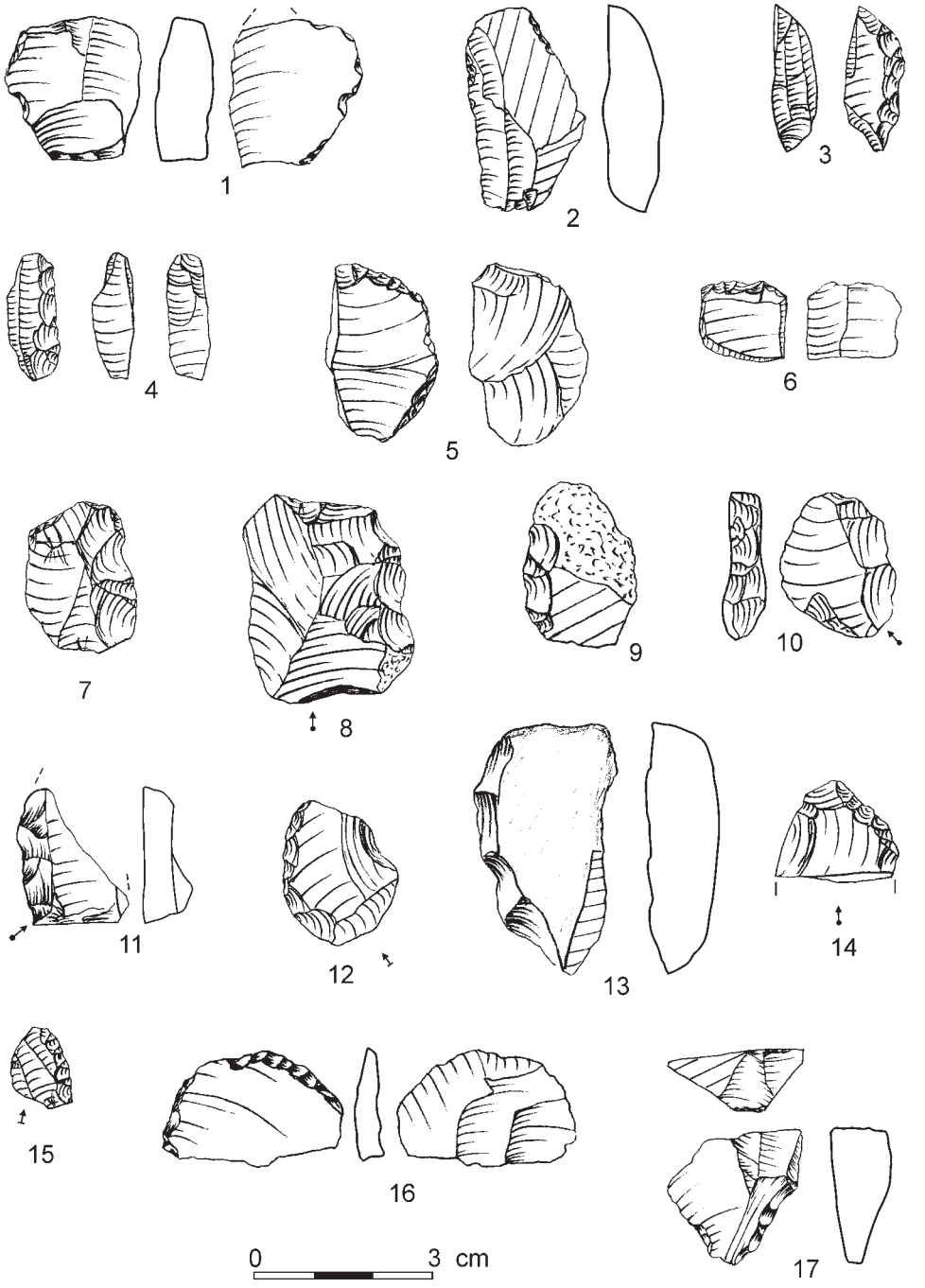

Pl. 15. Kerame 1: 1-6 – retouched flakes, 7-17 – side-scrapers

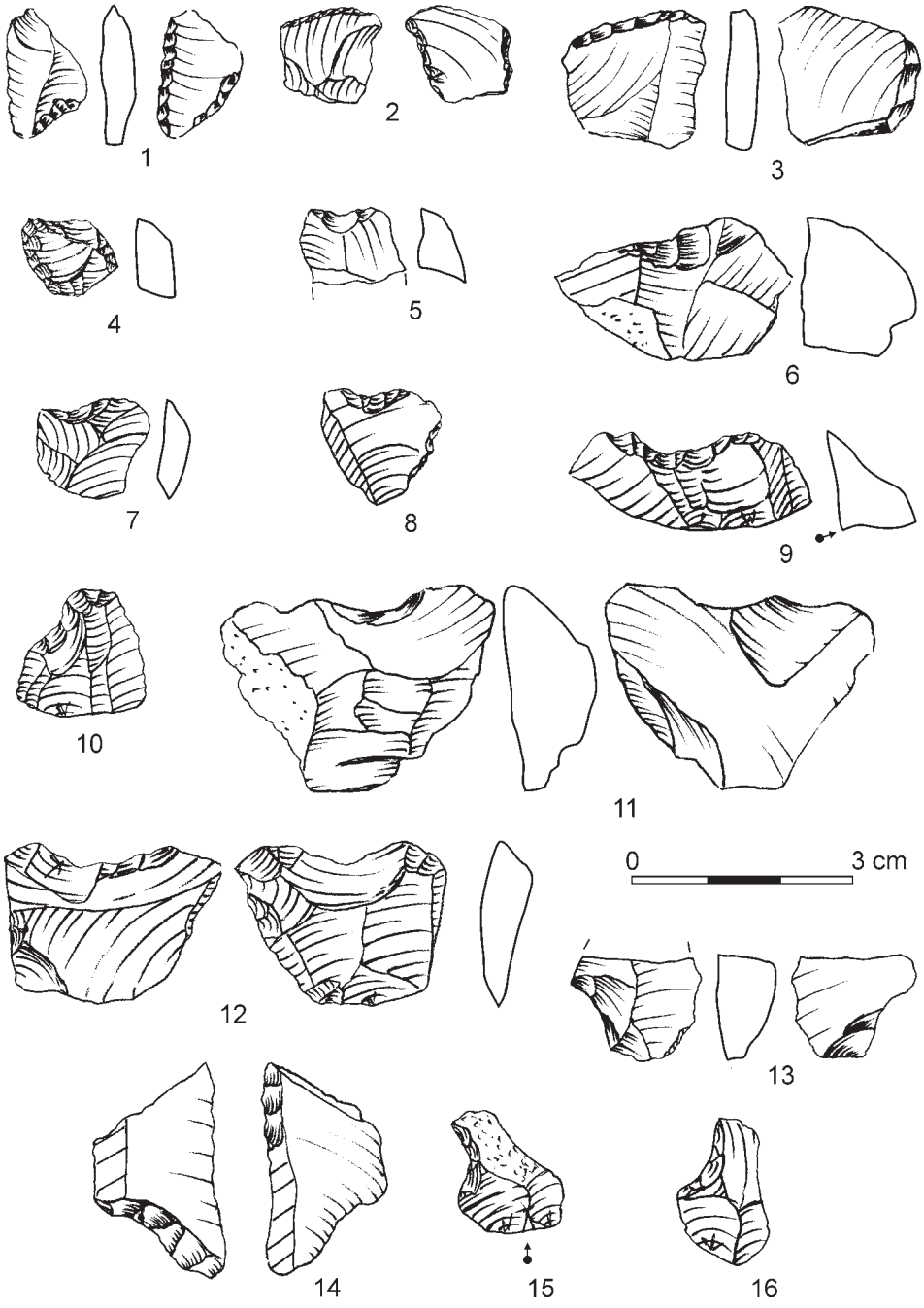

Pl. 16. Kerame 1: 1-4 – *raclettes*, 5-16 – denticulated-notched tools

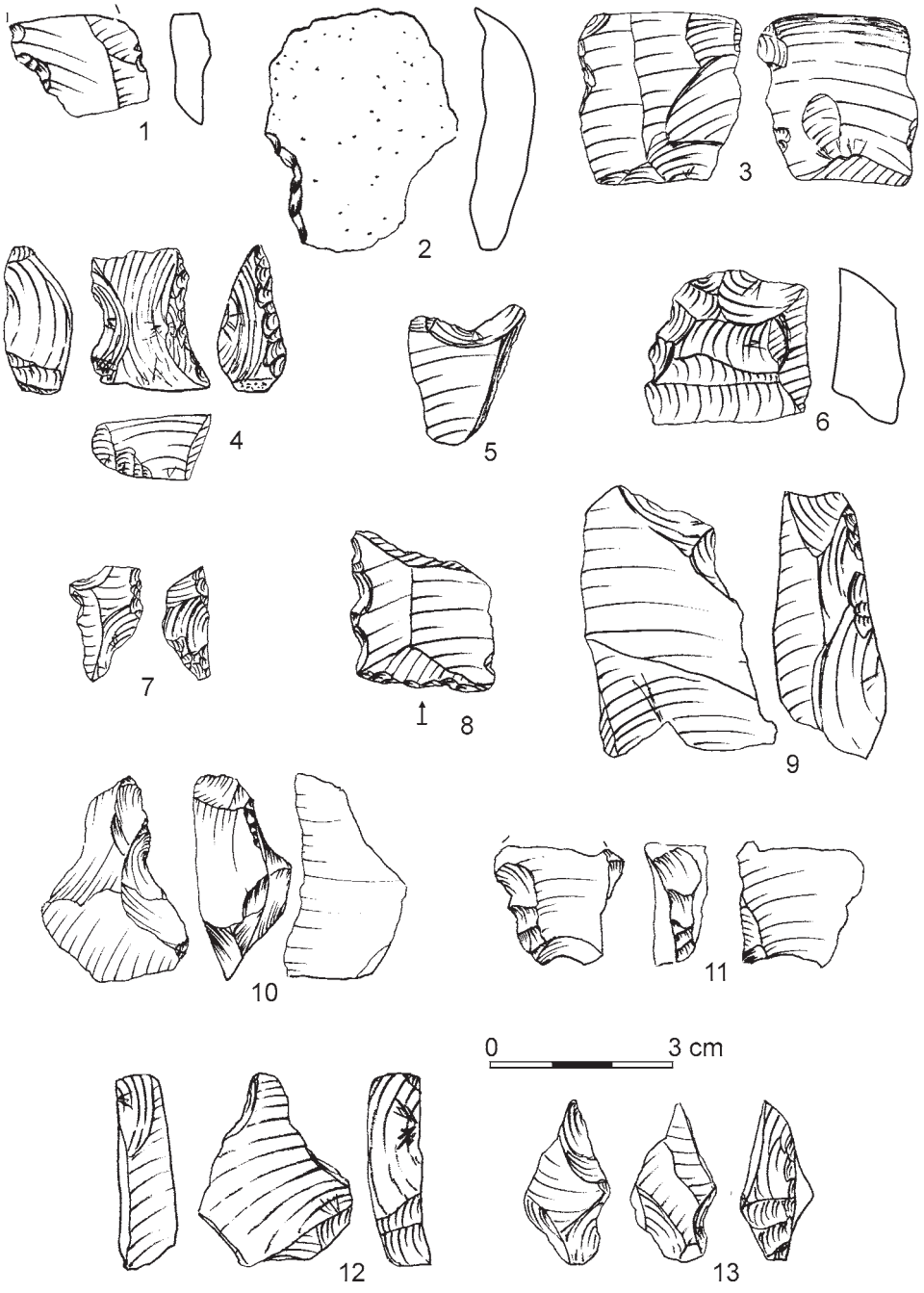

Pl. 17. Kerame 1: 1-13 – denticulated-notched tools

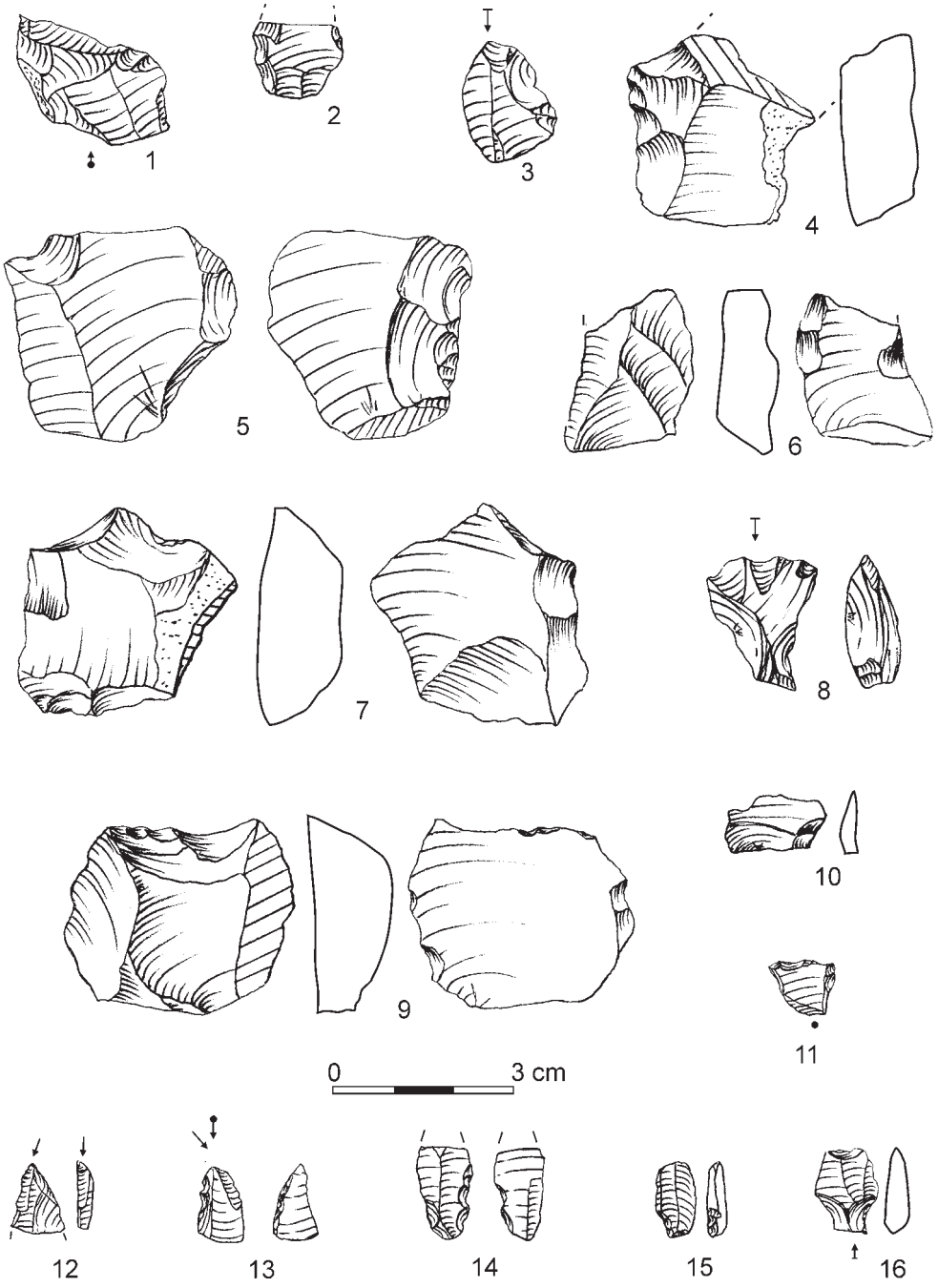

Pl. 18. Kerame 1: 1-11 – denticulated-notched tools, 12-14 – bladelets with impact fractures, 15, 16 – bladelets with basal notches

1

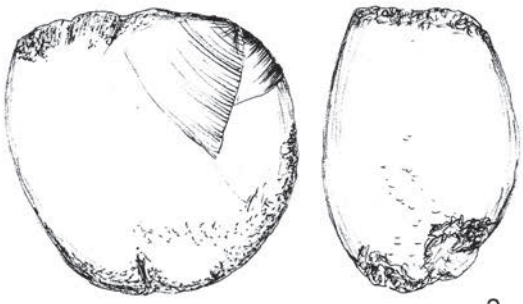

2

0 3 cm

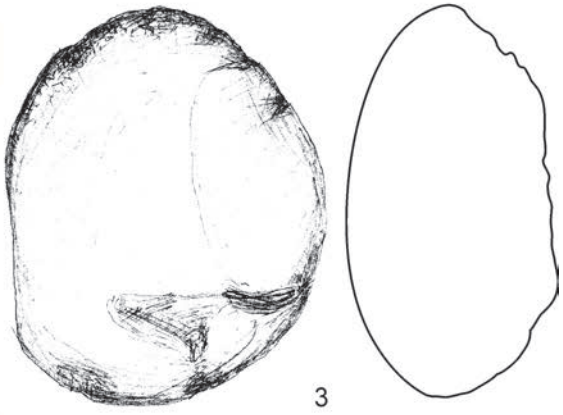

3

Pl. 19. Kerame 1: 1-3 – hammerstones/grinders

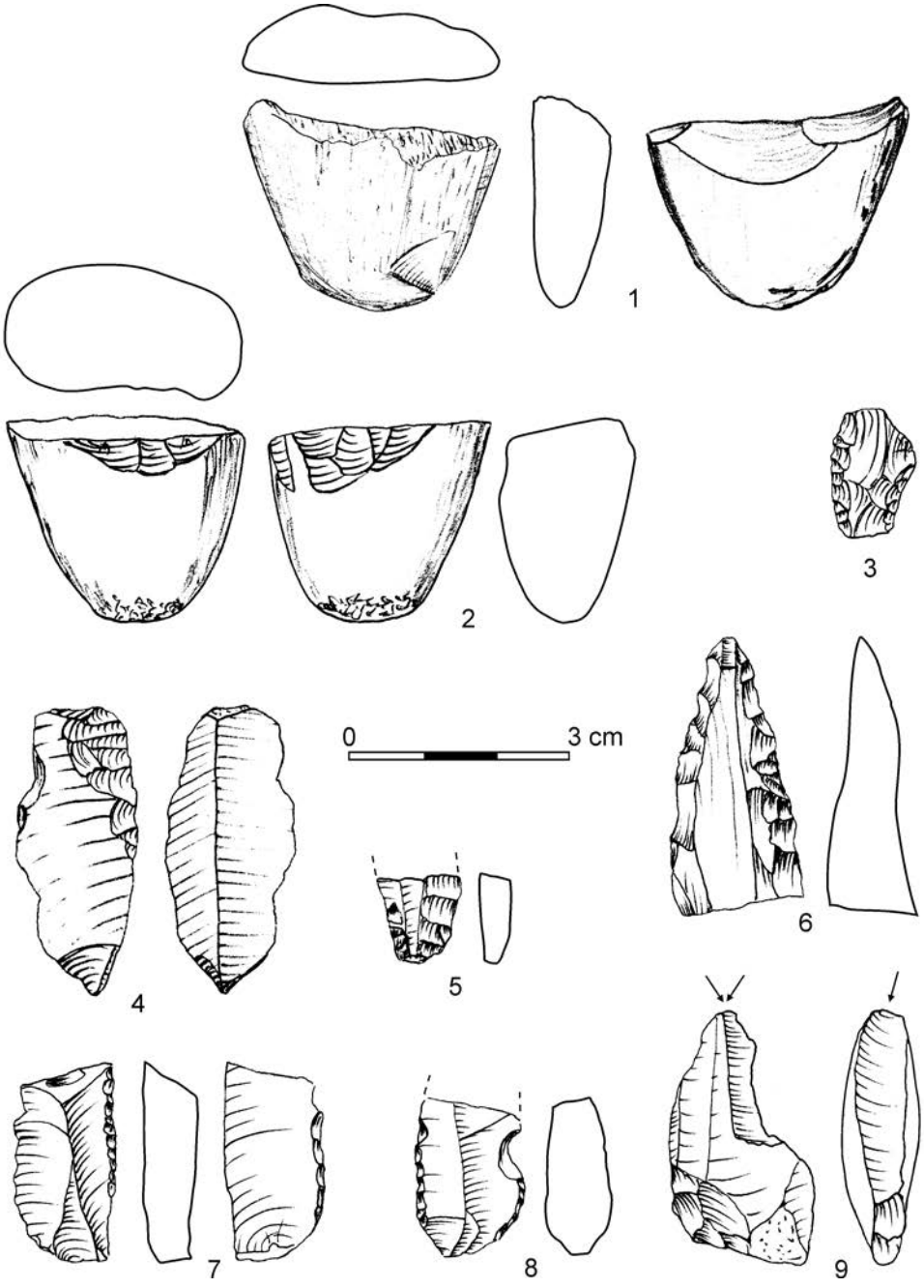

Pl. 20. Kerame 1: 1-9 – Neolithic admixtures

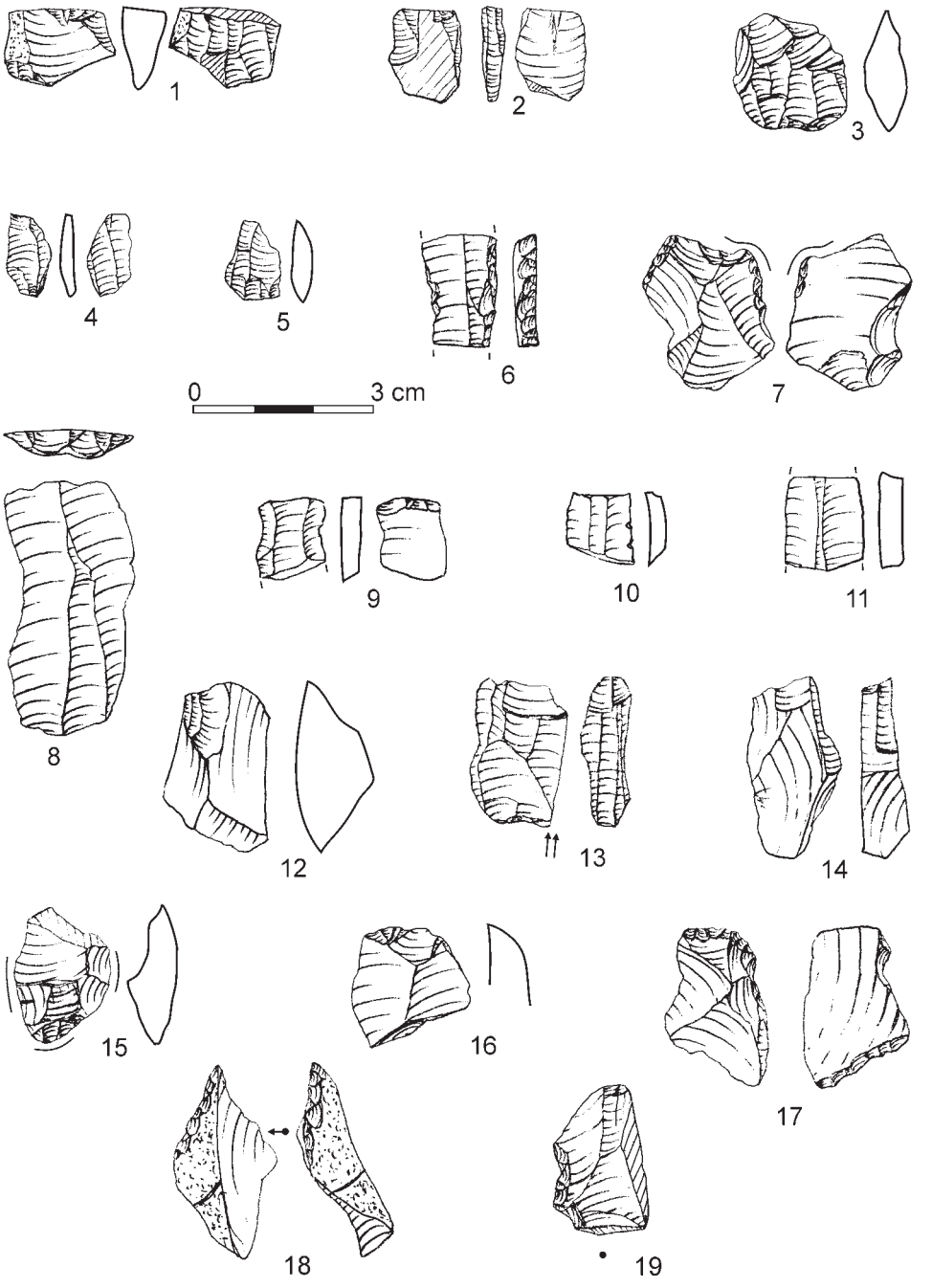

Pl. 21. Other Mesolithic sites: 1-11 – Nyfi 2, 12-19 – Nyfi 3

REFERENCES

Adamiec G. and Aitken M.J., 1998. Dose-rate conversion factors: update. Ancient TL **16**: 37-50.

Ambrose W. R., 1998. Obsidian Hydration Dating at a Recent Age Obsidian Mining Site in Papua, New Guinea. In: M. S. Shackley (Ed.), Archaeological Obsidian Studies: Method and Theory. Plenum Press, New York: 205-222.

Broodbank C., 2006. The origins and early development of Mediterranean maritime activity. Journal of Mediterranean Archaeology **19**: 199-230.

Crank J., 1975. The Mathematics of Diffusion. Oxford University Press, Oxford.

Facorellis Y., Damiata B.N., Vardala-Theodoru E., Ntinou M. and Southon J., 2010. AMS radiocarbon dating of the Mesolithic site Maroulas on Kythnos and calculation of the regional marine reservoir effect. In: The Prehistory of the Island of Kythnos (Cyclades, Greece) and the Mesolithic settlement at Maroulas. PAU, Kraków: 127-136.

Friedman I. and Smith R., 1960. A new dating method using obsidian. Part I: the development of the method. American Antiquity **25**: 476-522.

Geological Map of Greece 1: 50,000, Ikaria Island sheet, 2005. IGME, Athens.

Georgalas G.C., 1953. Les terrasses littorales de la côte sud-orientale de l'île de Nikaria (Mer Égée). Proceedings of the Academy of Athens **28**: 425-434.

Georgiadis M., 2008. The obsidian in the Aegean beyond Melos: an outlook from Yali. Oxford Journal of Archaeology **27(2)**: 101-117.

Kaczanowska M. and Kozłowski J.K., 2008. Chipped stone artefacts. In: A. Sampson (Ed.), The cave of the Cyclops, Mesolithic and Neolithic networks in the northern Aegean, Greece, Intra site analysis, Local Industries, and Regional Site Distribution. INSTAP Academic Press, Philadelphia, Pennsylvania: 169-178.

Kaczanowska M., Kozłowski J.K. and Sobczyk K., 2010. Upper Palaeolithic human occupation and material culture at Klissoura Cave 1. Eurasian Prehistory **7(2)**: 133-286.

Katsaros T., 2006. Ikariaka Symeikta (in Greek). Athens.

Kopaka K. and Matzanas C., 2009. Palaeolithic industries from the island of Gavdos, near neighbour to Crete in Greece. Antiquity Project Gallery **83**: 321.

Kozłowski J.K. and Kaczanowska M., 2009. The Mesolithic of the Aegean Basin: how to interpret the pre-Neolithic settlement of the Aegean island and its role in the Neolithization of south-eastern Europe. In: J.J. Shean and D.E. Lieberman (Eds.), Transitions in Prehistory. Oxbow, p. 357-384.

Ktenas C.A., 1927. Découverte du Pliocène inférieur marin dans l'île de Nikaria (Mer Égée).

Comptes Rendus de l'Academie des Sciences de Paris **184**: 756-758.

Ktenas C.A., 1969. La géologie de l'île de l'Ikaria (Rédigée des restes de l'auteur par G. Marinos). Geological and Geophysical Researches, Athens **13**: 57-85.

Lambeck K., 1996. Sea-level change and shore-line evolution in Aegean Greece since Upper Palaeolithic time. Antiquity **70**: 588-611.

Laskaris N., 2010. Application of spectroscopic and microscopic methods of analysis for the improvement of the Obsidian Hydration Dating (in Greek). Unpublished Ph.D. thesis, University of the Aegean, Department of Mediterranean Studies, Rhodes.

Laskaris N., Sampson A., Mavridis F. and Liritzis I., 2011. Late Pleistocene/Early Holocene seafaring in the Aegean: new obsidian hydration dates with the SIMS-SS method. Journal of Archaeological Science **38**: 2475-2479.

Liritzis I., 2006. SIMS-SS. A new obsidian hydration dating method: Analysis and theoretical principles. Archaeometry **48(3)**: 533-547.

Liritzis I., Diakostamatiou M., Stevenson C.M., Novak S.W. and Abdelrehim I., 2004. Dating of hydrated obsidian surfaces by SIMS-SS. Journal of Radioanalytical and Nuclear Chemistry **261**: 51–60.

Liritzis I., Bonini M. and Laskaris N., 2008a. Obsidian hydration dating by SIMS-SS: surface suitability criteria from atomic force microscopy. Surface and Interface Analysis **40**: 458-463.

Liritzis I., Laskaris N. and Bonini M., 2008b. Nano- and micro- scale resolution in ancient obsidian artifact surfaces: the impact of AFM on the obsidian hydration dating by SIMS-SS. Physica Status Solidi **5(12)**: 3704-3707.

Liritzis I. and Laskaris N., 2009. Advances in obsidian hydration dating by Secondary Ion Mass Spectrometry: World examples, Nuclear Instruments and Methods. Physics Research B, **267**: 144-150.

Liritzis I. and Laskaris N., 2010. The SIMS-SS obsidian hydration dating method. In: I. Liritzis and C.M. Stevenson (Eds.), The Dating and Provenance of Obsidian and Ancient Manufactured Glasses. New Mexico Press, Albuquergue (in press).

Liritzis I. and Laskaris N., 2011. Fifty years of obsidian hydration dating in archaeology. Journal of Non-Crystalline Solids **357**: 211-219.

Liritzis I. and Stevenson C.M. (Eds)., 2011. Obsidian and Ancient Manufactured Glasses. University of New Mexico Press, Albuquerque.

Lomax J., Hilgers A., Twidale C.R., Bourne J.A. and Radtke U., 2007. Treatment of broad palaeodose distributions in OSL dating of dune sands from the western Murray Basin, South Australia. Quaternary Geochronology **2**: 51-56.

Lykousis V., Anagnostou C., Pavlakis P., Rousakis G. and Alexandri M., 1995. Quaternary sedimentary history and neotectonic evolution of the eastern part of the Central Aegean Sea, Greece. Marine Geology **128**: 59-71.

Michael C.T. and Zacharias N., 2000. A new technique for thick-source alpha counting determination of U and Th. Nuclear Instruments and Methods **439**: 167–177.

Murray A.S. and Wintle A.G. 2000. Luminescence dating of quartz using an improved single – aliquot regenerative – dose protocol. Radiation Measurements **32**: 57-73.

Papanikolaou D., 1978. Contribution to the geology of Ikaria island, Aegean sea. Annales Géologiques des Pays Helléniques **29**: 1-28.

Sampson A. (Ed.), 2008. The Neolithic and Bronze Age Occupation of the Sarakenos Cave in Boeotia. Cave Settlement Patterns and Population Movements in Central and Southern Greece. University of the Aegean and Polish Academy of Sciences, Athens.

Sampson A., 2010. Mesolithic Greece (in Greek). ed. Ion, Athens.

Sampson A. (Ed.), 2011. The Cyclops Cave on the island of Youra, Greece. Mesolithic and Neolithic networks in the Northern Aegean Basin. Bone tool industries, Dietary resources and the Paleoenvironment, and Archaeometrical Studies. INSTAP Monograph Series Vol. 2. Academic Press, Philadelphia.

Sampson A., Kaczanowska M. and Kozłowski J.K., 2008.The first Mesolithic site in the eastern part of the Aegean basin: excavations into the site Kerame 1 on the island of Ikaria in 2008. Rocznik PAU 2007/2008: 321-329.

Sampson A., Kaczanowska M. and Kozłowski J.K., 2010. The Prehistory of the Island of Kythnos (Cyclades, Greece) and the Mesolithic settlement at Maroulas. PAU, Kraków.

Sampson A., Kozłowski J.K. and Kaczanowska M., 2003. Mesolithic chipped stone industries from the Cyclops Cave, Youra. In: N. Galanidou and C. Perlès (Eds.), The Greek Mesolithic – Problems and Perspectives. British School at Athens Studies **10**: 123-130.

Spooner N.A., Questiaux D.G. and Aitken M.J., 2000. The use of sodium lamps for low-intensity laboratory safelighting for optical dating. Ancient TL **18**: 45-48.

Stevenson C.M., Abdelrehim I. and Novak S.W., 2004. High Precision Measurement of Obsidian Hydration Layers on Artefacts from the Hopewell Site Using Secondary Ion Mass Spectrometry. American Antiquity **69(3)**: 555–568.

Stiros S.C., Laborel J., Laborel-Deguen F., Papageorgiou S., Evin J. and Pirazzoli P.A., 2000. Seismic coastal uplift in a region of subsidence: Holocene raised shorelines of Samos Island, Aegean Sea, Greece. Marine Geology **170**: 41-58.

Strasser T., Thompson N., Panagopoulou E., Karkanas P., Runnels C., McCoy F., Murray P. and Wegmann K., 2010. Stone Age seafaring in the Mediterranean. Evidence from the Plakias region for Lower Palaeolithic and Mesolithic habitation of Crete. Hesperia **79**: 145-190.

Tsermegas I., 2007. Znaczenie procesów naturalnych i antropogenicznych dla współczesnych przemian rzeźby Ikarii (in Polish). In: I. Tsermegas (Ed.), Warsztaty Geomorfologiczne „Naturalne i antropogeniczne procesy rzeźbotwórcze w warunkach śródziemnomorskich", Grecja 26.04-06.05. 2007. WGiSR UW, SGP, NUA, Warszawa: 52-63.

Wintle A.G. and Murray A.S., 2006. A review of quartz optically stimulated luminescence characteristics and their relevance in single-aliquot regeneration dating protocols. Radiation Measurements **41** : 369-391.

GUIDE FOR AUTHORS

Folia Quaternaria is a scientific journal of the Commission for Quaternary Palaeogeography, Polish Academy of Arts and Sciences in Kraków. Original contributions dealing with different aspects of the Quaternary period (archaeology, geology, geomorphology, palaeogeography, palaebotany, palaeozoology, radiometric dating, sedimentology and others) are considered for publication. The language of the journal is English.

Manuscripts and all correspondence to editors should be sent to: Publication Department, Polish Academy of Arts and Sciences in Kraków, ul. Sławkowska 17, 31-016 Kraków, Poland, or directly to Prof. Dr. Witold Zuchiewicz (witoldzuchiewicz@geol.agh.edu.pl), AGH University of Science and Technology, Faculty of Geology, Geophysics and Environmental Protection, Al. Mickiewicza 30, 30-059 Kraków, Poland.

A cover letter should include, besides precise postal and e-mail addresses of all authors, a statement that the submitted paper has not been published previously (except in the form of an abstract); that it is not in consideration for publication elsewhere; that this publication has been approved by all co-authors if any, that if and when the manuscript is accepted for publication, the authors agree to automatically transfer of the copyright to the publisher, i.e. the **Polish Academy of Arts and Sciences in Kraków**; that written permission of the copyright holder is obtained by the authors for material used from other copyrighted holder; and that any costs associated with obtaining this permission are the author's responsibility.

Three copies of the manuscript, tables and figures (one original and two high-quality copies) as well as their electronic versions on CD should be submitted for editorial and reviewing purposes and should be compiled following the outline used in the recently published volumes of *Folia Quaternaria* (see www.pau.krakow.pl/index.php/Folia-Quaternaria.html).

All contributions are reviewed by two anonymous specialists. The reviews are sent to the (corresponding) author together (if necessary) with the editorial suggestions and with technical remarks. In such a case the author is expected to send back one printout of the corrected material (text, illustrations) as well as the copies with reviewers' notes to the *Folia Quaternaria* editorial office for final acceptation.

Proofs should be sent back to the *Folia Quaternaria* editorial office as soon as possible. Additions are not normally being made at the proof stage; if necessary the author may be charged for their costs.

Organisation of the manuscript:

* Title of the paper;
* Name(s) of the author(s);
* Abstract;
* Key words;
* Author(s) address(es) and e-mail(s);
* Main text (introduction, regional setting, material and methods, results, discussion, conclusions);
* Acknowledgements (if any);
* References;
* Appendices (if any);
* Figure captions, starting from a new page. Captions for illustrations should be as precise as possible, and all symbols used should be explained. Captions numbers should be typed in consecutive order;
* Tables;
* Figures.

The manuscript should be printed on one side of white A-4 paper. Text should be double spaced, at a font size of 12 point (Times New Roman) with no hyphenation. The entire manuscript should be paginated and should not have justified right margin. Tab stops, not the space bar, should be used for indents. All uncommon symbols should be clearly defined at their first occurrence or in a separate list.

The references in the text should be carefully cross-checked with the list of references in order to ensure completeness and consistency in spelling of names and dates. A reference in the text to a publication should be made using name (with initials only when two or more authors of the same name appear) and year. Abbreviations et al. should be used if there are more than two authors but never in the list of references. The tables and figures from the cited papers should not be capitalized. In the list of references, all references in the text, tables, figure captions and appendices should be included. The order is alphabetical by authors' names and chronological for multiple papers by the same author(s). For the papers by the same author(s) from the same year lower-case letters are added to the date (e.g., 2012a, b). Titles should be given in English for the papers in English and those which have English summary or abstract. In the latter case, original language should be indicated in the parentheses, e.g. (in Polish with English summary). For entirely non-English papers the original language should be used if alphabet is Latin or transliterated if non-Latin. The names of periodicals should be given unabbreviated.

Figures and plates should be numbered consecutively in Arabic numerals, and each one must be referred to in the text. Each figure should be labelled with the author's name

and figure number. The approximate position of each figure, plate and table should be indicated in the printout and manuscript file. Each figure should be saved as a separate file and should not be embedded in to the text file.

Computer-prepared black and white photographs can be submitted in TIFF format (600 dpi) at publication size.

Tables should be typed on separate sheets, not included as part of the text. Tables with graphic elements must be prepared in graphics software (e.g., CorelDraw) and submitted at publication size. Each table should be saved as a separate computer file.